UNIVERSIDADE DA BEIRA INTERIOR
Ciências

Optimization of a gellan gum support by experimental design for recombinant proteins partition

Filipe dos Santos Frias

Dissertação para obtenção do Grau de Mestre em

Bioquímica

(2º ciclo de estudos)

Orientadora: Prof. Doutora Ângela Maria Almeida de Sousa
Co-orientador: Prof. Doutor Luís António Paulino Passarinha

Covilhã, Junho de 2015

Acknowledgments

First of all, I would like to express my sincere gratitude to my parents and brother for all their sacrifices, encouragement, support and unconditional love.

Furthermore, I would also like to give a special thanks to my supervisors Professor Doctor Ângela Sousa and Professor Doctor Luís Passarinha for all their availability, guidance, expertise, patience and trust. Their help, efforts, vast knowledge, criticism and suggestions were crucial for the development of this project. It was a privilege to work and learn with them.

I would also like to acknowledge the University of Beira Interior, in particular the Health Sciences Research Center, where all the work was developed.

I am also grateful to all people involved in the Health Sciences Research Center of the University of Beira Interior, particularly to my colleagues in the Biotechnology and Biomolecular Sciences group whose advice and companionship made my work much more easy and pleasant.

Finally, I am extremely thankful to all my friends. Their constant availability, support, belief, motivation and love through all this time was crucial to surpass the most difficult times.

Resumo alargado

A cromatografia é um dos métodos mais usados para a separação e purificação de diferentes biomoléculas terapêuticas. É uma técnica que tem sido muito explorada, ao longo dos últimos anos, nas áreas da indústria farmacêutica e biotecnológica para a obtenção de proteínas e ácidos nucleicos com elevado grau de pureza.

Os suportes cromatográficos têm sido alvo de grandes desenvolvimentos a fim de encontrar uma matriz que reúna as características ideais como porosidade, estabilidade química e física, elevada eficiência de transferência de massa, baixo custo de produção associado, biocompatibilidade, hidrofilicidade, boa capacidade de manutenção do fluxo e capacidade de reutilização após vários ensaios cromatográficos.

A goma de gelana é um polímero polissacárido natural linear que tem uma vasta gama de aplicações em diversas áreas, desde a indústria alimentar (agente espessante e gelificante), cosmética (loções, cremes, maquilhagem, etc), indústria biotecnológica (como um substituinte do agar), indústria farmacêutica (sistema de entrega direcionada de fármacos e microencapsulações) e medicina (construção de "*scaffolds*" para regeneração de tecidos). Devido às suas propriedades como versatilidade, biocompatibilidade, biodegradabilidade e elevada estabilidade, a gelana tem atraído grande interesse por parte do mercado e tem ganho crescente importância entre as diferentes indústrias.

A gelana possui a capacidade de, em determinadas condições e na presença de catiões divalentes, sofrer uma alteração conformacional formando uma forte rede tridimensional devido às interações entre a gelana, os iões e as moléculas de água dando origem a um gel termoreversível, resistente a altas temperaturas e a extremas condições ácidas.

Tendo em conta as características apresentadas, o presente trabalho teve como objetivo otimizar a formulação de uma matriz cromatográfica pela técnica de emulsão água-em-óleo a fim de ser usada em diversos processos cromatográficos. A inovação deste projeto tem como base a produção de microesferas através de um método de emulsão água-em-óleo, usando dois líquidos imiscíveis, a água e um óleo alimentar vegetal. Trata-se de uma técnica que não requer o uso de instrumentos complexos, é de fácil manuseamento, tem baixo custo associado e permite o fácil controlo dos parâmetros associados a este processo. A preparação das esferas foi feita de acordo com os seguintes parâmetros: concentração da goma de gelana (1 % - 2,5 %), velocidade de agitação (250 rpm – 750 rpm) e temperatura (20 ºC – 100 ºC). Considerando que todos estes fatores afetam a estabilidade e estrutura das microesferas, foram feitas várias formulações utilizando um desenho experimental, estratégia que permitiu obter as condições ótimas no sentido de se produzirem micropartículas com o mínimo diâmetro possível. As condições ótimas fornecidas pelo desenho foram 1,41 % de concentração de gelana, 749,47 rpm de velocidade de agitação e 99,20 ºC para obter microesferas com um tamanho de 277,08 µm. Para a formulação deste suporte

cromatográfico, foi necessário a presença de catiões divalentes numa solução de reforço, para onde as esferas foram transferidas a fim de aumentar a estabilidade. O catião escolhido foi o bário, que devido ao seu grande tamanho iónico é considerado bastante eficaz na gelificação da gelana, pois contribui largamente para a formação da estável e rígida rede tridimensional. Além disso, o bário também permitiu a formação de esferas uniformes de tamanho reduzido com um pequeno *ratio* de inchaço.

Para a validação do modelo fornecido pelo *software* do desenho experimental, foi necessário efetuar cinco réplicas de dois pontos previstos dados pelo programa. A visualização das esferas produzidas foi feita através de microscopia ótica que permitiu a medição dos diâmetros das micropartículas e através de microscopia eletrónica de varrimento, que tornou possível a análise estrutural das esferas num estado liofilizado, bem como a análise topográfica e morfológica da sua superfície. Além disso, esta última metodologia também permitiu avaliar a porosidade das esferas, de onde foi constatado a ausência de canais interiores, sugerindo que qualquer interação estabelecida com a matriz de goma de gelana se dê apenas na sua superfície.

Aproveitando a natureza aniónica do polímero de gelana e o facto de não ter que ser funcionalizada com ligandos como os suportes cromatográficos comerciais, foi possível explorar diferentes interações com as proteínas modelo albumina sérica bovina (BSA), α-quimotripsina e lisozima, bem como com um extracto parcialmente purificado da proteína catecol-*O*-metiltransferase humana na isoforma solúvel (hSCOMT). Nos ensaios com as proteínas modelo, o tampão usado foi o MES a pH 6.2, o que conferiu carga negativa à BSA e cargas positivas à α-quimotripsina e lisozima devido aos seus pontos isoelétricos. Assim, a BSA não ligou à matriz tendo sido eluída após a injeção da amostra na coluna, ainda com a passagem do tampão sem sal, enquanto as outras duas proteínas interagiram devido à oposição de cargas, tendo sido eluídas com o aumento da força iónica. Quanto à amostra pré-purificada de SCOMT, foi usado um tampão de pH 4.0 nas condições de equilíbrio, o que conferiu carga positiva a esta proteína. Esta condição permitiu a interação desta proteina com a coluna, tendo sido maioritariamente eluída através da manipulação do pH (alterando o pH do tampão para 6.4), permitindo assim a eliminação de algumas proteínas contaminantes presentes na amostra.

A fim de se caracterizar melhor esta nova matriz cromatográfica, foi determinada a capacidade dinâmica de ligação utilizando uma estratégia de saturação da coluna com uma solução de lisozima 0,5 mg/mL a 1 mL/min. Os valores obtidos na capacidade de ligação das microesferas de goma de gelana a 10 % e 50 % da curva de saturação foram 2,43 mg/mL e 4,73 mg/mL, respetivamente. Comparando com outras matrizes cromatográficas comerciais e tendo em conta que apenas a área de superfície das microesferas de gelana é funcional, estes valores estão dentro do esperado.

Estes estudos permitiram concluir que a estabilidade da matriz cromatográfica de gelana foi incrementada com o desenvolvimento deste projecto de mestrado e que permitiu a interação

com proteínas de várias naturezas, através de estratégias de eluição com manipulação de força iónica e pH.

Em suma, os dados apresentados manifestam uma versatilidade da gelana em interagir com diferentes biomoléculas e, devido à sua capacidade de gelificação, foi possível a elaboração deste inovador e promissor suporte cromatográfico para a cromatografia de troca catiónica, a partir de microesferas da goma de gelana.

Palavras-chave

Cromatografia de troca iónica; Matriz cromatográfica; Microesferas de gelana; Purificação de proteínas; Técnica de emulsão água-em-óleo

Abstract

Chromatography is one of the most studied methods, due to its simplicity, versatility and high reproducibility, to separate and purify molecules that can have therapeutic, industrial and biotechnological interest. In recent years, the development of new chromatographic matrices has been continuously increased in order to afford rapid and efficient separations and decrease the use of resources. Gellan gum is a natural anionic exopolysaccharide and, in the presence of divalent cations, has the ability to form thermos-reversible strong gels resistant to temperature and extreme acidic conditions.

In this work, it was proposed the preparation of gellan gum microbeads to be used as a stable chromatographic stationary phase. In order to produce the matrix, a low-cost water-in-oil emulsion technique was adopted. To obtain optimal conditions to the bead formulation, experimental design was applied, which allowed the optimization of the experimental conditions and to produce microbeads with the smallest diameter possible. Due to the negative charge of gellan gum, it was possible to study the interactions established with three model proteins (BSA, α-chymotrypsin and lysozyme) and with a therapeutic complex protein, SCOMT. In the model protein assays, MES buffer with pH 6.2 was used, which conferred negative charge to BSA and positive charge to α-chymotrypsin and lysozyme, due to its isoelectric points. Thus, BSA did not bind to the matrix while the other two proteins were retained to the gellan gum, being eluted with an increase of ionic strength. Regarding to pre-purified SCOMT sample, a buffer with pH 4.0 was used under equilibrium conditions, conferring positive charge to the protein, thus, it also interacted with the column and was majorly eluted by pH manipulation (by changing the buffer pH to 6.4), allowing the elimination of some protein contaminants.

Dynamic binding capacity assay of the gellan gum microbeads was made, in order to characterize this support as a novel chromatographic matrix. The values of DBC of the gellan gum stationary phase to 10 % and 50 % of breakthrough were 2.43 mg/mL and 4.73 mg/mL, respectively. These DBC values are satisfactory when compared to commercial resins used in affinity chromatography, taking into account that protein interaction only occurred at the gellan bead surface. These results indicated that gellan gum microbeads obtained by water-in-oil emulsion technique can be used as an innovative and promising chromatographic support due to its gelling ability and versatility to interact with different biomolecules.

Keywords

Chromatographic matrix; Gellan gum microbeads; Ion exchange chromatography; Protein purification; Water-in-oil emulsion technique

Contents

List of figures

List of tables

List of acronyms

3,5-DNC	3,5-dinitrocatechol
AC	Affinity chromatography
ANOVA^{+}	Analysis of variance
$BaCl_2$	Barium chloride
BSA	Bovine serum albumin
CCD	Central composite design
CG	Gas chromatography
CI	Confidence interval
COMT	Catechol-O-methyltransferase
CV	Coefficient of variation
DBC	Dynamic binding capacity
D-Glc	D-glucose
D-GlcA	D-glucuronic acid
DoE	Design of experiments
EPS	Extracellular polysaccharides
FDA	Food and Drug Administration
G1P	Glucose-1-phosphate
G6P	Glucose-6-phosphate
GSLs	Glycosphingolipids
HA-gellan	High acyl gellan
HCl	Hydroclorich acid
HIC	Hydrophobic interaction chromatography
hMBCOMT	Human membrane catechol-*O*-methyltransferase
hSCOMT	Human soluble catechol-*O*-methyltransferase
IDA	Imino diacetate
IEC	Ion-exchange chromatography
IMAC	Immobilized metal-chelate chromatography
JECFA	Joint Expert Committee on Food Additives
LA-gellan	Low acyl gellan
LC	Liquid chromatography
L-Rha	L-rhamnose
MES	4-Morpholineethanesulfonic acid
NaCl	Sodium chloride
NPC	Normal phase chromatography
NTA	Nitrotriacetic acid
O/W	Oil-in-water

OAc	O-acetyl
OGl	O-glyceryl
OMA	Outer membrane auxiliary
OVAT	One-variable-at-a-time
PCPs	Polysaccharide co-polymerases
PD	Parkinson´s disease
PFC	Prefrontal cortex
PgmG	Phosphoglucomutase
pI	Isoelectric point
PSA	Ammonium persulfate
PVDF	Polyvinylidene fluoride
RmlA	TDP-glucose pyrophosphorylase
RmlB	dTDP-D-glucose-4,6-dehydratase
RmlC	dTDP-6-deoxy-D-glucose-3,5-epimerase
RmlD	dTDP-6-deoxy-L-mannose dehydrogenase
RPC	Reverse phase chromatography
RSM	Response surface methodology
SAM	S-adenosyl-$_L$-methionine
SCOMT	Soluble catechol-*O*-methyltransferase
SDS	Sodium dodecyl sulfate
SDS-PAGE	Sodium dodecyl sulfate polyacrylamide gel electrophoresis
SEC	Size-exclusion chromatography
SEM	Scanning electron microscopy
TBS	Tris-buffered saline
TED	Tris(carboxylmethyl) ethylene diamine
TEMED	N,N,N',N'-tetramethylethylenediamine
Tris	Tris(hydroxymethyl)aminomethane
UgdG	UDP-glucose dehydrogenase
UgpG	UDPglucose pyrophosphorylase
W/O	Water-in-oil

Chapter I

Introduction

1 Gellan gum

1.1 Gellan gum as a microbial polysaccharide

In recent years, the use of microbial polysaccharides in different industrial sectors like food, pharmaceuticals, chemicals, cosmetics, oil drilling, and paper manufacturing has strongly increased because of its several physicochemical and rheological properties. Moreover, it has gained much importance due to its novel property of forming thermo-reversible gels when heated and cooled [1,2].

Microbial extracellular polysaccharides, produced by a wide range of bacteria, are high molecular weight biopolymers, presenting an extreme diversity in terms of chemical structure and composition [3]. Some of the applications of the biopolymers include their utility as emulsifiers, stabilizers, binders, gelling agents, coagulants, lubrificants, film formers, thickening agents, and have additionally potential use in catalysis, separation of materials, tissue engineering and drug delivery in the form of tablets, capsules, beads and hydrogels [4].

Among the extracellular polysaccharides (EPS), gellan is a multifunctional gelling agent produced in high yields. Gellan gum is the generic name for the anionic water-soluble extracellular heteropolysaccharide produced by bacterium *Pseudomonas elodea*. It was previously referred to by codename S-60 and PS-60. The gellan gum producing microorganism was isolated from the elodea plant tissue [5]. In 1994, it was discovered that the gellan gum producing bacterium was a new non-pathogenic bacterial strain of species *Sphingomonas paucimobilis ATCC* 31461, and classified in α-4 subclass of the proteobacteria [6]. *Sphingomonas* is a group of gram negative, rod shaped chemoheterotrophic with a single flagellum, strictly aerobic bacteria that produce yellow pigmented colonies and contains glycosphingolipids (GSLs) in their outer membranes instead of lipopolysaccharides [7].

1.2 Molecular structure

The native exopolysaccharide product gellan from *Sphingomonas paucimobilis* is composed of a linear repeating tetrasaccharide of D-glucose (D-Glc), D-glucuronic acid (D-GlcA) and L-rhamnose (L-Rha) in the ratio of 2:1:1 (Figures 1 and 4 *a A6*). It has O-acetyl (OAc) and O-glyceryl (OGl) moieties on the D-glucosyl residue adjacent to the D-glucuronyl residue as the side chain [8]. The native gellan is partially esterified: the 1,3-DGlc residue can be linked to L-glycerate at C-2 and/or to acetate at C-6 (Figure 1) and there is 1 mol of glycerate and 0.5 mol of acetate per repeating unit [9].

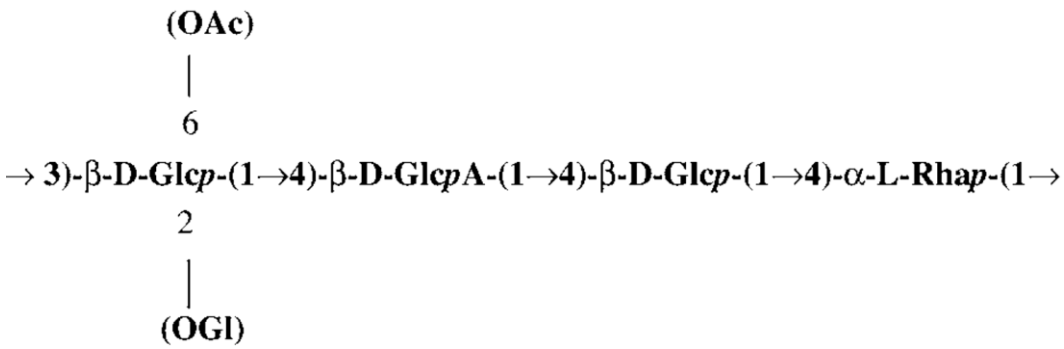

Figure 1. Repeating unit of the exopolysaccharide gellan produced by *S. paucimobilis ATCC* 31416. In the native polymer, O-acetyl (OAc) is present at 0.5 mol per repeating unit and O-glyceryl (OGl) at 1 mol per repeating unit. D-Glc, D-glucose; D-GlcA, D-glucuronic acid; L-Rha, L-rhamnose [9].

1.3 Chemical, physical and gelling properties

Gellan gum, an anionic heteropolysaccharide because of the presence of free carboxylate groups, has an average molecular mass of about 500 kDa. It has been shown to dissolve readily in water, adopting a disordered conformation (random coil) at higher temperatures (>~ 40 ºC) which subsequently undergoes a disordered-to-ordered transition on cooling. X-ray diffraction studies on gellan gum have shown that the ordered conformation is a threefold, left-handed, parallel double helix [10]. The double-helical structure is stabilized by interchain hydrogen bonding occurring regularly along the helix between hydromethyl groups of the 4-linked glucosyl units in one chain and carboxylate groups in the other. The aggregation of the gellan gum helices occurs in aqueous solutions and is strongly influenced not only by the polymer concentration but also by the temperature and the presence of cations [11]. While helical ordering at low temperatures may impart weak gels characteristics, the formation of a true hydrogel network is achieved through cation-mediated association of helices (Figure 2). This association can be facilitated through either monovalent or divalent cations, although divalent cations produce stronger gels. The mechanism of gelation involves the formation of double helical junction zones followed by

aggregation of double helical segments to form a three-dimensional network by complexation with cations and hydrogen bonding with water [10].

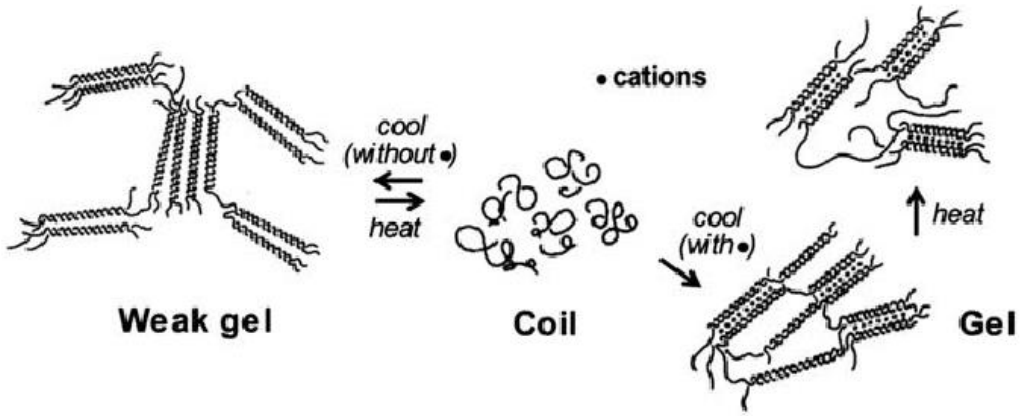

Figure 2. Schematic model of the conformational transitions and gelation of low acyl gellan gum through temperature changes with and without added cations [12].

Increasing the ion or polysaccharide concentration in the medium raises the gelling and melting point of the polysaccharide gels. The presence of the cations increases the number of junction zones and decreases the rotational freedom. The structures are rendered more heat resistant and the elastic modulus of the gel is increased [13]. It has been suggested that the O-acetyl group on the native polysaccharide has only a weak effect on aggregation of gellan molecules, whereas the L-glyceryl residue seems to be detrimental in crystal packing [14].

The organization of double helices in the unit cells portrays the junction zone implicated in the gelation process. In the presence of monovalent cations, such as K^+, pairs of gellan helices are aligned in an antiparallel fashion with their helix axes apart and connected by strong carboxylate---K^+---water---K^+---carboxylate interactions. On the other hand, when divalent ions, such as Ca^{2+}, are used for gelation, each K^+---water---K^+ bridge in this arrangement is expected to be replaced by a single Ca^{2+} ion so that gellan molecules are linked by obviously stronger carboxylate---Ca^{2+}---carboxylate interactions. This rearrengement of the junction zone provides a convincing structural explanation for the ability of calcium to make gellan gels of a desired strength and texture at a significantly lower ionic strength than that of potassium or other monovalent ion. Divalent cations act as direct bridges by site binding between pairs of carboxyl groups, while monovalent cations induce aggregation by suppressing electrostatic repulsions [10]. For that reason, we can say that divalent counter ions promote greater gelation compared to monovalent ones [15].

The physical properties of gellan vary considerably and are functions of EPS concentration, temperature, aqueous environment, and the presence of monovalent and divalent cations in the solution. The gellan gum is one of the EPS most widely used in fermentation materials

which offers a solution to many problems encountered in the current gelling agents, because it can form a transparent gel in the presence of multivalent cations, which is resistant to heat and acid. Therefore, gellan gum is one of the most intensively studied polysaccharides and an appropriate model in order to study thermo-reversible sol-gel transitions [16].

The gellan gum, in its native form, contains two acyl substituents, L-glycerol and acetyl, being known as high acyl gellan (HA-gellan). The substituents may be removed by alkaline hydrolysis to give deacetylated gellan, also called low acyl gellan (LA-gellan). The acyl substituents drastically affect the rheology of the gels formed with various cations. HA-gellan usually produces elastic, soft (weak), non-brittle, and opaque gels while LA-gellan enables the formation of non-elastic, hard (firmer, strong), brittle, and transparent gels under optimal gelling conditions [17]. Therefore, a wide range of structures, with varied rheological properties and appealing textures may be designed by controlling the acyl content. Structure of gellan gum along with native and deacetylated gellan gum, as well the chemical composition of the different types of gellan are illustrated in Figure 3 and Table 1, respectively [18].

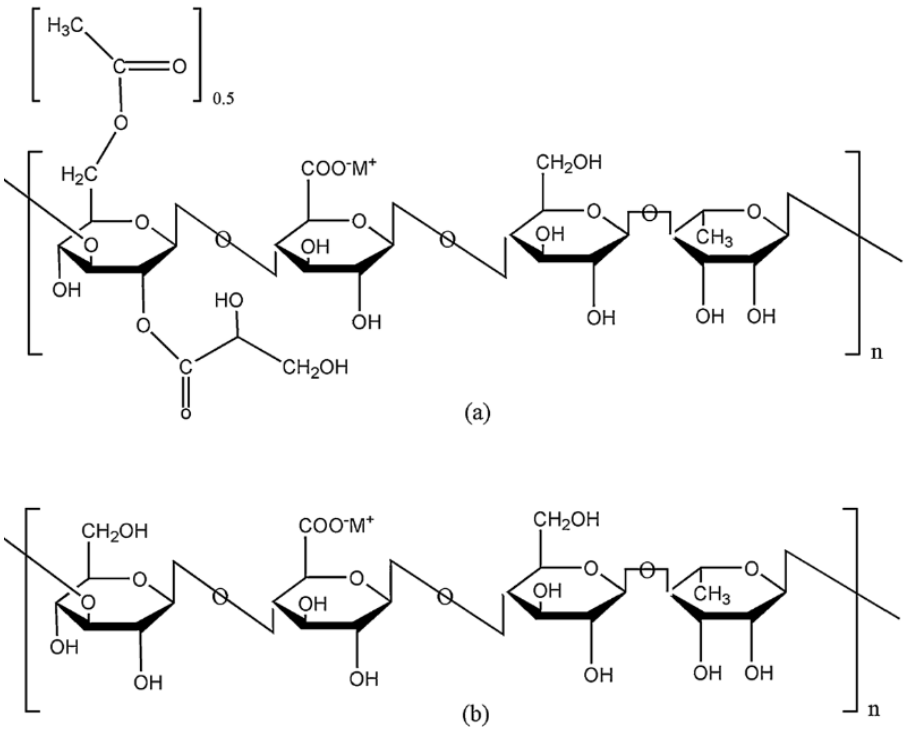

Figure 3. Chemical structure of *(a)* native and *(b)* deacetylated gellan gum [19].

Table 1. Chemical composition of different types of gellan gum (modified from [18]).

Gellan gum	*Neutral sugars Glc/Rha=6/4*	*Uronic acid %*	*Acetyl group %*	*Protein %*	*Ash %*
Native	69	11	3	10	7
Deacetylated	62	13	0	17	8
Deacetylated and clarified	66.5	22	0	2	9.5

The approximated chemical composition of gellan gum is glucose 60 %, rhamnose 20 % and glucuronic acid 20 %. In addition to these, it contains considerable amounts of non-polysaccharide material such as cell protein and ash, which can be removed by filtration or centrifugation [20,21].

The clarified gellan gum results from filtration of hot and deacetylated gellan gum and is used for enhanced removal of cell proteins. Clarification of gellan gum is of value especially when the gum is to be used as an agar substitute [22].

1.4 Production of gellan gum

1.4.1 Fermentation process

Figure 4 shows a fermentation process for gellan gum production and its purification at a laboratory scale. Gellan production is a growth-associated process with a maximum production of 12 g/l (Figure 4 *b*). The viscosity of the culture medium increases during the exponential and stationary phases and reaches a very high value at the end of the process. This characteristic creates great difficulty in terms of separating gellan from the cells, and the dilution of culture broth prior to isopropyl alcohol precipitation is required. After repetitive isopropyl alcohol precipitation steps, gellan is resuspended in water, followed by dialysis and lyophilization. Finally, gellan can be resuspended in water to produce a gel (Figure 4 *a*) [23].

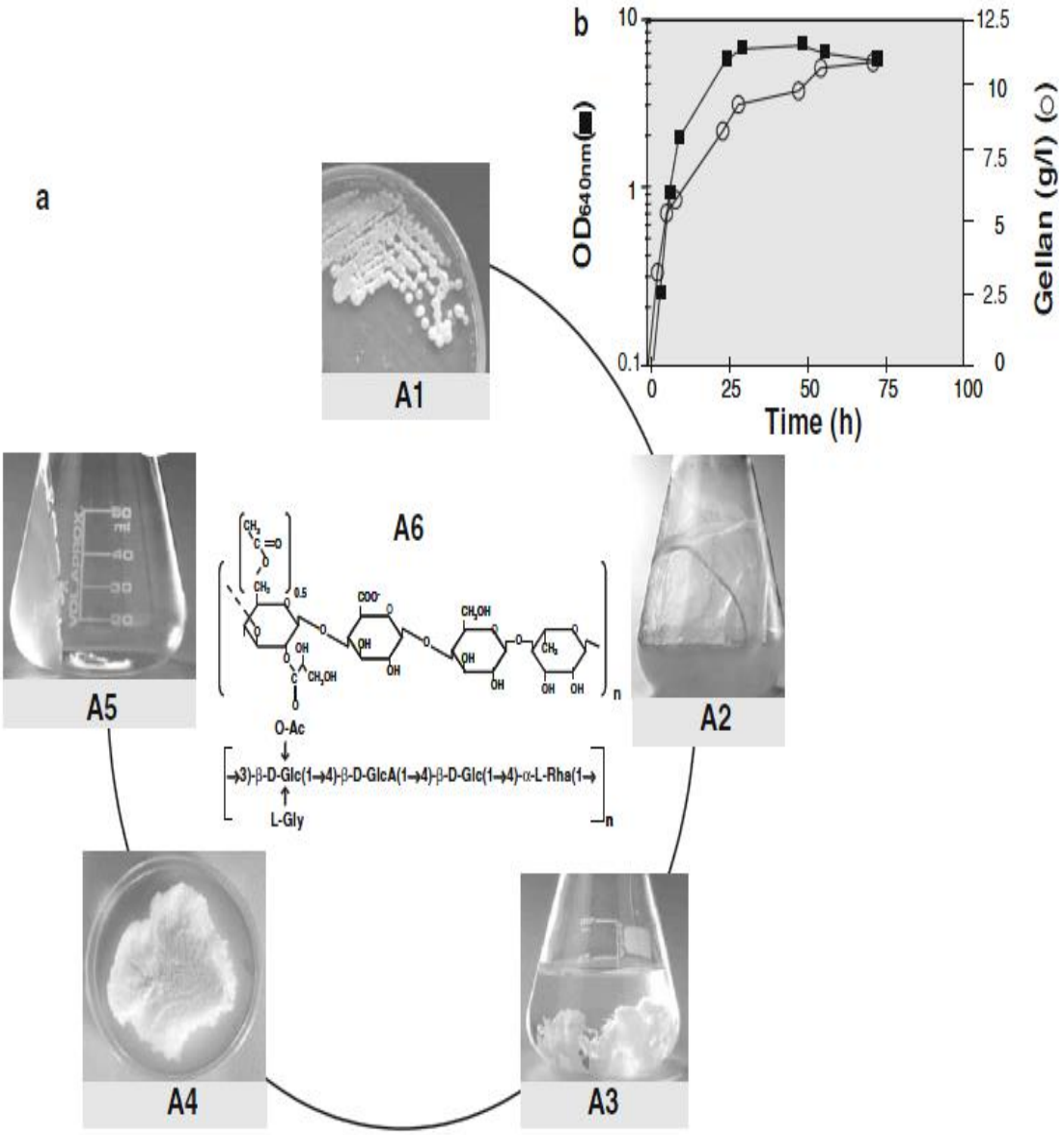

Figure 4. *(*a) Typical fermentation process for gellan production and its purification at a laboratory scale. *A1* Mucoid phenotype of the gellan producing strain *S.elodea ATCC* 31416, *A2* culture broth after 72 h of growth, *A3* gellan precipitated with isopropyl alcohol, *A4* lyophilized gellan, *A5* gellan gel (1 g/l), *A6* molecular structure of the repeat unit of gellan, Glc glucose, GlcA glucoronic acid, Rha L-rhamnose, Ac acetate, Gly glycerate. (b) Time of course of growth and gellan production by *S. elodea ATCC* 31416 at 30 ºC during a batch growth in a defined medium with 20 g/l glucose at initial pH of 8.0. The procedure adopted to recover gellan from the culture broth involves a dilution (with saline solution) in order to reduce its viscosity, followed by centrifugation to separate the cells. The supernatant is precipitated with cold isopropyl alcohol and the dried EPS quantified. The viscosity of the broth increased significantly during growth [23].

The pH plays an important role in the production of gellan gum by *S. paucimobilis*, as it significantly influences both cell growth and product formation. The optimal pH value for bacterial polysaccharide production is higher that of fungal glucan production. The recommended pH value for gellan production ranges from 6.5 to 7.0 [24,25]. More acidic or more alkaline environment reduces the cell growth and, consequently, gellan production [26].

1.4.2 Biosynthetic pathway

The gellan biosynthetic pathway is a multi-step process that can be divided into three sequential steps: *(a)* the intracellular synthesis of the sugar-activated precursors (Figure 5); *(b)* the assembly of the tetrasaccharide repeat units linked to the inner membrane (Figure 6); *(c)* translocation of the repeat unit to the periplasmic space followed by their polymerization and exportation of the polymer through the outer membrane (Figure 6) [23]. The gellan biosynthesis starts with the cytosolic formation of the nucleotide-sugar precursors, UDP-D-glucose, UDP-D-glucuronic acid, and dTDP-L-rhamnose. The enzymes required for the synthesis of these sugar nucleotides are phosphoglucomutase (PgmG), UDPglucose pyrophosphorylase (UgpG), UDP-glucose dehydrogenase (UgdG), TDP-glucose pyrophosphorylase (RmlA), dTDP-D-glucose-4,6-dehydratase (RmlB), dTDP-6-deoxy-D-glucose-3,5-epimerase (RmlC), and dTDP-6-deoxy-L-mannose dehydrogenase (RmlD) [9].

Glucose-1-phosphate occupies a key position from which two routes derive, one leading to UDP-D-glucose and UDP-D-glucuronic acid and the other leading to dTDP-L-rhamnose. The identification and biochemical characterization of genes/enzymes involved in the formation of the following gellan precursors were carried out: the *pgm*G gene, encoding a phosphoglucomutase (EC 5.4.2.2), which catalyses the reversible conversion of glucose-6-phosphate into glucose-1-phosphate [27]; the *ugp*G gene, encoding a glucose-1- phosphate uridilyltransferase (or UDP-glucose pyrophosphorylase; EC 2.7.7.9), which catalyses the reversible conversion of glucose-1-phosphate and UTP into UDP-D-glucose and diphosphate [28]; the *ugd*G gene, encoding a UDP-glucose dehydrogenase, which converts UDP-D-glucose into UDP-D-glucuronic acid [29]; and *rml*A, the first gene of the 4-gene rml cluster, which encodes a glucose-1-phosphate thymidilyltransferase (or TDP-glucose pyrophosphorylase; EC 2.7.7.24) that converts glucose-1-phosphate and TTP into TDP-D-glucose, necessary for the formation of dTDP-L-rhamnose [30]. Among the gellan biosynthetic enzymes, the PgmG protein plays a pivotal role, presumably being an ideal target for metabolic engineering. Indeed, this enzyme catalyses a step representing a branch point in carbohydrate metabolism; G6P enters catabolic processes to yield energy and reducing power and G1P is a precursor of sugar nucleotides that are used by cells in the synthesis of various polysaccharides [23].

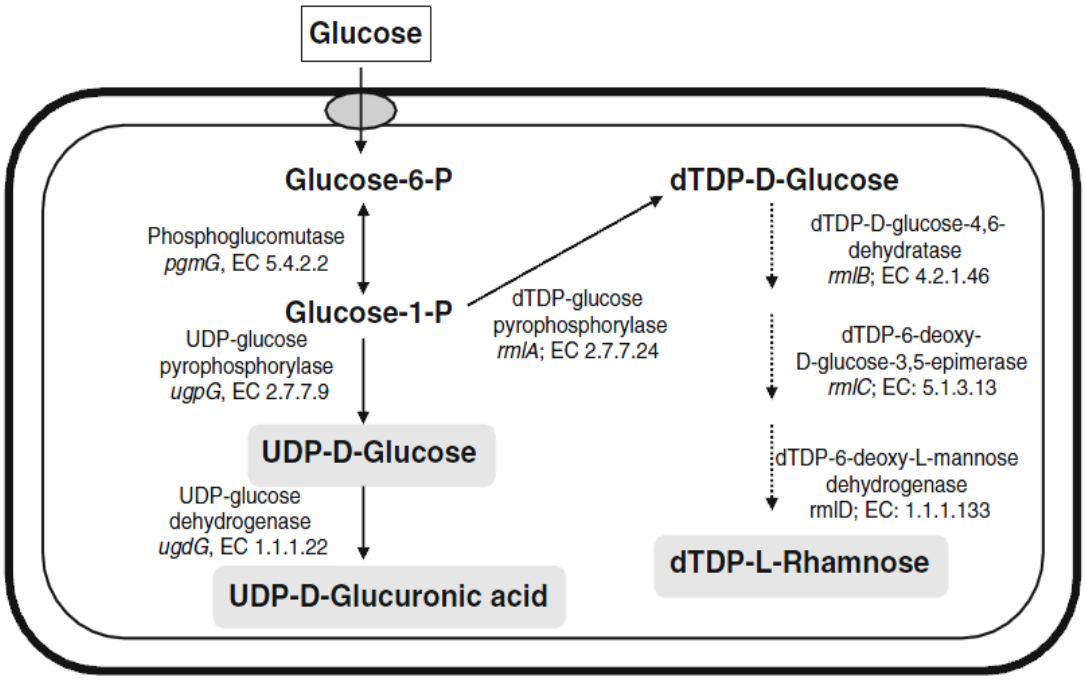

Figure 5. Proposed pathway leading to the nucleotide sugar precursors, UDP-D-glucose, UDP-D-glucuronic acid and dTDP-L-Rhamnose, involved in gellan gum biosynthesis with glucose as the substrate [9].

The synthesis of the sugar precursors is followed by the formation of the repeat units by sequential transfer of the sugar donors to an activated lipid carrier by committed glycosyltransferases. Then, gellan gum polymerization and exportation (Figure 6) are the next steps. Most of these gellan-specific processes are catalyzed by enzymes encoded by the gel cluster of genes that contain at least 22 genes (Figure 6 a) [9,31].

Gellan tetrasaccharide repeat units are assembled on a lipid carrier (Figure 6 step 2). The priming glycosyltransferase is encoded by the gene gelB, which is homologous to spsB from *Sphingomonas sp. ATCC* 31554 [31]. SpsB was demonstrated to be a glycosyl-isoprenylphosphatate transferase that transfers glucose-1-phosphatase from UDP-glucose to the lipid carrier [32]. The addition of the second sugar, glucuronic acid, from UDP-glucuronic acid into the glucosyl-α-pyrophosphorylpolyprenol intermediate is catalyzed by GelK [27]. Pollock and co-workers proposed the gene *sps*L for encoding a glucosyl-(β1–4)-glucuronosyl transferase. Due to the strong homology between *sps*L and *gel*L genes, it is possible that the glycosyltransferase GelL catalyses the addition of the third sugar (glucose) to the repeat unit. Finally, the enzyme that adds the last sugar to the tetrasaccharide repeat unit, rhamnose, is putatively encoded by the remaining gene with homology to glycosyltransferases, *gel*Q [9,31]. The assembly of the repeat unit will only be complete after the addition of the substituent groups, acetate and glycerate, to the first glucose residue. These reactions are catalyzed by two enzymes having acetyltransferase and glyceryltransferase activities, respectively [31].

The next step in polysaccharide biosynthesis is the polymerization of the repeat units to form longer chains. The genes involved in this process of gellan polymerization and the export to the cell surface have been identified and located in the gel cluster region IV and are named *gel*S and *gel*G, respectively. GelS is the translocase of the repeat units and GelG is the polymerase (Figure 6 *b*, *step* 3). The determination of length distribution of the synthesized polysaccharide chains is controlled by a family of proteins termed polysaccharide co-polymerases (PCPs), which interact both with the polymerase enzyme and the secretion machinery. The PCP enzyme in *S. elodea* is encoded by the genes *gel*C and *gel*E. GelE also plays an important role by regulating GelC activity, in fact, GelE seems to have ATPbinding activity. GelC shows the typical PCP N- and C-terminal transmembrane helices separated by a segment with a predicted coiled-coil region located in the periplasm. A computational analysis of GelE structure reveals a potential amphipathic helix at the C-terminal region, which may be involved in the association of GelE to the plasma membrane and, therefore, interacting with GelC [33].

The next step, the exportation of the polysaccharide, is mediated by integral outer membrane proteins from the outer membrane auxiliary (OMA) family, which forms a protein channel through the membrane that allows the polysaccharide to gain access to the cell surface. This exportation process is mediated by the OMA protein homologue encoded by the gene *gel*D in *S. elodea* [34,35].

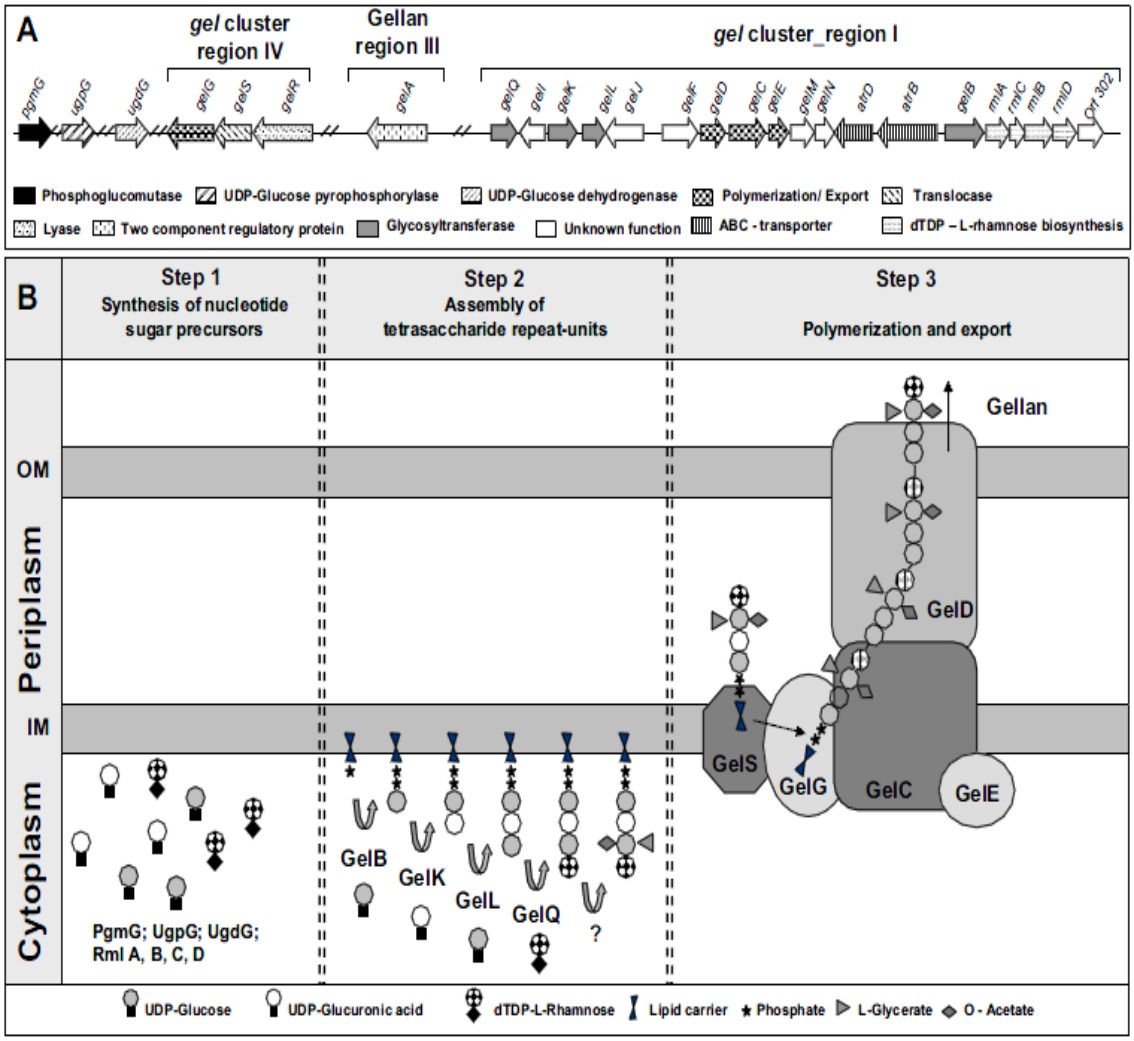

Figure 6. (a) Organization of the gellan biosynthetic *gel* clusters (from *S. elodea ATCC* 31461. (b) A model for biosynthesis and assembly of gellan. Activated sugar nucleotides are sequentially added to a lipid carrier to form repeat units of the polysaccharide. The undecaprenyl pyrophosphate (und-PP)-linked tetrasaccharide repeat unit is assembled at the interface between the cytoplasm and the inner membrane by sequential activity of GelB, GelK, GelL, and GelQ glycosyltransferases. These newly synthesized und-PP-linked repeat units are then translocated across the membrane in a process requiring GelS. These repeat units provide the substrate for GelG polymerization and also require GelC/GelE proteins, possibly by forming oligomers that connect polymerization to export and regulate polysaccharide chain length. Gellan chains are then exported by GelD, which acts as a channel. *IM* Inner membrane, *OM* outer membrane [23].

1.5 Gellan applications

Most polysaccharide´s applications are related to their behavior in aqueous media. Their physical and chemical characteristics, such as water binding capacity, high average molecular weight, polyelectrolyte behavior, molecular structure, and the possibility of being chemically modified, enables this type of molecules to present diverse functional properties like thickening, film forming, gelling, emulsion stabilizing, flocculating and nano/microstructures production abilities [36]. Furthermore, in the case fucose and rhamnose-rich bacterial polysaccharides, they also present interesting biological activities that render these

molecules to be used in a wide range of applications, particularly in added value products like cosmetics, pharmaceuticals, medical devices, and functional food products [37,38]. As examples, rhamnose is commonly used as precursor for the productions of aroma and flavors, and together with fucose has attracted more attraction since it has been found to counteract with several of the mechanism involved in skin aging [39].

In 1992, successful toxicity trials were completed and approval has been granted by the Food and Drug Administration (FDA) in the USA. Gellan gum was accepted to be used as a food additive [40]), and specifications, as summarized in Table 2, were prepared at the 46th Joint Expert Committee on Food Additives (JECFA) in 1996 [18]. Since then, gellan has been used in the food industry as additive that functions, not only as versatile gelling agent, but also as texturizing, stabilizing, suspending, film-forming, and structuring agent. Types of food products that contain gellan gum include bakery fillings, dairy products, low-fat spreads, frostings, icing and glazes, desserts gels, puddings, jams and jellies, sauces, structured foods and toppings [41].

Table 2. Specifications of gellan gum (modified from [18]).

Property	*Value*
Definition	Gellan gum is a high molecular weight polysaccharide produced by a pure culture fermentation of carbohydrates by *Sphingomonas elodea*, purified by recovery with isopropyl alcohol, dried and milled
Molecular mass	Approximately 500 kDa
Description	Off-white powder
Functional uses	Thickening agent, gelling agent, stabilizer, etc
Solubility	Soluble in water, forming a viscous solution, insoluble in ethanol
Loss on drying	Not more than 15 % (105 °C, 2.5 h)
Lead	Not more than 2 mg/kg
Nitrogen	Not more than 3 %
Gel test with calcium ion	Add 1 g of sample, 0.5 g sodium chloride, heat to 80 °C for 1 min. Allow solution to cool. A firm gel is produced
Gel test with sodium ion	To 1 % solution of sample, add 0.5 g sodium chloride, heat to 80 °C and stir for 1 min. Allow solution to cool. A firm gel is formed
Isopropyl alcohol	Not more than 750 mg/kg
Microbial criteria:	
1. Total plate count	Not more than 10,000 colonies/gm
2. *E. coli*	Negative by test
3. Salmonella	Negative by test
4. Yeasts and molds	Not more than 400 colonies/gm

Gellan is commercially available in three forms: no, low, and high acyl content with the respective denominations of Gelrite®, Kelcogel® F, and Kelcogel® LT100. Kelgogels are food-grade gellans used as gelling agents in food and personal care applications (lotions, creams, sunscreens, make-up, face masks, hair care products, air freshener and toothpastes) [42].

In the biotechnology industry, Gelrite® is used as a substituent of agar in plant tissue culture media and it is particularly useful for the culture of thermophilic bacterial species, as the gels are thermostables and can withstand prolonged incubations at high temperatures. In these microbiological media applications, the high purity of gellan gum and the water-like clarity of the gels are distinct additional advantages [43]. It also has potential environmental applications like the biodegradation of gasoline [44] and the transportation of gel-encapsulated cells protected from biotic and abiotic stress, such as predation by protozoa and bacteriophages, and the inhibitory effect of toxic compounds, respectively [45].

In the medicine field, the use of gellan has been investigated for tissue engineering (construction of 3D scaffolds, cartilage reconstruction and guided bone regeneration) and wound healing (in wound dressings to inhibit postsurgical adhesion and scar formation). Gellan sulfate derivatives are promising materials for rheumatoid arthritis, as they have a tendency for selective binding of fibronectin molecules, and for the development of cell-hybrid materials for artificial veins design due to the anticoagulant activity of such derivatives [46].

In pharmaceuticals technology, gellan gum can be used to produce easy-to-swallow solid dosage forms, such as hydrogels, beads and coated tablets, and to modify the rate of release of active ingredients from tablets and capsules. Gellan gum is also conveniently used for controlled or sustained release of various drugs and also for microencapsulating preparation. Formulations based on gellan gum for oral, ophthalmic, gastric, and nasal applications have also been developed [47].

Gells of gellan gum are also used as solid matrix for separation of DNA fragments onto electrophoresis and DNA isolation [48] and, more recently, gellan gum has been applied in the development of a new gel matrix for ionic exchange chromatographic approaches [49].

In summary, we can argue that gellan gum has gained importance among several industries and attracted a considerable market interest, as we can see in Table 3. Due to its unique properties, versatility, stability, biocompatibility, and biodegradability, the large variety of applications as well as the high and steadily increasing number of patents filing, it is suggested that gellan gum has been adopted as one of the most important commercialized bacterial exopolysaccharides and, due to its potential, it will be even more significant in the future [18].

Table 3. Several areas highlighting the utility of gellan gum as a polymer (modified from [18]).

Drug used	*Formulation*	*Action*	*Application*
Clarithromycin	In situ floating gel	Anti-bacterial	Gastric ulcers
Levofloxacin hemihydrates	In situ floating gel	Anti-bacterial	Helicobacter pyroli infections, peptic ulcers
Naproxen	In situ floating gel	Anti-pyretic and NSAID	Rheumatic arthritis, inflammation
Cimetidine	In situ floating gel	H2 receptor antagonist	Peptic ulcer
Acetohydroxamic acid	Floating bead	Anti-bacteria	Helicobacter pyroli infections
Mometasone furoate	Nasal in situ gel	Corticosteroid	Allergic rhinitis
Metoclopramide HCl	Intranasal microspheres	Anti-emetic	Cancer therapy, nausea, vomiting, pregnancy migraine
Glipizide	Gellan gum beads	Hypoglycaemic agent	Diabetes
Gellan gum and beverage or food component	Spherical flavored gel bead	Flavourant	Food industry
Carvedilol	Hydrogel microspheres	Anti-hypertensive	Hypertension, Angina pectoris
Gatifloxacin	Ocular inserts	Fluoroquinolone antibiotic	Bacterial conjunctivitis
Indomethacin	Ophthalmic in situ gel	NSAID	Uveitis, inflammation of eyes
Metformin	Gum cordial/gellan beads	Hypoglycaemic agent	Diabetes
Propranolol	Gellan beads	B-blocke	Hypertension
Paracetamol	Oral in situ gel	-	-
Ascorbic acid	Gellan gum films	Nutritional and antioxidante property	Food industry

2 Chromatography

2.1 Chromatographic process

The development of techniques and methods for protein separation and purification has been essential for many of the recent advancements in biotechnology research. The chromatographic technology is undoubtedly one of the most diverse and powerful purification methods for downstream process applications. The diversity and quantity of biomolecules present in crude extracts as well the similarities between impurities and the target biomolecule are considered the critical challenges in the extraction and purification steps. Thus, the global aim of a protein purification process in not only the removal of unwanted contaminants, but also the concentration of the desired protein and their transfer to an environment where it is stable, biologically active, with a high purity degree and in a form ready for the intended application [50].

Chromatography is widely used due to its simplicity, robustness, high resolving power, versatility, high reproducibility and can be applied in the purification of a large variety of biomolecules [51]. Depending on the physical and chemical characteristics, such as charge, molecular size, hydrophobicity and polarity of each target biomolecule and matrices, several chromatographic techniques ca be used, by exploiting different interactions between the solute in the mobile phase with the stationary phase. There are two mechanisms used for chromatographic separation of proteins: adsorption (ion exchange, hydrophobic interaction, reverse phase and affinity chromatography) and molecular filter chromatography (size exclusion chromatography) [47,50].

Ideally, a chromatographic stationary phase should be selective, macroporous, incompressible, reusable, mechanical and chemically stable with low unspecific adsorption and high binding capacity, present an adequate mass transfer and maintain good flow properties [52].

The solutes can stay in the mobile phase or be distributed in the stationary phase by promoting specific interactions. The stationary phase is packed into a vertical column and should be insoluble in the buffer whereas the mobile phase is pumped through the column. The differential separation occurs due to continuous addition of mobile phase, as known as elution, resulting from alterations on ionic strength and pH or by addition of a competitive agent, causing a sequence of separated peaks that reflect the concentration of biomolecules versus time or volume of eluent at the column exit, which is tipically represented in a chromatogram [53].

The purification of the biomolecule of interest may happen by two different processes. The target molecule can be separated from the contaminants by binding to the stationary phase,

followed by selective elution or by binding impurities, allowing the biomolecule to pass through the column without being retained (negative chromatography) [54].

2.2 Preparative chromatography

Chromatography can be applied in a preparative or an analytical scale [55]. Analytical chromatography aims at separating complex mixtures to identify and quantify the components of mixtures, simple or complex of a small sample. Once the required signals have been acquired for a component, the analyte is discarded. The purpose remains the rapid determination of the component structure, through the direct acquisition of the proper information, and the calculation of its concentration, through calibration of the detector signal. The preparative chromatography aims to isolate and purify the target molecules from impurities using a large amount of sample to be applied in a further goal. However, some concerns remains, like the need to produce as concentrated a fraction as possible, to collect and transfer it without pollution, and to do the separation as quickly and cheaply as possible [56].

In the preparative chromatography, maximum throughput at a high purity is the principal consideration. Therefore, an adsorption/desorption mode is preferred. The process can be divided into several steps: equilibration (adjusting mobile phase and stationary phase to binding conditions); sample application/loading (loading of the sample solution onto the column); washing (removal of unbound material, often with several steps); elution (desorption of the desired compound by stepwise or continuous change of the mobile phase composition); regeneration/cleaning (desorption of sticky impurities, colors, endotoxins and lipids); preservation/sanitation (change of mobile phase to avoid microbial contamination during storage) [55].

2.3 Chromatographic methods

General properties of proteins are used to isolate them from other proteins or non-protein contaminants. Minor differences between various proteins, such as size, charge, hydrophobicity and biospecific interactions (Figure 7) are used to purify the target protein with the application of several chromatographic methods [57].

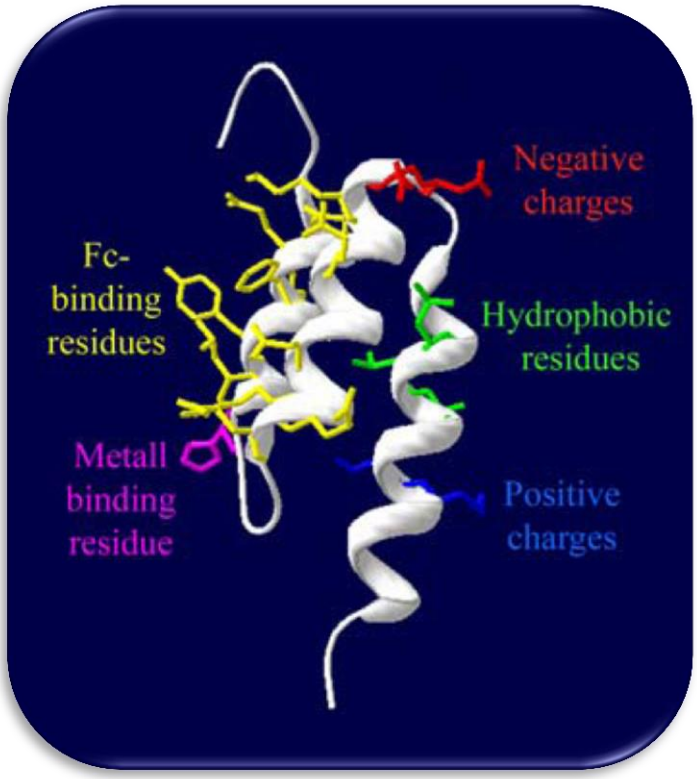

Figure 7. Selective protein properties. Example of properties that are used to separate one protein from another [57].

Currently, several different action principles are employed for chromatography of biomolecules (Table 4). These action principles are gel filtration or size-exclusion chromatography (SEC), ion-exchange chromatography (IEC), hydrophobic interaction chromatography (HIC), reverse phase chromatography (RPC) and affinity chromatography (AC) [58].

Table 4. Action principles in protein purification (modified from [58]).

Name	*Action principle*	*Separation by*
Size-exclusion chromatography	Size exclusion	Molecular size and shape
Ion-exchange chromatography	Ionic binding	Surface charge
Hydrophobic interaction chromatography	Hydrophobic complex formation	Hydrophobicity and hydrophobic patches
Reversed-phase chromatography	Hydrophobic complex formation	Hydrophobicity
Affinity chromatography	Biospecific adsorption/desorption	Molecular structure and chemical structure

2.3.1 Size-exclusion chromatography (SEC)

Size-exclusion chromatography, also designated as gel filtration, is an entropically controlled separation technique that depends on the relative size or hydrodynamic volume and shape of a macromolecule with respect to the average pore size of the packing. With a properly calibrated SEC column, all the statistical average molecular weights of a polymer can be determined, as well as its molecular weight distribution. For protein separations, composite packings particles, such as the Superdex series, are increasing in popularity because of their high pore volume, inertness and small particle size availability [59].

The separation process depends on the different ability of various proteins to enter all, some or none of the channels in the porous beads. Molecules running through a SEC column have to solve a maze which becomes more complex to smaller the molecule is, because small molecules have more potential channels that they can access. On the other hand, larger molecules are, for steric reasons, excluded from the channels, and pass quickly between the beads. The detour through the channels will thus retard smaller molecules in comparison to larger proteins (Figure 8). Although the separation in SEC is generally assumed to be according to its molecular weight, it is more accurate to claim that SEC separation is achieved by the differential exclusion or inclusion within porous particles. The ease of diffusion is dependent on the hydrodynamic volume, which is the volume created by the movement of the molecule in water. The difference between hydrodynamic volume and molecular weight is the shape. Proteins tend to be globular molecules while DNA or polysaccharides tend to be linear molecules. Linear molecules have much larger hydrodynamic volume than globular molecules, so a 10.000 MW DNA molecule will elute much earlier than a 10.000 MW protein [57].

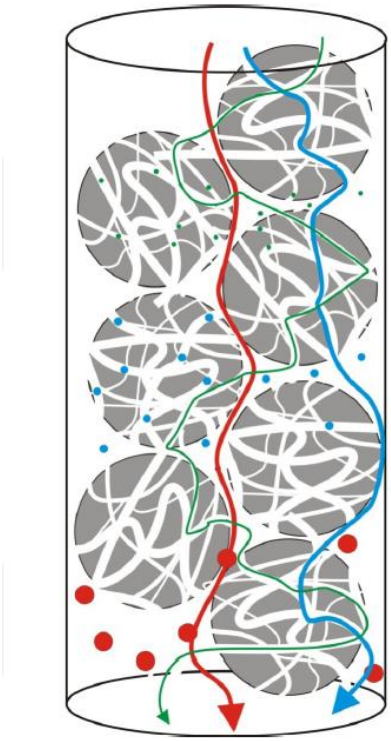

Figure 8. In SEC, large molecules run through the space between media with a shorter pathway, while the smaller molecules run through inside the packing particles with a longer pathway [60].

Sample components are eluted isocratically (single buffer, no gradient) and separation can be performed within a broad pH, ionic strength, and temperature range. The medium accepts a variety of additives: co-factors, protein stabilizers, detergents, urea and guanidine hydrochloride. The buffer composition does not usually affect resolution, although including a low salt concentration, for example 25 to 150 mM NaCl, is recommended to eliminate any weak electrostatic interactions between proteins and the SEC matrix. The buffer conditions are selected to suit the sample type and to maintain target protein activity, because the proteins are transferred to the buffer used for equilibration of the column. Equilibration buffer can thus be selected according to the conditions required for further purification, analysis, storage or use [54].

SEC is a powerful method for purification of proteins that have passed one or several initial purifications steps. After those steps, the material has been concentrated and bulk impurities have been removed. Gel filtration can now be used to remove remaining impurities and it will also remove oligomers or aggregates of the target protein [54]. Therefore, the SEC separation method gives the least resolution with the lowest capacity and largest dilution of the sample with respect to all other forms of chromatography. Still, this technique is frequently used due to its simple performance and some other features not found in other methods. The principal

advantage of SEC is its gentle non-interaction with the sample, enabling high preservation of biological activity. Moreover, since the separation is not dependent on any adsorptive property of the molecule, SEC provides a method for separating multimers that are not easily distinguished by other chromatographic methods.

SEC is a non-binding method, which means that no concentration of the sample components take place. Since separation starts directly as the sample is applied on the column, the cross section must be large enough to cope with the desired sample volume. In fact, the sample zone is broadened during the passage through the column resulting in dilution of the sample [54]. However, the length of the column is also significant since it affects both resolution and process time, thus a relationship between the quantity of injected sample and the column volume (maximum 5 %) must be complied in order to guarantee an efficient separation between the molecules. Consequently, SEC is preferably used as a final polishing step when sample volumes have been reduced [57].

2.3.2 Ion–exchange chromatography (IEC)

Ion-exchange chromatography separates biomolecules according to differences in their surface charge to give separation with high-resolution and high sample loading capacity. The net charge of a protein depends on its amino acid sequence (proteins can have both positive and negative charges) and on the pH of the buffer in which it has been solubilized. At its isoelectric point (pI), the net charge of a protein is neutral. At pH values above this pI, the protein is negatively charged being considered an anion. Therefore, if the matrix has positively charged groups (an anion exchanger) it can be used to purify the protein if the buffer pH is above the pI of the protein. On the other hand, at pH values below the pI, the protein is positively charged, hence, a cation exchange may bind this protein (Figures 9 and 10) [53]. The pH interval in which ion exchange chromatography is carried out is restricted by the pH range in which the protein is stable. To achieve good adsorption, the pH of the buffer chosen should be at least one pH unit above or below the isoelectric point of the analytes to be separated [57].

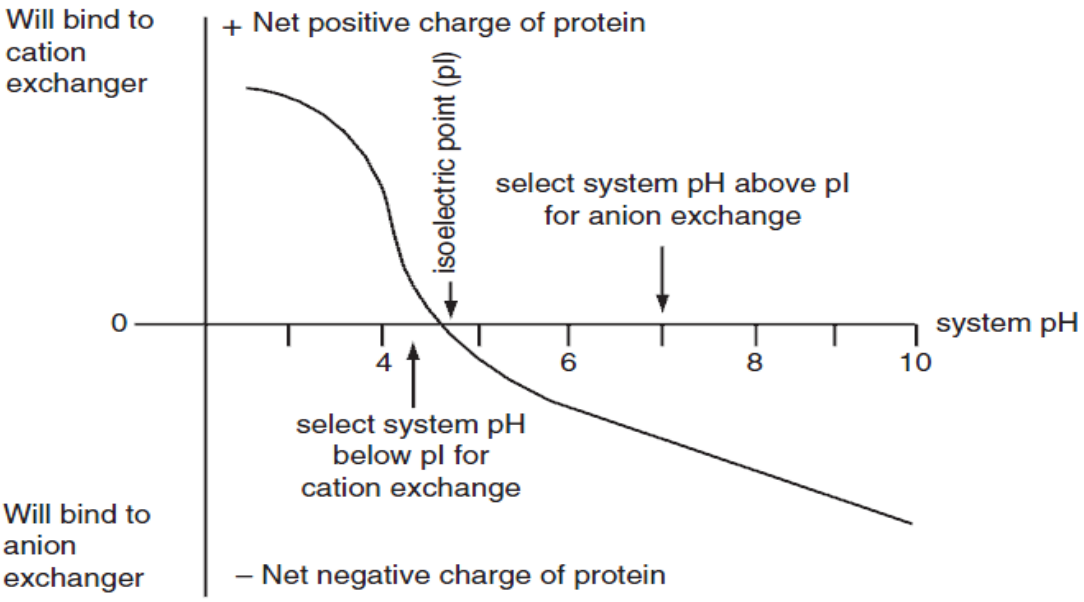

Figure 9. Net charge of a protein as function of pH, showing the pH ranges in which the protein is positively or negatively charged [61].

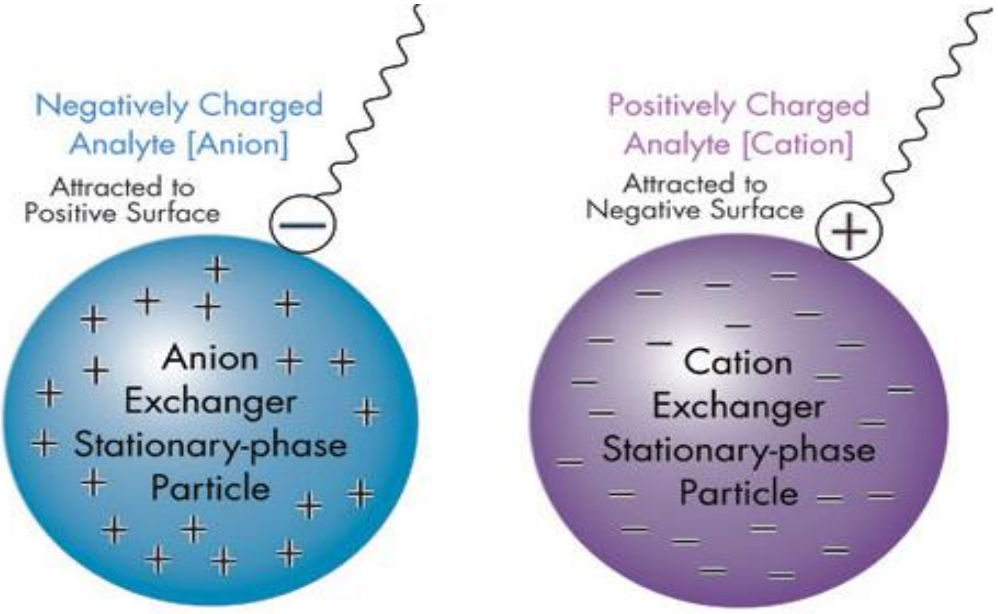

Figure 10. Types of ion exchangers (modified from [62]).

Proteins bind as they are loaded onto a column at low ionic strength and then, the ionic conditions are altered so that bound substances are desorbed differentially. Elution is usually performed by increasing salt concentration or changing pH, in a linear or stepwise gradient.

The most common salt is NaCl, but other salts can also be used to modulate separation, for example, K^+, Ca^{2+}, Mg^{2+}, CH_3COO^-, SO_4^{2-}, I^-, Br^- [54].

IEC is one the more powerful protein purification methodology available and probably the most frequently used chromatographic technique for the separation of proteins, polypeptides, nucleic acids, polynucleotides, and other charged biomolecules. An advantage of this method is that elution normally takes place under mild conditions, so that the protein can maintain its native conformation during the chromatographic process. In general, ion exchangers are more densely substituted than other adsorbents used in protein chromatography and its capacity for protein binding is very high. Its broad specificity also allows the removal of significant impurities such as deamidated forms, endotoxins and unwanted glycoforms. Still, non-specific interactions with proteins due to hydrophobic or other non-ionic interactions are low. Additional reasons for the success of IEC are the straightforward separation principle and ease of performance and controllability of the method. Moreover, ion exchanger resins are very robust and can be sanitized in place and used for hundreds of cycles. The main disadvantage of IEC is its limitation in selectivity [57].

2.3.3 Hydrophobic interaction chromatography (HIC)

Hydrophobic interaction chromatography takes advantage of the hydrophobicity of proteins promoting its separation on the basis of reversible hydrophobic interactions between immobilized hydrophobic ligands and non-polar regions on the protein surface. The adsorption increases with high salt concentrations in the mobile phase and the elution is achieved by decreasing the salt concentration of the eluent (Figure 11) [50]. Therefore, the term “salt-promoted adsorption” could be used for this type of chromatography [63]. The different types of elution conditions can be used for purification of complex mixtures of proteins that would be difficult to separate using other chromatographic techniques. In fact, HIC has been successfully used for separation purposes as it displays binding characteristics complementary to other protein chromatographic techniques [64].

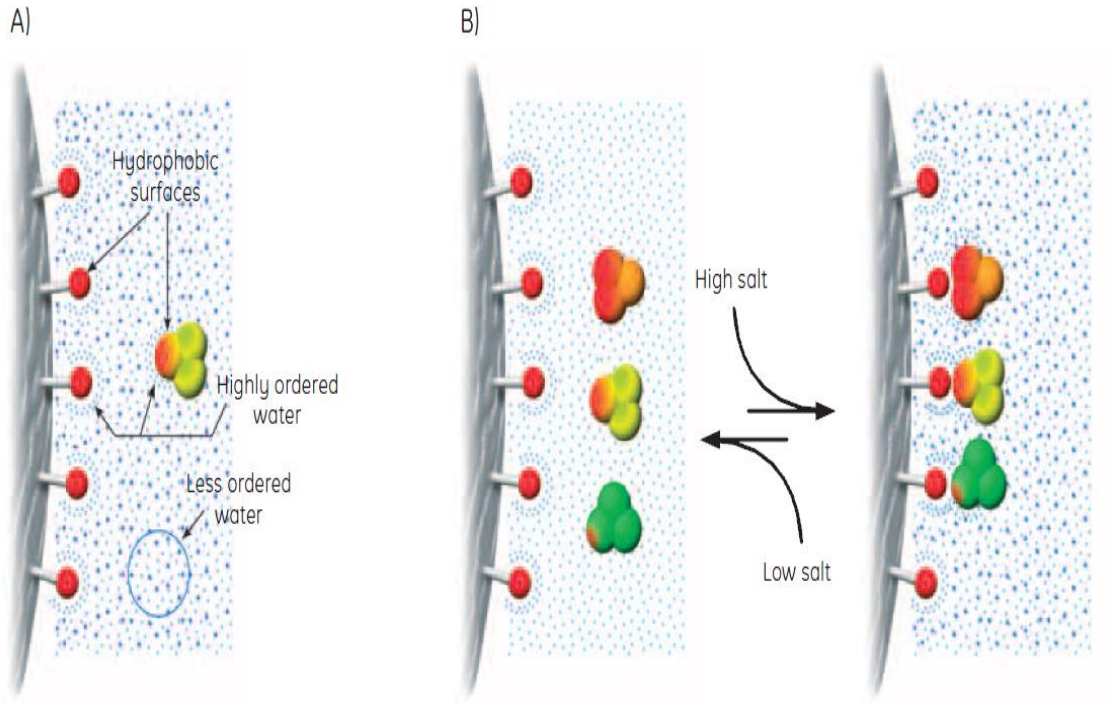

Figure 11. A) Highly ordered water shells surround the hydrophobic surfaces of ligands and proteins. Hydrophobic substances are forced to merge to minimize the total area of such shells (maximize entropy). Salts enhance the hydrophobic interaction. B) The equilibrium of the hydrophobic interaction is controlled predominantly by salt concentration [65].

The hydrophobic ligands on HIC media can interact with the hydrophobic surfaces of proteins. In pure water, any hydrophobic effect is too weak to cause interaction between ligand and proteins or between the proteins themselves. However, certain salts enhance hydrophobic interactions because they remove the hydration water, leaving the hydrophobic groups available to interact, thus, adding such salts, brings about binding (adsorption) to HIC media. For selective elution (desorption), the salt concentration is lowered gradually and the sample components elute in order of hydrophobicity (Figure 11 *B*) [65].

Hydrophobic interaction chromatography can be used for capture, intermediate to other techniques or as polishing steps in a purification protocol. It allows the protein separation that differs in one amino acid residue, separating a native protein from incorrectly folded proteins. The structural damage to the biomolecule is minimal, certainly due to the stabilizing influence of salts. Still, recoveries are often high. Thus, HIC combines the non-denaturating characteristics of salt precipitation and the precision of chromatography to yield activity recoveries. Therefore, at laboratorial and industrial scales, the biomolecule purification such as serum proteins, nuclear proteins, recombinant proteins, membrane proteins, enzymes, and hormones is extremely performed by HIC [66].

2.3.4 Reversed-phase chromatography (RPC)

Reversed-phase chromatography separates molecules according to differences in their hydrophobicity. In theory, HIC and RPC are closely related techniques since both are based upon reversible interactions between hydrophobic patches on the surface of biomolecules and the hydrophobic surfaces of a chromatography medium. However, in practice, the techniques are very different. The surface of an RPC medium is usually more hydrophobic than that of a HIC medium. This leads to stronger interactions that, for successful elution, must be reversed using non-polar, organic solvents such as acetonitrile or methanol (Figure 12). HIC media offers an alternative way of exploiting the hydrophobic properties of the biomolecules by working in a more polar and less denaturing environment [65].

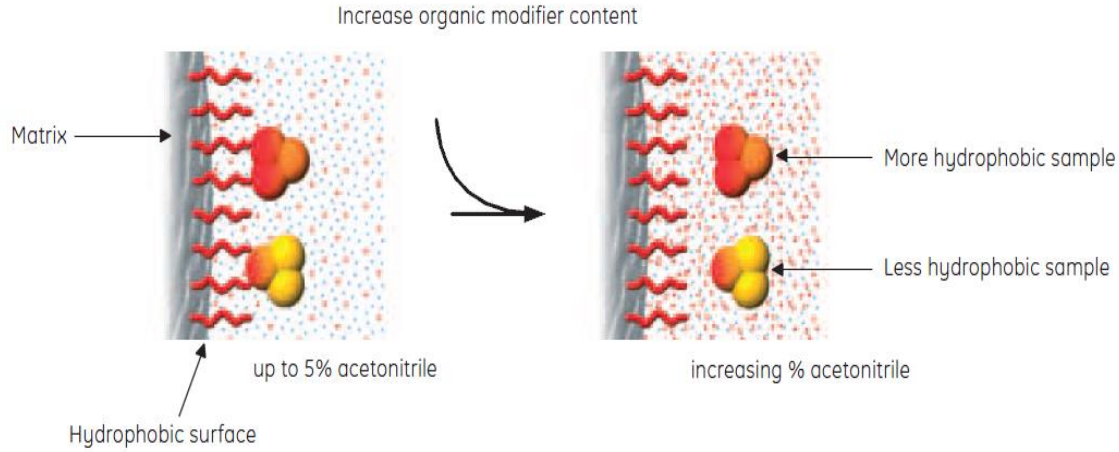

Figure 12. Proteins and peptides bind to an RCP medium under aqueous conditions and elute as the eluent becomes more hydrophobic [54].

Separation relies on the sample molecules existing in an equilibrium between the eluent and the surface of the medium. The distribution of the sample depends on the properties of the medium, the hydrophobicity of the sample and the composition of the eluent (mobile phase), as illustrated in Figure 12. Initially, conditions favor an extreme equilibrium state where essentially 100% of the sample is bound. Since proteins and peptides carry a mix of accessible hydrophilic and hydrophobic amino acids and are rather large, the interaction with the medium has the nature of a multi-point attachment. To bring about elution, the amount of organic solvent is increased so that conditions become more hydrophobic. Binding and elution occur continuously as sample moves through the column. The process of moving through the column is slower for those samples that are more hydrophobic. Consequently, samples are eluted in order of increasing hydrophobicity [65].

RPC is a high-resolution method and is widely used for purity check analysis when activity and tertiary structure are not a focus. Because many proteins are denaturated by organic solvents, this technique is not generally recommended for preparative protein purification because the recovery of activity and native tertiary structure is often compromised. Proteins tend to denature and bind strongly to the RPC medium, making elution very difficult to achieve. However, due to its high resolving power, in the polishing phase, when the majority of protein impurities have been removed, RPC is excellent, particularly for small target proteins that are less commonly denaturated by organic solvent [67].

2.3.5 Affinity chromatography (AC)

Affinity chromatography (AC) is a type of adsorption chromatography in which the molecule to be purified is specifically and reversibly adsorbed by a complementary binding substance (ligand) immobilized on an insoluble support (matrix). AC involves the formation of a reversible complex between the target protein with the ligand and it can be applied to a wide variety of macromolecule-ligand systems. The target protein from the crude extract interacts with the immobilized ligand and remains bound; the other constituents of the crude extract (contaminants) are removed. In some cases, a "*spacer arm*" is introduced between the ligand and the matrix to improve binding conditions (Figure 13). Desorption of the bound target molecule is generally accomplished by a non-specific elution method (changing, for example, pH, ionic strength, or polarity) or using, under mild conditions, a competitive ligand [68].

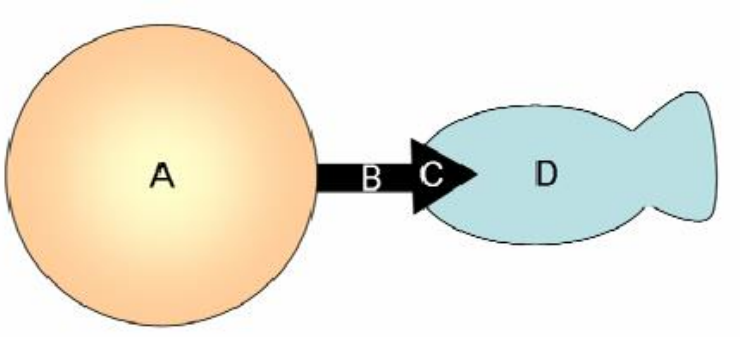

Figure 13. An affinity matrix binding to its target protein. A - the bead; B - the space arm; C - the ligand; D - the target protein [57].

The recognition that occurs between two complementary molecules, such as enzyme-substrate or antigen-antibody, is due to the involvement of several interactions. An immobilized natural ligand is covalently attached to an inert chromatographic matrix and

specifically interacts with the desired protein. The binding can involve a combination of electrostatics or hydrophobic interactions as well as short-range molecular interactions such as Van der Walls forces and hydrogen bonds [53].

The stationary phase must possess suitable chemical groups to which the ligand can be covalently coupled and have a relatively large surface area available for attachment. It must also be inert in solvents and buffers that are employed in the process, which can be harsh, especially during elution of the protein. Hydrophilic and neutral matrices are preferred and they should be macroporous to accommodate free interaction of large proteins with the ligands, but also exhibit good flow properties [57].

The immobilized ligand is the key factor that determines the success of any affinity chromatographic method. Ligands can be extremely selective and bind to only one single or a very small number of proteins. Examples are antibodies, protein receptors, steroid hormones, vitamins and certain enzyme inhibitors. The ligand normally is a synthetic molecule that is stable, safe, inexpensive, provides high selectivity and is compatible with the solvents used during the couple procedure. It is essential that the ligand possesses, at least, one functional chemical group by which it can be immobilized to the matrix. The most common of such groups are amines thiols, carbohydroxides and hydroxyl groups [68].

To facilitate the access and recognition of the target protein by the ligand, it is generally advantageous to interpose a spacer arm between the ligand and the matrix (Figure 13). In this way the ligand is distanced from the surface of the matrix which reduces steric hindrance of the binding that can occur when the ligand is bound directly to the bead. Spacer arms should neither chemically or structurally affect the sample or the ligand [69].

AC is a high resolution purification technique that simplifies the isolation process by using pre-existing ligand-binding relationship that is developed to be highly specific. As a consequence, affinity chromatography is capable of giving very high purification power, even from complex mixtures, in one simple process step. Moreover, the ligand may be reutilized for multiple experiments and this method only requires short periods of time of execution. Other advantage of affinity chromatography is its broad range of applications for protein purification, like immunoaffinity, purification of immunoglobulins, glycoconjugates, DNA-binding proteins, receptor proteins, enzymes and isolation of cells and nucleotides [57].

2.3.5.1 Immobilized metal-ion affinity chromatography (IMAC)

Considering the nature of the ligand, there are several types of affinity chromatography. The immobilized metal-ion affinity chromatography (IMAC), also named as metal-chelate chromatography, is a type of AC. It is based on the interaction of proteins with histidine

residues (or Trp and Cys) on their surface with divalent metal ions (Ni^{2+}, Cu^{2+}, Zn^{2+}, Co^{2+}) immobilized via a chelating ligand (Figure 14). Amino acids are especially suitable for binding and histidine is the one that exhibits the strongest interaction, as the electron donor groups on the imidazole ring in histidine readily form coordination bonds with the immobilized transition metal. The histidine-tagged proteins have an extra high affinity in IMAC because of the multiple (6 to 10) histidine residues and are usually the strongest binder among all the proteins in a crude sample extract (for example a bacterial lysate), while other cellular proteins will not bind or will bind weakly [54].

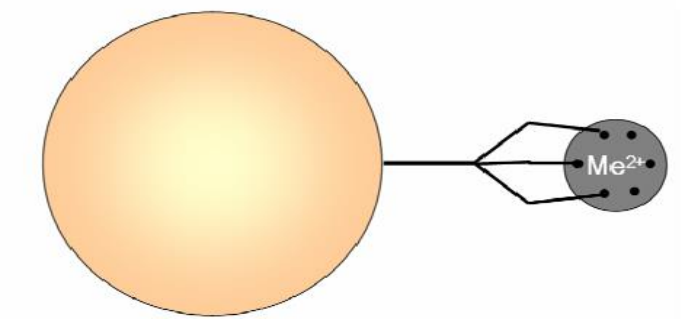

Figure 14. A bead of a typical IMAC matrix with an attached chelator that coordinates a metal ion [57].

The requirements of the support in IMAC are the same as applied to affinity chromatography: easy to derivatize, exhibit no unspecific adsorption and have good physical, mechanical and chemical stability. A suitable spacer arm, plus a simple chelator, is attached to the matrix (Figure 14). Some commonly chelators are imino diacetate (IDA), nitrotriacetic acid (NTA) and tris(carboxylmethyl) ethylene diamine (TED). Electron-donor atoms (N, S, O) present in the chelators are capable of coordinating metal ions and forming metal chelates. The affinity of a protein for a metal chelate strongly depends on the metal ion involved in coordination. Compared to other affinity separation technologies, IMAC cannot be classified as highly specific, but only moderately so. However, benefits like ligand stability, high protein loading, mild elution conditions, simple regeneration and low cost makes this method highly useful for recombinant protein [57].

2.4 Matrices and ligands

The structure of chromatographic supports has been continuously developed to afford rapid and efficient separations, as well as, the application of specific ligands to improve the selectivity for the target molecule. As stated above, the support format should ideally be

solid, macroporous, hydrophilic, insoluble in the solvent, chemical and physically stable, exhibit low nonspecific adsorption with high binding capacity and mass transfer, and maintain good flow properties throughout the process. Consequently, the stationary matrix must be incompressible, inexpensive, simple to use, reusable in several chromatographic runs, and stable to sanitization by alkaline conditions [52].

2.4.1 Chemical features of chromatographic supports

In general, the chemical composition of chromatographic supports determines the preferential interactions established with the target molecule, allowing its retention whereas undesirable molecules are eluted. In this way, the chemical nature of the functional groups will determine the chromatographic action principles that will be reflected in the effectiveness of the purification steps [76,77].

The possibility to perform chemical modifications or to immobilize specific ligands on the surface of the chromatographic supports should result in an increased stability of the matrix and in the improvement of the established interactions. On the other hand, the physical and structural characteristics of the solid supports will determine the availability and accessibility of the functional groups to the target molecules [51].

The balance between the structural shape and the number of available binding sites is required to take advantage of a high binding capacity and productivity. Therefore, the combination of the ideal chemical and structural characteristics of the chromatographic matrices can result in a suitable purification process to obtain pharmaceutical-grade biological samples for therapeutic applications [51].

The constituent material of chromatographic supports can be classified, according to the chemical properties, in natural polymers, synthetic polymers, inorganic material and composite material (Table 5). Several chromatographic supports with different structural and physical properties have been used in purification (Figure 15) [51].

Table 5. Examples of different basic material constituents of chromatographic supports applied in purification (modified from [51]).

Category	*Basic material*	*Physical shape*	*Trade name*
Natural polymer	Cellulose	Fibrous cross-linked	CELBEADS
	Nitrocellulose	Fibrous	-
	Dextran	Particles	Sephacryl S
		Particles cross-linked	Sephadex G
	Agarose	Particles	Sepharose 4B
Synthetic polymer	Polyacrylamide derivate	Cryogel	Trisacryl or Hyper
	Polymethacrilate	Porous continuous bed	CIM
	Polystyrene	Microparticles	-
Inorganic material	Hydroxyapatite	Porous crystal	-
	Silica	Particles	-
	Glass	Coated with polystyrene	-
Composite material	Methacrylate + cryogel	Supermacroporous	PHEMAH

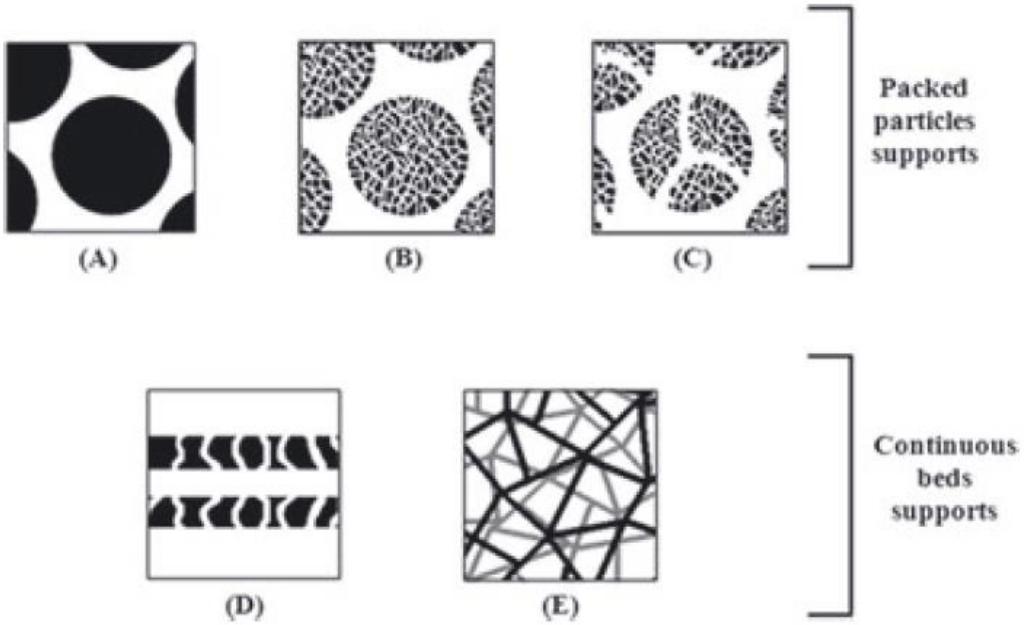

Figure 15. Schematic representation of the physical and structural properties of the constituent materials of different chromatographic supports. (A) Diffuse nonporous particles; (B) Diffuse porous particles; (C) Perfusion superporous particles; (D) Two stacked membranes sheets; (E) Monoliths [51].

2.4.2 Physical and structural features of chromatographic supports

Physical characterization of the support material in terms of its particle size, pore size, pore volume and pore surface will help in determining the mass transfer rate of solutes within the chromatographic bed and its effective ligand binding capacity [72].

The ideal features of a medium suited for protein chromatography are summarized in Table 6. It is often not possible to reconcile all features and, therefore, compromises have to be searched. The chemical nature of proteins determines the surface properties of the media, while the large size of proteins determines its physical properties. First of all, a large surface is requested to get a high binding capacity [58].

Table 6. Features of media suited for protein chromatography (modified from [58]).

Feature	*Dimension*
Surface area (m^2/cm^3)	10 - 400
Functional group (μmol/cm^3)	1 - 100
Porosity (εP):	
Non-porous	0
Porous	0.25 - 0.75
Pore size (nm):	
Conventional	10 - 100
Monolith	1000 - 5000

Pore dimension is correlated with the exclusion limit, which defines the size range of molecules that can enter or be excluded from the pore. Hence, for an adequate chromatographic support, the size of the pores should be at least five times larger than an average size of the target biomolecule for its easy access to immobilized ligands inside the pore, increasing the binding capacity. In reality, the pore size of a matrix is inversely correlated to its surface area, which in turn directly affects the amount of immobilized ligand and, thus, the binding capacity [73].

The non-porous particles are more useful for quality control, on-line monitoring and purity evaluation of biomolecules than for preparative purposes. They allow quick separations and analysis with high efficiency because the mass transfer resistance and intraparticulate diffusions are eliminated. The absence of internal pore structure allows good recovery, avoiding conformational changes of the biomolecules. However, the column loading capacity is relatively low due to small surface area of the particles. The porous particles overcome some limitations of the non-porous particles. They increase the surface area and, consequently, they increase the binding capacity. Porous particles allow faster mass transfer and higher flow rates by maintaining an efficient capture. The superporous particles, also named perfusion particles, contain a network of large through-pores that allow intraparticle mass transport by molecular convection, improving the effect of mass transfer resistance resulting from the mobile phase stagnated inside the pore. The application of superporous materials in chromatography leads to lower efficiency loss with increased flow rate without sacrificing resolution [58].

Membrane technology is often used for filtration, to concentrate samples, to separate large molecules from small ones, and also in downstream processes to remove cell debris. Thereby, membrane adsorbers arise as potential supports for enhanced chromatographic resolution, efficiency and productivity. Membranes are very thin layers, therefore, scale up is not possible while preserving this structure, however, they can be stacked to provide additional volume and, consequently, improve capacity. Membranes can also be considered as monoliths due to the extreme geometry, but the dimension of the axial direction is very short, since they are used as a single sheet. The structural appearance of the monolith disks resembles several stacked membrane sheets, but in reality they are polymerized directly into a column as a single unit. In this way, some problems, like air bubbles, are eliminated. This monolithic method allows fast separations with higher mass transfer at low pressure and the columns are characterized by specific permeability resulting from their morphological and physical properties. This fact allows high surface availability, accessibility and uniform frontal migration throughout the support. Owing this remarkable characteristics, monoliths have the ability to maintain both resolution and capacity, independently of the flow rate [51].

2.4.3 Ligand features on chromatographic supports

The preparation of appropriate supports for specific chromatography requires the immobilization of ligands with restricted desired characteristics, either to porous or nonporous material. The association of adequate ligands with solid supports takes advantage of higher selectivity and specificity for the target biomolecule, allowing an efficient and directed purification [51].

To be stable, the ligand should be covalently coupled to the support by some functional groups that can be easily and conveniently derivatized. For an ideal activation/coupling chemistry, it must have desirable characteristics such as (1) rapid, efficient formation of a stable, uncharged, covalent bond under mild conditions with no side reactions, (2) easy blocking of residual activated groups with simple, hydrophilic, uncharged groups and (3) use of inexpensive, non-toxic reagents in procedures which can be scaled up [72].

General ligands can be classified as biological (natural) (examples are nucleotides, lectins, protein A and protein G) or non-biological (synthetic), such as dyes, metals, and amino acids. Natural ligands have high specificity, however, the high specificity means low dissociation constants and stronger elution buffers. Moreover, they are often unstable and so its use is limited at ambient or high temperatures or under harsh conditions. Synthetic ligands are robust and not susceptible to denaturation. They are also more stable under strong elution conditions and more cost effective than their biological counterparts [72].

The ligand immobilization procedure consists on activating the matrix to make it reactive with the ligand functional group. Then, the ligand is covalently coupled to the matrix and unreacted groups are blocked by low molecular weight substances, such as etholamine [53]. When small ligands are immobilized, a spacer arm between the ligand and the matrix should be introduced to increase the ligand availability and reduce steric hindrance [74].

2.5 Dynamic binding capacity

One way to characterize and accomplish the applicability and potential use of a new chromatographic support for a specific purification purpose is by determining the dynamic binding capacity (DBC) under optimized conditions. High DBC is especially important for obtaining high yield of the target protein on a preparative scale, where productivity is essential [75].

This parameter reflects the impact of mass transfer limitations that may occur when the flow rate is increased. Besides, the performance of protein-ligand adsorption can be characterized by this parameter. DBC of a chromatographic support predicts the amount of target protein in the solution that will bind under adequate binding and flow conditions before significant breakthrough of unbound protein is achieved. The breakthrough curve can be used to determine how much of column capacity has been used, how much protein has been wasted during the adsorption phase, the processing time or applied volume, and the production rate [76].

Dynamic binding capacity values are obtained by subtracting the value obtained under non-binding conditions, according to the following equation (Equation 4):

$$\mathrm{DBC} = \frac{(\mathrm{VL} - \mathrm{V0}) \times \mathrm{Cp}}{\mathrm{Vc}} \quad (4)$$

where DBC is the dynamic binding capacity (mg/mL), VL corresponds to the volume loaded up to the breakthrough point (mL), V0 is the void volume of the column (mL), Cp corresponds to the concentration of protein (mg/mL) and Vc is the volume of the columns (mL) [49].

The binding capacity of the support is directly proportional to its surface area and, consequently, is affected by the amount of immobilized ligand. The larger is the surface area, the greater is the amount of immobilized ligands. On the other hand, surface area increase with decreasing porous size. All these parameters are important for evaluating the application of a new matrix in purification processes [51].

2.6 Chromatographic supports for protein purification

As seen in section 2.4.1, the chemical nature of the functional groups will determine the chromatographic matrix action principles, such as the medium charge, that will be reflected in the effectiveness of the purification steps [76,77].

Over the last several decades, the evolution of ion-exchange media accompanied the development of stationary phases. The driving force for development of new media has been the need for better mechanical stability, reduced tendency to unspecific adsorption, higher binding capacity, and accelerated mass transfer [77].

A strategy for the development of new materials must balance the contradictive physical characteristics on the chromatographer´s wish list: large particles allow a low-pressure drop but slow mass transfer kinetics due to long diffusional pathways through the porous network of the bead. Large pores enable fast mass transfer but reduce the available surface area and, thus, the equilibrium capacity. Mechanical stability also suffers from oversized pores [78].

The chemical composition of the stationary phase (natural or synthetic polymers, inorganic materials) places intrinsic limits for the preparation of porous spherical materials. Traditionally, common stationary phases in chromatography of biomolecules are tipically composed of a bead-shaped matrix comprising liquid filled pores [78].

A variety of materials has been used in the design of chromatographic matrices. Among these, the most common are polysaccharides (cellulose, dextran, and agarose), synthetic organic polymers (polyacrylamide, polymethacrylate, polysterene), and inorganic materials (silica, hydroxipatite). To produce a mechanically stable and functional matrix, the materials are chemically cross-linked and provided with a functional ligand. The physical and chemical conditions of the raw materials present in the production (solvents, concentration of base materials and cross-linkers, temperature, etc.) determine the properties of the stationary phase. Particles sizes of such media range from 2 μm for analytical purposes up to about 200 μm for low-pressure preparative applications. Pores sizes are in the range of 10-100 nm. In many cases, chromatographic media exhibit a typical size distribution of both particles and pores [77]. A selection of several ionic exchangers commonly used in IEC for the separations of proteins is given in Table 7.

Table 7. Chromatographic supports used in IEC (modified from [77]).

Stationary phase	*Base matrix*	*Mean particle diameter*	*Mass transport mechanism*	*Typical application and features*
SP Sepharose fast flow	Cross-linked agarose	90	Pore diffusion	Preparative protein capture
Capto S	Highly cross-linked agarose with flexible dextran surface extender	90	-	Preparative protein capture; salt tolerant, very high capacity
UNOsphere rapid S	Polyacrylamide network	80	Parallel diffusion (pore and surface diffusion)	Preparative protein capture; very high capacity
S-HyperD M	Ceramic shell filled with polyacryalamide soft gel	80	Surface diffusion	Preparative protein capture; very high capacity
CIM SO_3	Polymethacrylate monolith	1 - 2	Convective mass transport	Ultrafast analytical separations
Fractogel EMD SO3 – M	Polymethacrylate with Polyacrylamide surface extender	65	-	Preparative protein capture; salt tolerant, very high capacity
POROS HS	Polystyrene-divinylbenzene with through pores	50	Pore diffusion, convective mass transport	Preparative protein purification, improved purificaiton
Source 30 S	Polystyrene-divinylbenzene monobeads with hydrophilic coating	30	Pore diffusion	Preparative protein purification, iproved resolution
Toyopearl SP-650 M	Polymethacrylate	65	Pore diffusion	Preparative protein capture
GigaCap S	Polymethacrylate with flexible polymeric surface extender	65	-	Preparative protein capture; salt tolerant, very high capacity

All these materials present advantages and disadvantages for a purification process. For example, some materials develop good selectivity by the target biomolecule but also poor flow properties, or in other cases, lost the binding capacity. The ideal chromatographic support should be biocompatible with low nonspecific adsorption, physically stable and simple to use in order to maintain good flow properties and to be reusable in several chromatographic runs [49].

Gellan gum is an anionic polymer and has some properties that are important in a chromatographic matrix, including porosity, hydrophilicity, low unspecific adsorption, high binding capacity and negative charge to establish ionic interactions with positively charged biomolecules [12,51,52]. Since in the presence of metallic ions, gellan gum forms clear gels resistant to temperature and extreme acidic conditions, it can be used as a low-cost and easy production chromatographic stationary phase and, taking into account that gellan has negative charge, it can be applied in cation exchange chromatography to separate and purify proteins and biopharmaceuticals [49].

After showing great potential to become a chromatographic matrix and presenting some advantages such as biodegradation, biocompatibility and low-toxicity, Gonçalves and co-workers studied the behavior and applicability of gellan gum as a chromatographic gel matrix [49]. However, gellan gum gels presented some disadvantages. Gellan gel often loses its stability, its integrity and is not reusable after several chromatographic runs, since it presents poor flow properties [49].

To eliminate these disadvantages, an optimization of the physical and structural properties of gellan gum as a chromatographic support for protein purification is necessary in order to increase its stability, its integrity and improve flow characteristics.

2.7 Preparation of microbeads by water-in-oil emulsion

One of the common production methods for polymeric microparticles is the emulsion technique. An emulsion is a two-phase system of two immiscible liquids with one of the liquid being dispersed as small spherical droplets in the other liquid. Emulsions can be conveniently classified according to the relative spatial distribution of the different phases. An emulsion consisting of oil droplets dispersed in an aqueous phase is referred to as an oil-in-water (O/W) emulsion (milk, ice-cream, dressings, mayonnaise, beverages, soup and sauces) (Figure 16), while a system presenting water droplets dispersed in an oil phase is considered as a water-in-oil (W/O) emulsion (butter, margarine and some spreads). The liquid that makes up the droplets is usually referred to as the “dispersed phase” or “discontinuous phase whereas the material that makes up the surrounding liquid is known as the “dispersing phase” or “continuous phase” [81].

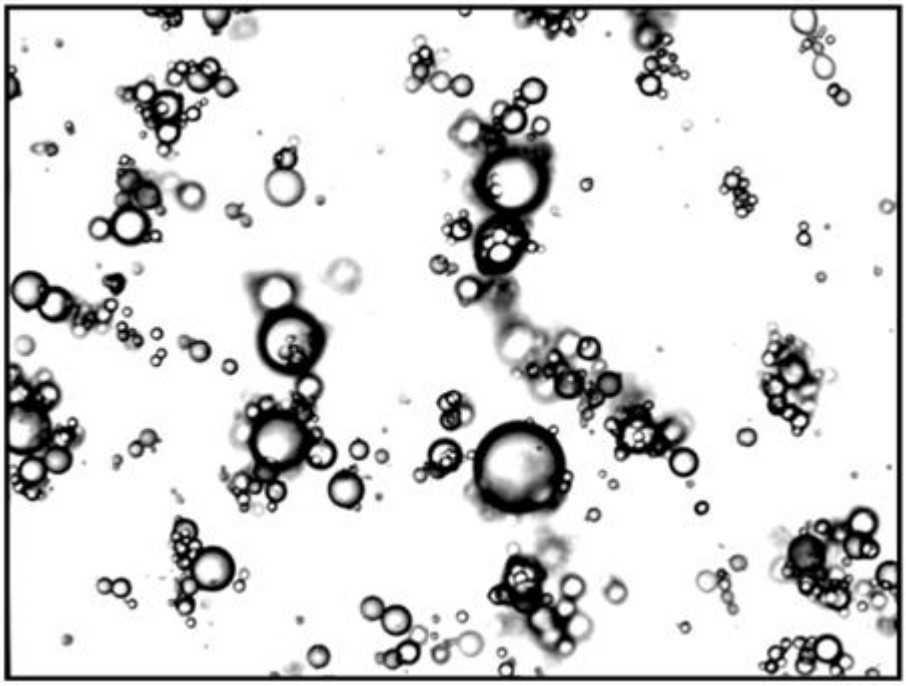

Figure 16. Photomicrograph of a polydisperse oil-in-water emulsion consisting of oil droplets in a continuous aqueous phase. There is evidence of droplet flocculation in this system [82].

The process of converting bulk oil and bulk water into an emulsion, or of reducing the size of the droplets in an already existing emulsion, is known as "homogenization". It is achieved by applying an intense mechanical agitation to the liquid mixture. However, it can occur flocculation (Figure 16), which is the process whereby two or more droplets "*stick*" together to form an aggregate. Nonetheless, each of the initial droplets retains its individual integrity. Moreover, two or more droplets can merge together to form a single larger droplet, in a process denominated coalescence [82].

Gelation of polysaccharides by association of chains into ordered junction zones involves a massive loss of conformational entropy, which must be more than balanced by enthalpically favorable interactions (non-covalent bonds) between the participating strands. When the chains are charged, intermolecular electrostatic repulsion presents a further barrier to close packing. Network formation by anionic polysaccharide often requires neutralization of screening of charge by appropriate cations, therefore, in the emulsion method, it is used a reinforcement solution where the microspheres can be stabilized. This solution contains a high density of positively charged cations, which, due to the complexation between oppositely charged species, allows the formation of a more rigid network with higher tensile strength [83]. Moreover, with an increase in ion density, smaller microspheres are produced due to the formation of a more rigid network as a result of increased cross-link density [84].

The most direct way in which counter-ions can promote association is by incorporation as an integral part of the intermolecular assembly in an "*egg-box*" model, which involves arrays of site-bound cations sandwiched between the polymer chains [85].

The counter-ions used can be divided into two major categories: low molecular weight counter-ions ($CaCl_2$, $BaCl_2$, $MgCl_2$, $CuCl_2$, $ZnCl_2$, $CoCl_2$) and high molecular weight ions (octyl sulphate, lauryl sulphate, hexadecyl sulphate, cetylstearyl sulphate) [86].

Due to its characteristic properties of temperature-dependent and cation-induced gelation, gellan gum allows the preparation of microbeads which can have multiple utilities, such as being used as microparticles in controlled drug delivery systems [87].

2.8 Experimental design

The water-in-oil emulsion technique is one of the methods used in production of biomicroparticles, however, it is necessary to control the process parameters, such as stirring velocity, temperature and polymer concentration. Therefore, the optimization of these parameters is a topic of central importance in laboratory research and industrial scale, with particular attention to biotechnological production processes, in which a small improvement can be critical for commercial success [88].

The optimization of various conditions is laborious, tedious, time-consuming and can lead to misinterpretation of results when performed by using conventional techniques such as one-variable-at-a-time (OVAT) method. This kind of conventional design techniques does not depict the interactive effects among the variables, not guaranteeing the determination of the most favorable conditions [89].

The need to maximize the efficiency of scientific experimentations, in order to minimize waste and cost, has caused researchers to do a set of experiments that give the most information possible with the fewest assays performed. These limitations can be eliminated by employing specific design of experiments (DoE), a structured and efficient methodology for planning experiments such that statistically valid relationships between factors affecting the bead production and its outputs can be established. This method is a time-saving technique and minimizes the error in determining the effect of the parameters involved. It can be used at various phases of optimization process, such as for screening experiments or variables and for finding optimum conditions for a desired response [90].

In the DoE method, the user has to define the factors of study (normally two to four factors) like temperature, pH, flow rate, composition of mobile phases or gradient parameters. Then, the minimum and maximum values for each factor in the experimental domain should be set.

These values represent the design levels needed to establish the group of experiments to be done. One of the design used to determine the response surface is the central composite design (CCD), which is commonly used for optimization with great efficiency [91].

The CCD is a very efficient and the most popular class of design used for fitting the second-order model. This CCD is so named because it combines a two-level factorial design with a star design and center points. The star and factorial points can lie equidistant from the center (Figure 17), can lie within the space of the factorial design or they can also lie on the faces of the factorial design points (faced) [91].

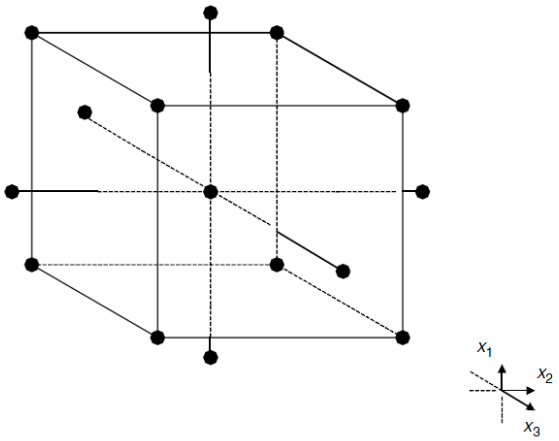

Figure 17. Central composite design for three factors. Each point represents the factor values for one experiment (run) [92].

This design consists in a 2^k factorial with n_F runs, 2k axial or star runs, and n_C center runs, where k is the design order, n_C the number of center points and n_F the number of factorial points. It is important, in a second-order model, to provide good conditions throughout the region of interest. For that, it is necessary to require the model to have a reasonably consistent and stable variance of the predicted response at the points of interest [93].

Rotatability is an adequate basis for the selection of a response surface methodology (RSM) design. Since the purpose of the method is the optimization and the location of the optimum conditions that are unknown prior to running the experiment, it makes sense to use a design that provides equal precision and estimation in all directions. The CCD is made rotatable by the choice of α value, which depends on the number of points in factorial portion of the design. In fact, $\alpha = (n_F)^{1/4}$ yields a rotatable central composite design where n_F is the number of points used in the factorial portion of the design [94].

RSM is a collection of statistical and mathematical methods that are useful for modeling and analyzing problems in which a response of interest is influenced by several variables. The

objective is to optimize the response, to develop a mathematical model of a second-order response surface with the best fit, to determine the optimal set of experiments parameters that produce a maximum or minimum value of response, and to represent the direct and interactive effects of the process parameters through two and three-dimensional (3D) plots. If all variables are assumed to be measurable, the response surface can be expressed as follows:

$$y=f(x_1,\ x_2,\ldots,\ x_k) \qquad (1)$$

where y is the answer of the system, and x_1, x_2,…, x_k are the variables of action called factors. This response is characterized by a geometric representation obtained when a response variable is plotted as a function of the quantitative factors (Figure 18). The counter plots are a series of lines and curves that identify values of factors for which the response is constant, corresponding to a particular height of the response surface [92].

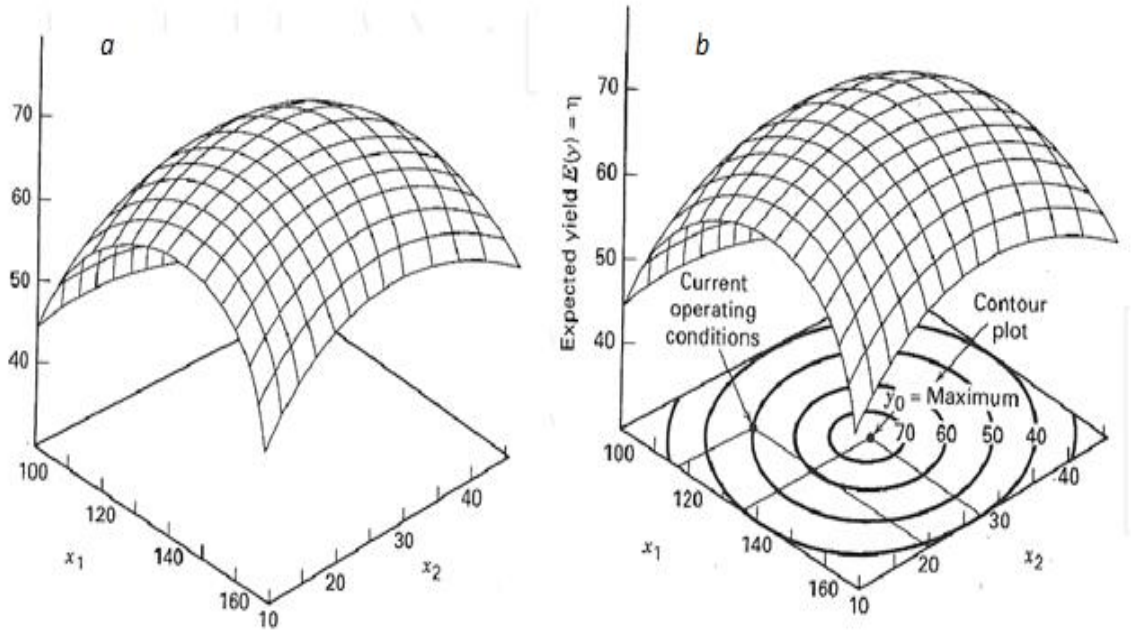

Figure 18. (*a)* A three dimensional response surface plot showing the expected performance (η) as a function between x_1 and x_2. (*b)* A contour plot of variables interaction of a response surface [94].

Usually, one of the RSM problems is that the form of relationship between the response and the independent variables is unknown. Thus, the first step in RSM is to find a suitable approximation for that functional relationship. Polynomial models of first and second order (linear and quadratic equations with interactions) are normally used to model the response surface. If the response is well modeled by a linear function of the independent variables, then the approximating function is the first order model (Equation 2).

$$y = \beta_0 + \beta_1 x_1 + \beta_2 x_2 + \ldots + \beta_k x_k + \epsilon \qquad (2)$$

where, y is the response, B_0 is the model intercept and $B_{1,..,\,k}$ is the linear coefficient, and x_i is the level of the independent variable. If there is curvature in the system, then a polynomial of higher degree must be used, such as the second order-model (Equation 3).

$$y = \beta_0 + \sum_{i=1}^{k} \beta_i x_i + \sum_{i=1}^{k} \beta_{ii} x_i^2 + \sum\sum_{i<j} \beta_{ij} x_i x_j + \epsilon \qquad (3)$$

where, y is the predicted response, x_i and x_j the input variables, B_0 a constant, B_i the linear coefficients, B_{ii} the squared coefficients and, B_{ij} the cross-product coefficients [93].

The goal is to optimize the response variable (y) and an important assumption is that the independent variables are continuous and controllable by experiments with negligible errors. The task then is to find a suitable approximation for the true functional relationship between independent variables and the response surface [95].

So, the RSM in conjunction with CCD, which is a design for fitting the second-order model, can be applied in modeling and in the optimization of a wide range of bioprocesses, becoming a successful statistical method in the present-day for biotechnology [93].

3 Catechol-*O*-methyltransferase (COMT)

3.1 General overview of catechol-*O*-methyltransferase

Catechol-*O*-methyltransferase (COMT, E.C. 2.1.1.6) is a methyltransferase enzyme that catalyses, in the presence of Mg^{2+}, the transfer of the methyl group from S-adenosyl-$_L$-methionine (SAM) to one of the hydroxyl groups of the catechol substrate, leading to their degradation [96]. This methylation reaction is a sequentially ordered mechanism, with SAM being the first to bind to the enzyme, followed by the Mg^{2+} ion and finally the substrate (Figure 19) [97].

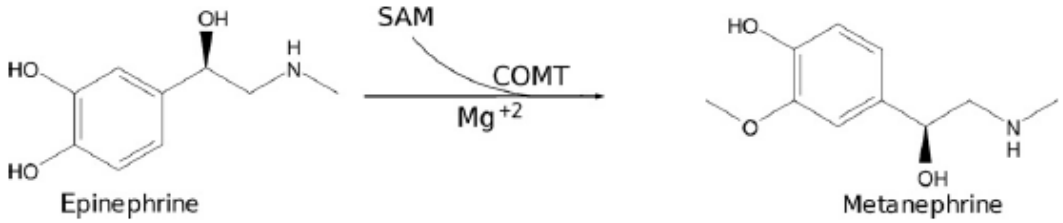

Figure 19. Reaction catalyzed by catechol-*O*-methyltransferase (COMT). COMT, in the presence of magnesium (Mg^{2+}) transfers a methyl group from S-adenosyl-$_L$-methionine (SAM) to a hydroxyl group of the substrate [98].

In human tissues, two distinct COMT isoforms can be found: a soluble form (hSCOMT) present in the cytoplasm of various tissues, such as liver, kidney and spleen, and a membrane-bound form associated to rough-endoplasmatic reticulum (hMBCOMT), which is predominant in the brain. Thus, it is not surprising that COMT has many physiological roles and has been suggested by several authors to be a trait marker in human neuropsychiatry disorders, such as major depression, schizophrenia, Alzheimer´s and Parkinson´s disease (PD) [105,106].

Soluble catechol-*O*-methyltransferase (SCOMT) shows that it is a monomeric protein of 221 amino acids residues with a predicted molecular mass of 24 kDa, while membrane-bound catechol-*O*-methyltransferase (MBCOMT) has a molecular weight of 30 kDa and possess 50 additional amino acid residues, of which around 20 constitute the membrane anchor region domain [99]. The general function of COMT is the elimination of biologically active or toxic catechols and other metabolites, while playing a particularly important role in the metabolism of catecholamines, especially in the breakdown of the neurotransmitters dopamine, epinephrine and norepinephrine [101].

The three-dimensional structure of rat recombinant SCOMT in complex with the co-substrate SAM, one magnesium ion and the competitive inhibitor 3,5-dinitrocatechol (3,5-DNC) was resolved for the first time by Vidgren and collaborators. COMT is composed by one single domain with α/ß-folded structure, containing eight α-helices arranged around a central mixed ß-sheet (Figure 20) [102].

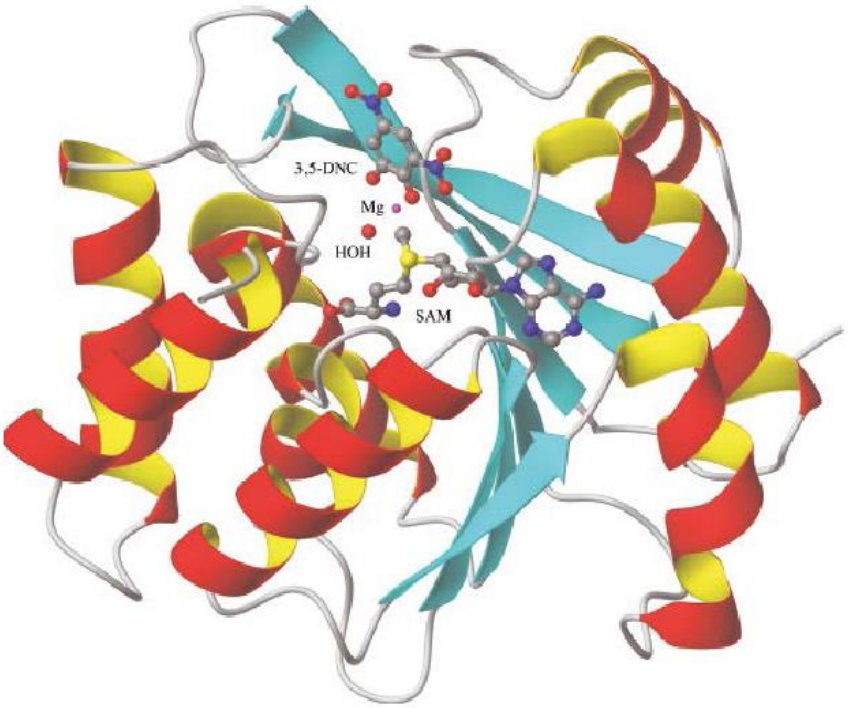

Figure 20. Schematic representation of the three-dimensional structure of COMT. The S-adenosyl-$_L$-methionine (SAM) co-substrate, the inhibitor 3,5-dinitrocatechol (3,5-DNC), the magnesium ion (Mg^{2+}), and the coordinated water molecules are depicted [102].

3.2 Physiological functions of COMT in catecholamine metabolism

Physiologically, COMT is one of the major enzymes responsible for the inactivation and breakdown of catecholamine neurotransmitters, with special importance to dopamine in the prefrontal cortex (PFC) and to the methylation of levodopa (dopamine precursor) to 3-O-methyldopa in levodopa/aromatic amino acid decarboxylase inhibitor-treated Parkinson´s disease patients [108,109]. COMT acts as an enzymatic detoxifying barrier between the blood and other tissues, shielding them from the negative effects of hydroxylated xenobiotics [97]. COMT also modulates some excretory functions in the kidney and intestinal tract by modulating the dopaminergic tone, as in the brain, where COMT activity regulates the levels of dopamine, namely in the PFC areas (Figure 21). Moreover, COMT has been suggested to be associated to the modulation of several behavior and cognitive processes [101].

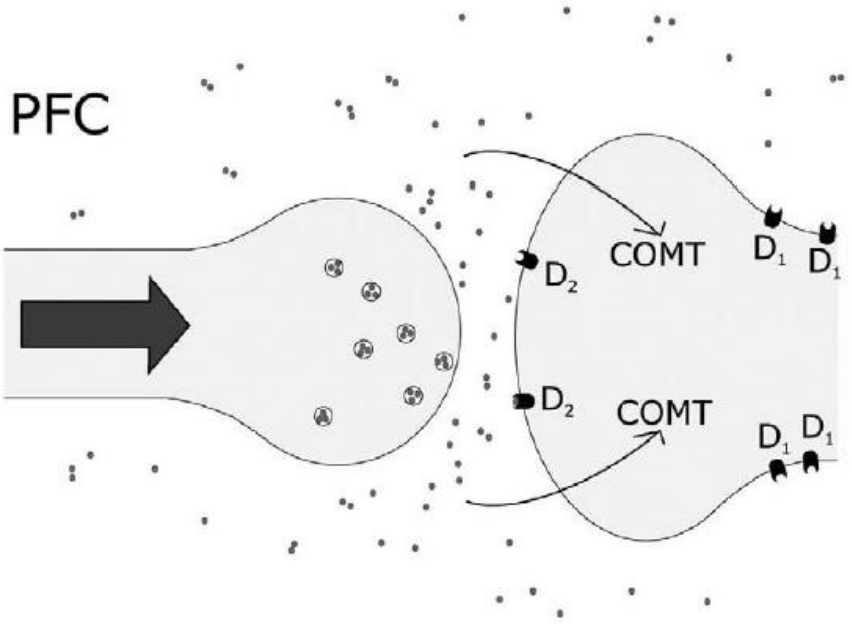

Figure 21. Dopaminergic transmission in prefrontal cortex (PFC). The lack of dopamine transporter (DAT) in the synapse means that COMT plays a prominent role in inactivating dopamine [101].

3.3 Parkinson´s disease and COMT inhibitors

Parkinson´s disease, affecting 1 - 2 % of the worldwide population over 60 years, is the most neurodegenerative movement disorder, characterized by progressive and profound loss of dopaminergic neurons. Symptoms of PD include motor impairment (resting tremor, rigidity) and non-motoric symptoms (cognitive and psychiatric problems) [104].

Over the last decades, the lack of dopamine has been linked to Parkinson´s disease, and so, levodopa and dopamine agonists are currently the drugs of choice for PD when a significant symptomatic effect needs to be achieved. However, the use of COMT inhibitors plus levodopa is more effective at reducing PD symptoms when compared do levodopa alone [96].

The design of inhibitors has been in practice since the discovery of COMT. The first generation of COMT inhibitors such as tropolone, N-butylgallate, catechol, 2-hydroxylated oestrogens and U-0521 showed low efficacy *in vivo*, were short acting, lacked selectivity and were quite toxic. The second-generation inhibitors included nitrocatechols like entacapone, nitecapone and tolcapone. In the present, only two COMT inhibitors that have beneficial effect of prolonging the half-life of levodopa, are currently available, namely tolcapone and entacapone, a safer but less efficient compound (Figure 22) [98].

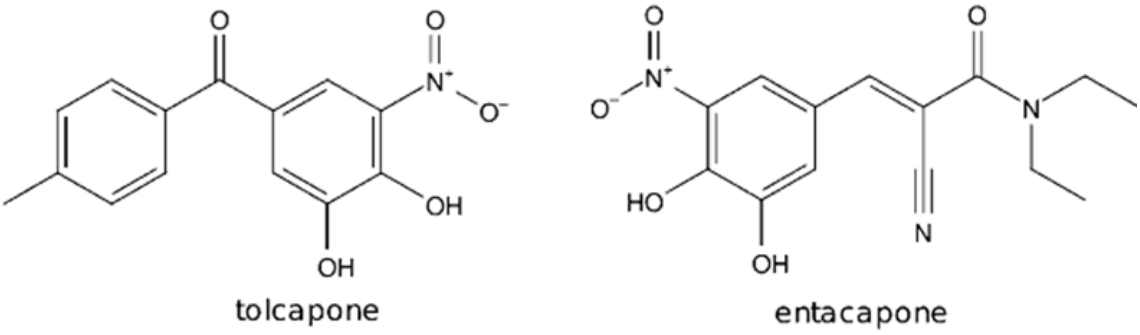

Figure 22. Chemical structures of tolcapone and entacapone, second-generation COMT inhibitors [98].

3.4 hSCOMT biosynthesis and purification

The best way to obtain considerable amounts of human proteins is by recombinant technology. The main source for recombinant hSCOMT production has been *E.coli* host system, since this expression has an ability to grow rapidly and at high cell density on inexpensive substrates [105].

This recombinant technology is an adequate host for expression of recombinant SCOMT since it lacks endogenous COMT enzyme. Indeed, with an optimized heterologous expression system in *E.coli* for recombinant hSCOMT production, it was possible to produce and recover the active monomeric enzyme directly from cell crude using, as lysis step, freeze/thaw cycles or ultrasonication [106]. More recently, due to a rapid grow of knowledge in area of biogenesis membrane proteins, others expression systems, such as the expression system based on *Brevibacillus choshinensis*, have been used to produce considerable amounts of recombinant hMBCOMT for structural, functional and pharmacological studies [107].

Over the years, the human SCOMT has been extensively studied and submitted to all kinds of purification procedures, such as hydrophobic interaction chromatography [112,114], cation and anion exchange chromatography [99], bioaffinity chromatography with immobilized amino acids [109] or size exclusion chromatography [110]. All these techniques intend to isolate and purify SCOMT, however, it is necessary to take into account the COMT activity, as well as the enzyme recovery, that some of these procedures present as drawback [110].

Chapter II

Objectives

Since the use of gellan gum as a chromatographic matrix is a relatively recent approach in the vast range of applications that this polymer presents, the main goal of this work is the optimization of physical and structural properties of the gellan gum as a chromatographic support and to reinforce the applicability of gellan as a chromatographic matrix with the purification of model proteins and more complex biomolecules with industrial, biotechnological and therapeutic interest.

Therefore, in a novel chromatographic approach, it is proposed the formulation of gellan gum microbeads that will allow the production of a more stable stationary phase. For that purpose, an easy and low-cost manufacturing strategy to produce the microspheres is going to be adopted, the water-in-oil emulsion. This technique allows the making of microbeads and, with the application of design of experiments, it will be possible to study, understand and optimize the effects and interactions of the different parameters that are going to be used in the bead formulation. Furthermore, it will be intended to explore and study the possible interactions between the matrix with loaded model proteins and with a more complex protein, recombinant human soluble catechol-*O*-methyltransferase (hSCOMT), exploiting the ion exchange chromatography. Moreover, it will be determined the dynamic binding capacity of the support in order to characterize the gellan gum beads as a novel chromatographic matrix.

Chapter III

Materials and Methods

1 Materials

Ultrapure water for all the solutions was obtained with a Mili-Q system from Milipore/Water (Billerica, MA, USA). Gellan gum (Gelrite ®), 4-Morpholineethanesulfonic acid (MES), barium chloride ($BaCl_2$), lysozyme, bovine serum albumin (BSA), α-chymotrypsin, sodium chloride (NaCl) and bromophenol blue were acquired from Sigma-Aldrich (St. Louis, MO). Acrylamide 30% / Bis-acrylamide solution was obtained from BioRad (Hercules, CA). Tris(hydroxymethyl)aminomethane (Tris) was bought from Fisher Scientific (Epson, United Kingdom). Sodium dodecyl sulfate (SDS) and glycerol were acquired from Himedia (Mumbai, India). Ammonium persulfate (PSA) was obtained from Eurobio (Courtaboeuf, France). N,N,N',N'-tetramethylethylenediamine (TEMED) and ß-mercaptoethanol were purchased from Merck (Darmstadt, Germany). NZYTech colour protein marker II was bought from NZYTech (Lisbon, Portugal). Anti-rabbit IgG alkaline phosphatase secondary antibody were purchased on GE Healthcare Biosciences (Uppsalla, Sweden). Monoclonal rabbit anti-COMT antibody was produced in BIAL (S. Mamede do Coronado, Portugal) using purified recombinant rat COMT. The buffer solutions were filtered through a 0.20 µm pore size membrane (Schleicher Schuell, Dassel, Germany) and ultrasonically degassed. All chemicals used were of analytical grade, commercially available and used without further purification.

2 Methods

2.1 Bead formation with water-in-oil emulsion

The preparation of the gellan gum beads by water-in-oil emulsion involved several steps. First, the default quantity of gellan was dissolved in water with constant stirring of 300 rpm at 90 ºC for 15 minutes. Then, this solution was transferred to a syringe attached to a laboratory stand/support and, with a 21G needle, it was dropwised of a height of 20 cm into a 100 % vegetable cooking oil solution with pre-defined constant stirring and temperature. The following step consisted in transferring the mixture into a 200 mM $BaCl_2$ (counter-ion) solution with the same constant stirring of the previous step during 30 minutes, at room temperature.

Finally, the beads were washed with ethanol 70 % and rinsed with deionized water in a vacuum filtration system with a filter paper, then recovered and stored in a 10mM MES buffer pH 6.2 solution at 4 ºC for posterior application.

In order to optimize the gellan gum chromatographic support, several experimental conditions were tested. The beads formulations involved various parameters: gellan gum concentration, from 1 % to 2.5 % (%(w/v)); temperature, from 20 ºC to 100 ºC; and stirring velocity, from 250 rpm to 750 rpm.

2.2 Optimization of the bead formation with DoE

Design of experiments was applied to define the optimal experimental conditions that allowed the formation of the ideal gellan gum beads with the smallest diameter possible.

Central composite design (CCD) was used to predict the smallest bead size as function of the gellan concentration, stirring velocity and temperature. The CCD allowed the establishment of a second degree polynomial model with relationships between the factors and the dependent variable. Moreover, CCD can give information about the interaction between the variables (factors) in their relation to the dependent variable. The lowest and the highest levels of variables were given in Table 8.

Table 8. Levels of variables used in the central composite design.

Factor	*Variable*	*Low Actual*	*High Actual*	*Low Coded*	*High Coded*	*Mean*
A	[Gellan]	1.00	2.50	-1	1	1.75
B	Stirring (rpm)	250	750	-1	1	500
C	Temperature (ºC)	20	100	-1	1	60

After combining the concentration of gellan, the stirring velocity and the temperature, an experimental design with seventeen runs was performed, each one corresponding to a particular bead size response, as the final product. All the combinations obtained from the design of experiments can be seen in Table 9.

Table 9. Assays obtained by the conjugation of the different variables from the experimental plan for optimization of the gellan gum beads.

Run	*Factor A: Gellan (%)*	*Factor B: Stirring (rpm)*	*Factor C: Temperature (ºC)*
1	1	250	20
6	2.5	250	20
8	1	750	20
16	2.5	750	20
11	1	250	100
9	2.5	250	100
2	1	750	100
7	2.5	750	100
13	1	500	60
12	2.5	500	60
14	1.75	250	60
17	1.75	750	60
4	1.75	500	20
15	1.75	500	100
3	1.75	500	60
10	1.75	500	60
5	1.75	500	60

The experiments were designed by using the Design Expert software version 7.0 (State Ease Inc., Minneapolis, Mn, USA). A 2^3 factorial central face centered composite design with fourteen non-central points and three center points was employed for the optimization of the bead formation. The second-order polynomial (Equation 5), which includes all interactions terms, was used to calculate the predicted response. Also, the design expert software was used for regression and graphical analysis of obtained data.

$$\hat{Y}_i = \beta_0 + \sum_{i=1}^{3} \beta_i x_i + \sum_{i=1}^{3} \beta_{ii} x_i^2 + \sum_{i,j=1}^{3} \beta_{ij} x_i x_j \qquad (5)$$

2.3 Microscopic bead visualization and scanning electron microscopy (SEM)

The output proposed in the previous design was the evaluation of the diameter of the formed beads by the W/O emulsion technique. In order to visualize the microspheres and measure the average size, an inverted microscope was used. The beads, which were stored in a 10 mM MES buffer pH 6.2 solution at 4 ºC, were visualized in a hydrated state. A random sample form each bead formulation was collected, transferred to a microscopic slide, and viewed at different magnification lens (5x and 10x). In order to establish the average bead size, this visualization step was repeated three times for each assay (n=3).

To view the beads morphology, scanning electron microscopy (SEM) analysis was performed. This technique allows accessing the surface topography of the microbeads. For the visualization, the beads needed to be at a lyophilized state. The dried samples were transferred to an adequate aluminum support and coated with gold under vacuum using an Emitech K550 sputter coater. Finally, photomicrographs from the surface were obtained with a Hitachi S-2700 (Tokyo, Japan) scanning electron microscope with an acceleration voltage of 20 kV, at several magnifications degrees.

2.4 Ion exchange chromatography

After the optimization of the gellan gum beads, chromatographic assays using a workbench column (Econo-Pac column, BioRad, Hercules, CA) at room temperature with three model proteins, BSA (5 mg/mL), α-chymotrypsin (10 mg/mL) and lysozyme (10 mg/mL) and a more complex extract with catechol-*O*-methyltransferase (COMT) were made.

The column was packed with the beads formed from the optimal design point (1.41 % (w/v) gellan, 99.20 ºC and 749.47 rpm stirring speed) and equilibrated with 10 mM MES buffer pH 6.2. Furthermore, chromatographic assays with three protein samples, isolated or combined, were made with the purpose to establish their elution profiles based on their isoelectric points. It was injected in the equilibrated column 500 µL of each sample, both in the isolated and in the combined protein assays.

These assays consisted in two chromatographic steps. First, the column was equilibrated and the sample was loaded to the gellan beads matrix with 10 mM MES buffer pH 6.2. The second

step corresponded to the elution of bounded biomolecules. The elution was made with the same buffer, but with the addition of $BaCl_2$ and NaCl to maintain the matrix stability and to increase the ionic strength, respectively.

In each isolated protein chromatographic assay and in the combination of BSA with α-chymotrypsin and lysozyme, the elution buffer contained 100 mM $BaCl_2$ and 750 mM NaCl. In the assay with the combination between α-chymotrypsin and lysozyme, the equilibration buffer had 25 mM NaCl in the 10 mM MES pH 6.2 and the elution buffer was composed by 100 mM $BaCl_2$, 750 mM NaCl and 10 mM MES pH 6.2.

The assay with all the proteins combined consisted in three steps: the column was equilibrated with 10 mM MES buffer pH 6.2 and the protein mixture was loaded. A stepwise gradient of 25 mM NaCl in 10 mM MES buffer pH 6.2 was applied, and, finally, for the more retained protein elution, the buffer applied was constituted by 100 mM $BaCl_2$, 750 mM NaCl and 10 mM MES pH 6.2.

The recombinant human soluble catechol-*O*-methyltransferase (hSCOMT) protein expression and recuperation from *Pichia pastoris* lysate assays were made as described by Pedro and co-workers [111]. For the hSCOMT purification, an IMAC procedure, as described by Passarinha and co-workers [112], was made at 6 ºC in an AKTA Avant system with UNICORN 6 Software (GE Heatlhcare, Uppsala, Sweden), equipped with a 2 mL injection loop. For this SCOMT assay, it was injected 1 mL of a pre-purified and concentrated COMT sample in the column to study the profile that this enzyme had in the matrix and its chromatographic elution behavior. First, for preliminary studies the column was equilibrated with 10 mM MES buffer pH 6.2 and the sample was injected. Then, the elution buffers containing 50 mM $BaCl_2$, 100 mM NaCl and 10 mM MES pH 6.2 and 100 mM $BaCl_2$, 750 mM NaCl and 10 mM MES pH 6.2 were sequentially applied. These steps, were repeated in a second assay, however, the pH of the buffers was changed to 4.2.

Fractions of 1 mL were collected in each chromatographic step that was maintained for three column volumes. Then, the absorbance of the collected fractions was monitored at 280 nm in a Pharmacia Biotech Ultraspec 3000 spectrophotometer. At last, the fractions corresponding to the chromatographic peaks were concentrated and desalted using Vivaspin® 6 concentrators (Sartorius Stedim Biotech Goettingen, Germany) in centrifuges Macrosep® Advance and preserved at 4 ºC for further analysis by SDS-PAGE electrophoresis and dot-blot.

2.5 Electrophoretic and dot-blot analysis

The samples resultants from the chromatographic peaks were analyzed by reducing Sodium Dodecyl Sulphate-Polyacrylamide Gel Electrophoresis (SDS-PAGE). They were treated by adding 5 µL of a reduction buffer (500 mM Tris-HCl (pH 6.8), 10 % (w/v) SDS, 0.02 % bromophenol blue (w/v), 0.2 % glycerol (v/v), 0.02 % ß-mercaptoethanol (v/v)) to the 20 µL of concentrated samples. Then, they were denatured at 100 ºC during 10 minutes and electrophoretic assays were executed on 4.7 % stacking and 15 % resolving gels with a running buffer containing Tris (25 mM), glycine (192 mM), SDS (0.1 % w/v) at 120 V for 120 minutes. Finally, for the three model proteins, the gels were stained by Comassie brilliant blue whilst for the COMT samples, a silver color staining commercial kit was used.

For the dot-blot analysis, it was applied 60 µL of each sample into a PVDF membrane previously activated with pure methanol and equilibrated with Mili-Q water and TBS (20 mM Tris-HCl, 150 mM NaCl). Then, the membranes were dried before blocking non-specific sites by soaking in 5 % (w/v) non-fat milk in TBS-T (20 mM Tris-HCl, 150 mM NaCl, Tween 20) during 60 minutes. After the blocking step, the membranes were washed three times with TBS-T during 15 minutes and then incubated 1 hour, at room temperature, with each primary and secondary antibodies. The primary antibody is a rabbit anti-rat SCOMT monoclonal antibody, which cross reacts with the human protein, at 1:2500 dilution in TBS-T 1 %. Then, the membranes were again washed three times, during 15 minutes, with TBS-T and adherent antibody was detected by incubation for 1 hour with an anti-rabbit IgG alkaline phosphatase secondary antibody at 1:10000 dilution in TBS-T 1 %. Finally, the PVDF membranes were incubated with 200 µL of ECF for 5 minutes and enhanced by exposure to chemiluminescence detection.

2.6 Dynamic binding capacity

For the dynamic binding capacity studies, the prepared gellan gum beads formulation was the same as the chromatographic assays. The matrix was packed into a column C 10/10 (GE Healthcare, Portugal) to a total volume of 500 µL and then, the column was connected to an Akta Purifier system to determine the dynamic binding capacity. The column was equilibrated with 10 mM MES buffer pH 6.2. Thereafter, the column was overloaded with 0.5 mg/mL of lysozyme in 10 mM MES buffer pH 6.2, at a flow rate of 1 mL/min. Determination of dynamic binding capacity was carried out by recording breakthrough curves and calculating the amount of bound lysozyme per mL support at 10 % and 50 % of breakthrough curve. Dynamic binding capacity values were then obtained by subtracting the value obtained under non-binding conditions. Afterwards, the elution of the bound lysozyme was achieved by increasing the ionic strength to 750 mM NaCl in 100 mM $BaCl_2$ and 10 mM MES buffer pH 6.2.

Chapter IV

Results and Discussion

The development of new strategies for separation and purification of biomolecules has been a topic of great importance and with continuous progress. Chromatography, due to its simplicity, versatility and high reproducibility is a widely used purification method and plays an important key role in the separation of biomolecules with therapeutic and industrial interest [50].

Currently, there is a large variety of chromatographic supports, since natural polysaccharides and synthetic polymers to inorganic materials. These matrices are generally presented as inert and often require to be functionalized with specific ligands to give them a chromatographic character to explore. Thereby, the search of new chromatographic supports with different characteristics from the conventional ones, may constitute a valuable scientific asset in the purification of pharmacological biomolecules and in the biotechnological industry, by reducing the costs associated to the production of chromatographic matrices [51].

Gellan gum, due to its gelling ability and anionic nature can be used as a natural polysaccharide stationary phase and be applied, without being functionalized, in several chromatographic processes [49].

Since the main goal of this work is the morphology optimization of the gellan gum as a chromatographic support and to reinforce the applicability of gellan as a chromatographic matrix, it was proposed the formulation of gellan gum microbeads that allows the production of a more stable stationary phase.

1 Gellan gum beads production

In order to prepare the chromatographic matrix from gellan gum, an easy and low-cost manufacturing strategy to produce the microspheres was adopted, the water-in-oil emulsion. This technique allowed the making of the beads and, with the application of design of experiments, it made possible to study and to understand the effects and interactions of the different parameters that were used in the bead formulation.

The emulsion technique for microbeads production consisted in several steps. The first step was a gelation step. An aqueous solution, in which the polymer is dissolved to form a polymeric solution, was dispersed into an immiscible organic phase, 100 % vegetable cooking oil, and mixed in order to obtain an emulsion. Before the two phases were separated, the mixture was transferred into a room temperature solution with divalent ions that, by cooling, allowed the polymer drops to be hardened according to the sol-gel mechanism of gellan gum. Moreover, this counter-ion solution reinforced the polymer solution to form solid structures and promoted the gellan beads stabilization. The second step was the oil removal/washing phase, in which the oil was removed by vacuum filtration and the formed structures were washed with ethanol 70 % and rinsed with deionized water (Figure 23).

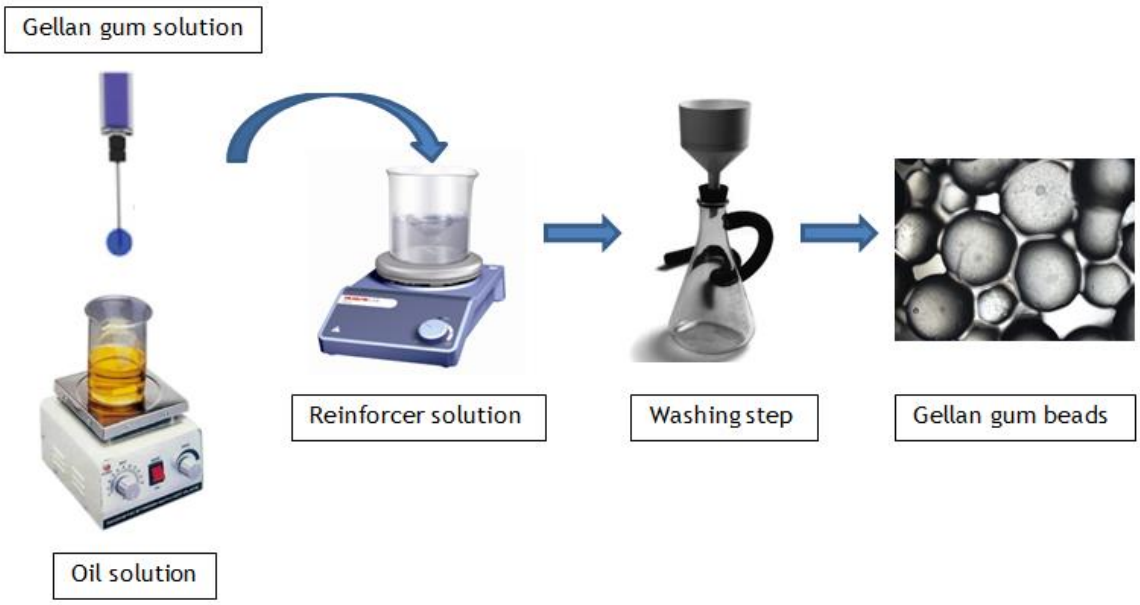

Figure 23. Scheme design of water-in-oil emulsion. An aqueous gellan solution is dropwised dispersed in an oil solution and transferred to a counter-ion reinforcer solution. Posteriorly the formed beads are washed in a vacuum filtration system.

Barium chloride was used in the reinforcerment solution as the counter-ion. As seen, divalent cations are considered very effective in the gelation of gellan gum and, taking into account that barium is an alkaline earth metal and a divalent positive ion, it was considered to be a suitable cation for the gellan gum gelation [113].

Furthermore, barium exhibits a large ionic size, when compared to other divalent ions like calcium, thus fitting more appropriately in the binding sites of gellan. This fact largely contributes to the formation a more rigid network with higher tensile strength and a more stable structure due to its entanglement with the polymer chains in an “egg box” model, where the cations are sandwiched between the negatively charged polymer chains [88,90].

Moreover, the negatively charged gellan gum also binds electrostatically to the Ba^{2+} ions to contribute towards the formation of the spherical beads [114].

Also, due to the high ion density and increased efficiency in cross-linking with gellan gum, barium allows the formation of smaller and uniform microspheres with low/none swelling ratios, which is important to maintain the original spherical form of the gellan gum beads. Moreover, Ba^{2+} cross-linked beads successfully protects proteins from acidic environments in drug delivery systems [115].

In addition, unlike other cations such as zinc and copper, the barium solutions have no color. Indeed, in all buffer solutions where the addition of a residual concentration of Ba^{2+} was required to maintain the bead stability in the presence of sodium salt, the absence of any color can guarantee no misread value because it does not interfere in all the necessary absorbance readings in the spectrophotometer. All these barium features made it ideal to use it as the counter-ion in the reinforcement solution of the water-in-oil emulsion technique to produce the gellan gum microbeads.

2 Optimization of the bead formation with DoE

In order to achieve the smallest bead size (output proposed) as function of the gellan concentration, stirring velocity and temperature (inputs), a central composite design (CCD) was used.

The CCD is a specific design of experiments which allows an efficient methodology for planning experiments such that statistically valid relationships between the factors affecting the bead production and its outputs can be established [90].

Central composite design was performed to predict the smallest bead size as function of the inputs. Moreover, this time-saving method was used because it permitted finding optimum conditions for the desired response and, due to its rotatability, it allowed the determination of the response surface, which is commonly used for optimization with great efficiency [91].

The combination of the three parameters enabled the formulation of different diameter beads (Figure 24) and allowed to study how they influence the formation of beads with several different sizes. All the combinations, with the respective bead diameter as output, can be seen in Table 10.

Table 10. Assays obtained by the conjugation of the different variables from the experimental plan for optimization of the gellan gum beads with the respective bead diameter as output.

Run	*Factor A: Gellan (%)*	*Factor B: Stirring (rpm)*	*Factor C: Temperature (ºC)*	*Response: Diameter (µm)*
1	1	250	20	2029.48
6	2.5	250	20	2980.41
8	1	750	20	1164.27
16	2.5	750	20	1887.05
11	1	250	100	1681.15
9	2.5	250	100	2422.69
2	1	750	100	320.65
7	2.5	750	100	1994.46
13	1	500	60	1478.38
12	2.5	500	60	2819.81
14	1.75	250	60	1556.31
17	1.75	750	60	640.55
4	1.75	500	20	2389.89
15	1.75	500	100	1209.92
3	1.75	500	60	1406.48
10	1.75	500	60	1747.59
5	1.75	500	60	1473.46

In order to measure the size of the formed beads, analyze and fill out the output response table with the mean diameter of each assay, microscopic visualization with different magnifications lens was performed (5x and 10x). The measurements of the beads diameter were made three times for each run, in order to settle the average bead size. Figure 24 shows several images obtained from different experimental runs. All the samples were collected from a hydrated state.

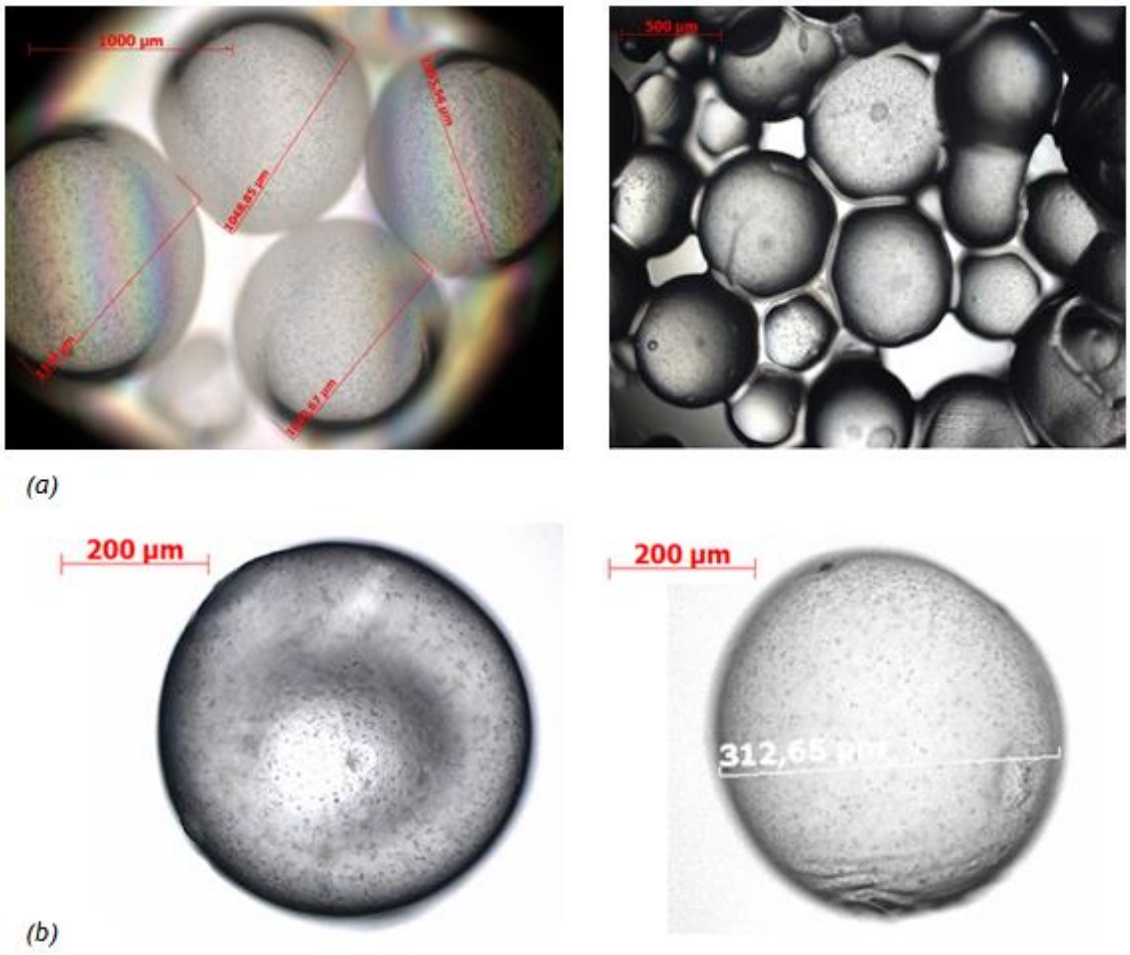

Figure 24. Microscopic visualization with different magnification lens of several sizes of the formed beads from different runs in a hydrated state. (a) Images obtained with a 5x magnification lens. (b) Images obtained with a 10x magnification lens.

2.1 Goodness of fit

The goodness of fit is given by the statistical coefficients resumed in Table 11. These different statistical calculations, by which the adequacy of a model can be judged, measures how good the model is, since they consider the contribution of all values together [116].

Table 11. Statistical coefficients of the model. ANOVA table for response surface reduced quadratic model.

R^2	R^2 Adj	R^2 Pred	Adeq Precision	Model F-value	p-value (Prob > F)
0.9117	0.8587	0.7244	15.260	17.20	< 0.0001

Analysis of variance, ANOVA, is an important diagnosis tool in regression analysis. In this study, A, B, C, AB, A^2, B^2 are significant model terms and had potential effect on the proposed output. According to the presented results, the model fitted the data and, among the independent test variables, a quadratic interaction is highly significant. The explained variation, R^2, has to be between 0 and 1, with larger values being more desirable, which represent a high significance of the model. On the other hand, the adjusted R^2 (R^2 adj) is a variation of the ordinary R^2 and is adjusted for the "size" of the model, that is the number of factors. If the adjusted R^2 decreases, non-significant terms are added to the model. The present results show that the model has a good adjusted R^2. The predicted R^2 is a measure of how good the model predicts a response value. The adjusted R^2 and predicted R^2 should be within approximately 0.20 of each other to be in reasonable agreement. If they are not, there may be a problem with either the data or the model. Adequate precision is a measure of the range in predicted response relative to its associated error, in other words, a signal to noise ratio. Its desired value is 4 or more. Since the radio indicates 15.260 we can say it indicates an adequate signal and this model can be used to navigate the design space. The model F-value of 17.20 implies the model is significant and there is only a 0.01 % chance that a "model F-value" this large could occur due to noise. Values of "prob > F" less than 0.05 indicate that model term are significant [117].

Moreover, for this regression model analysis, rather than plotting the observed and predicted values versus each of the independent variables in turn, it is simpler to generate a single plot of observed values versus the predicted values, in order to verify linearity (predicted versus observed plot). Therefore, for continuous responses the actual versus the predicted plot (Figure 25) shows how well the model fits the data. The diagonal line represents of where predicted and observed values are the same. For a perfect fit, all the points would be on this diagonal. As expected, the best points belong to central point because it is from these that the whole model is developed. The furthermost points of the line have higher residual value than those that are closer to the line. Additionally, the observation of a point with large residual value is called outlier. An outlier may indicate a sample peculiarity or may indicate a data error or other problem. Analyzing the Figure 25, it seems to no exist a significant observed value that could be considered as an outlier.

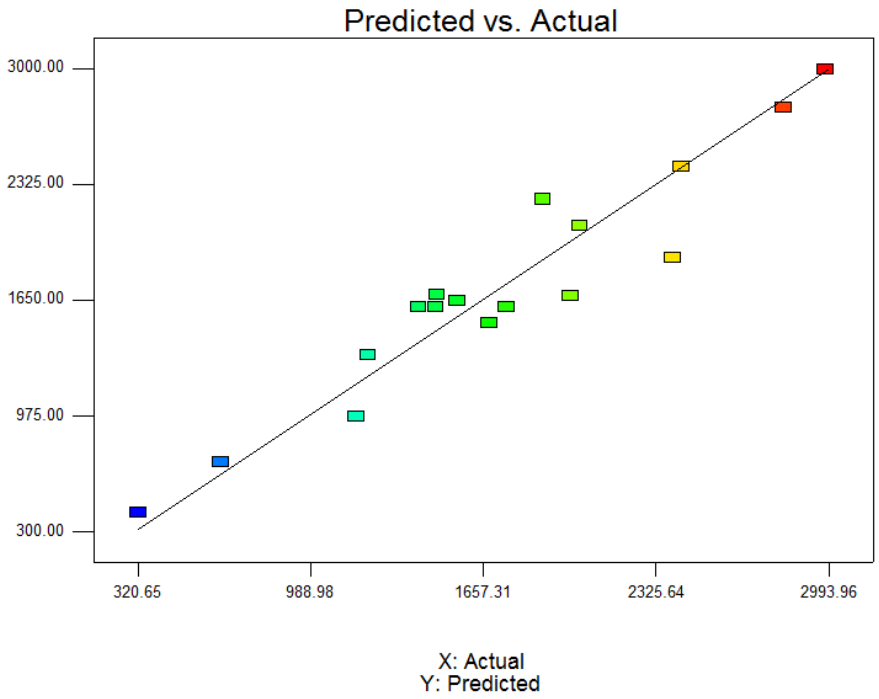

Figure 25. Predicted values versus observed values plot.

2.2 Model validation

From this design, predicted points could be selected in order to evaluate the minimum size bead. Conditions of optimum points were identified by introducing the data of DoE on Design Expert 7.0 software. The model was managed to predict points of the smallest bead sizes and two of them were chosen in order to replicate in laboratory and thus, validate the model. These points can be visualized in Table 12.

Table 12. Predicted points given by the program in order to obtain the minimum diameter bead.

Point number	*Factor A: Gellan (%)*	*Factor B: Stirring (rpm)*	*Factor C: Temperature (ºC)*	*Diameter desirability (µm)*
1	1.24	743.44	99.97	319.47
2	1.41	749.47	99.20	277.08

In order to validate the model by experimentation, five replicas of each optimal point were made (Table 13).

Table 13. Average bead diameter established by the visualization of five replicas from each optimal point.

Point number	*Replicas (μm)*	*Average of the replicas (μm)*
1	369.67 395.48 339.42 377.25 373.16	370.99
2	322.22 276.94 326.88 321.54 330.93	317.70

According to the program model, the confidence interval (CI) of 95 % is given in Figure 26 (*a*). The 95 % confidence interval represents the range in which the response should lie 95 % of the time.

Figure 26. (*a*) Diameter sizes for the validation of the DoE model given by Design Expert software version 7.0 in a confidence interval of 95 % and (b) considering all the sizes obtained from all the experiments.

Taking these values into account, this CCD design is validated. However, this interval has an overly range because it considers all the diameters obtained in all the experiments, including the minimum and maximum bead sizes (Figure 26 (*b*)), instead of only considering the confidence interval associated to the predicted points. Therefore, in order to validate the

model with more precision and accurate values, it was formulated a new confidence interval of 95% (Equation 6) for each predicted point given by the software:

$$IC_{\mu,95\%} = \left[\overline{X} \pm t \frac{S}{\sqrt{n}} \right] \qquad (5)$$

were n = 5; t de student: n – 1 → 5 – 1 = 4 → t = 2.77

For point 1:

$\overline{X}$ = 370.99

$S^2 = (369.67–370.99)^2+(395.48–370.99)^2+(339.42–370.99)^2+(377.25–370.996)^2+(330.96–370.99)^2$

S^2 = 3242.66

$$IC_{95\%} = 370.99 \pm 2.77 \frac{\sqrt{3242.66}}{\sqrt{5}}$$

$$IC_{95\%} = 370.77 \pm 70.69$$

300.08 *(µm)*_____370.77 *(µm)*_____441.47 *(µm)*

For point 2:

$\overline{X}$ = 317.70

$S^2 = (332.22–317.70)^2+(276.94–317.70)^2+(326.88–317.70)^2+(321.54–317.70)^2+(330.93–317.70)^2$

S^2 = 2146.25

$$IC_{95\%} = 317.70 \pm 2.77 \frac{\sqrt{2146.25}}{\sqrt{5}}$$

$$IC_{95\%} = 317.70 \pm 57.51$$

260.19 *(µm)*_____317.70 *(µm)*_____375.22 *(µm)*

The predicted bead diameters are 319.47 µm and 277.08 µm for point 1 and 2, respectively (Table 14). The replica experiments have an average bead size that fits in the 95 % confidence interval, confirming that the model is considered validated since the sizes are in these range of acceptance when any factor is changed, on design space.

Table 14. Range of bead size values in order to the model be validated in the 95% confidence interval for each predicted point by the software.

Point number	*Diameter desirability (μm)*	*95 % CI low*	*95 % CI high*	*Average of the replicas (μm)*
1	319.47	300.08	441.47	370.99
2	277.08	260.19	375.22	317.70

Moreover, another strategy to inquire if the model is or is not valid, is to calculate the error associated to these obtained values, trough BIAS and coefficient of variation (CV).

$$\% \text{ BIAS} = \frac{(Obs. - Predicted)}{Predicted} \times 100\% \qquad (6)$$

$$\% \text{ CV} = \frac{(Standard\ deviation))}{Mean} \times 100\% \qquad (7)$$

The % BIAS and the % CV permit to evaluate the error that is associated to the accepted parameters. The BIAS allows to calculate the mean relative error of accuracy and shows the model linearity. The accuracy describes the difference between the mean measured diameters for a sample obtained by the linear equation and the true diameter of the sample. Therefore, accuracy can be expressed as % Bias. Bias is considered valid if the value is situated between $\pm$ 15 %. The CV, ratio of the standard error of estimate to the mean value of the observed response, is also a measure of reproducibility of the model. It allows the measurement of the precision of an analytical method. Precision is defined as the repeatability of individual measurements of a sample, when these are done repeatedly with multiple aliquots of the same sample. Generally, a model can be considered reasonably reproducible if its CV is not greater than 10 % (Table 15) [118].

Table 15. % of BIAS and CV obtained from the error calculation of the values from the second 95% confidence interval obtained.

Point number	*Diameter desirability (µm)*	*Average of the replicas (µm)*	*Standard deviation*	*% BIAS*	*% CV*
1	319.47	370.99	36.43	16.13	9.82
2	277.08	317.70	28.73	14.66	9.04

Since the CV value indicated from the software was 15.36 %, these new % CV values (9.82 % CV for point 1 and 9.04 % CV for point 2) are very acceptable. Thus, we can say that, according to these results, the model is valid, since it has acceptable Bias values and shows a lower % CV than that the program suggested.

To better understand where the optimum conditions stand on the design space, Figure 27 represents two contour plots graphics with the two predicted responses, obtained with the established optimum conditions. The blueish areas, where it is possible to observe those predicted points, correspond to the space where the smallest sized beads can be found.

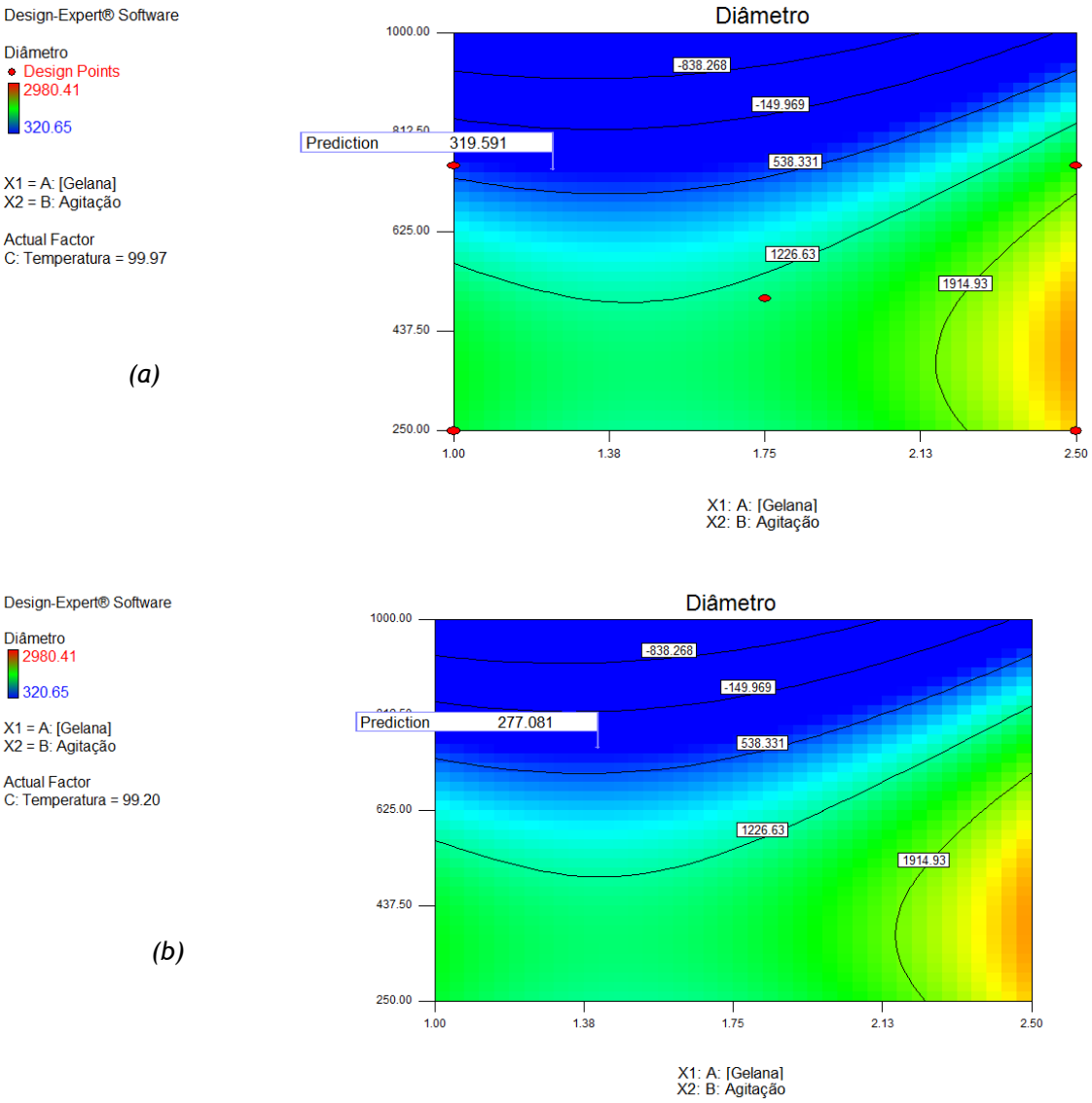

Figure 27. Contour plots for the predicted response (predicted bead diameter) of the defined optimal points. (*a*) Point 1. (*b*) Point 2. The blueish area corresponds to the smallest beads size.

2.3 Influence of one-factor and interaction plots on gellan gum beads production

In experimental design tests, if a variable influences another, this influence is called "effect". There are two different effects: the variable effects on another directly or via an interaction (or uses both mechanisms simultaneously). Because an interaction can magnify or diminish main effects, the evaluation of interactions is extremely important [119]. The following figures indicate the existence of interaction, or not, among the factors analyzed. For instance, Figure 28 represents interactions between stirring velocity and temperature.

A

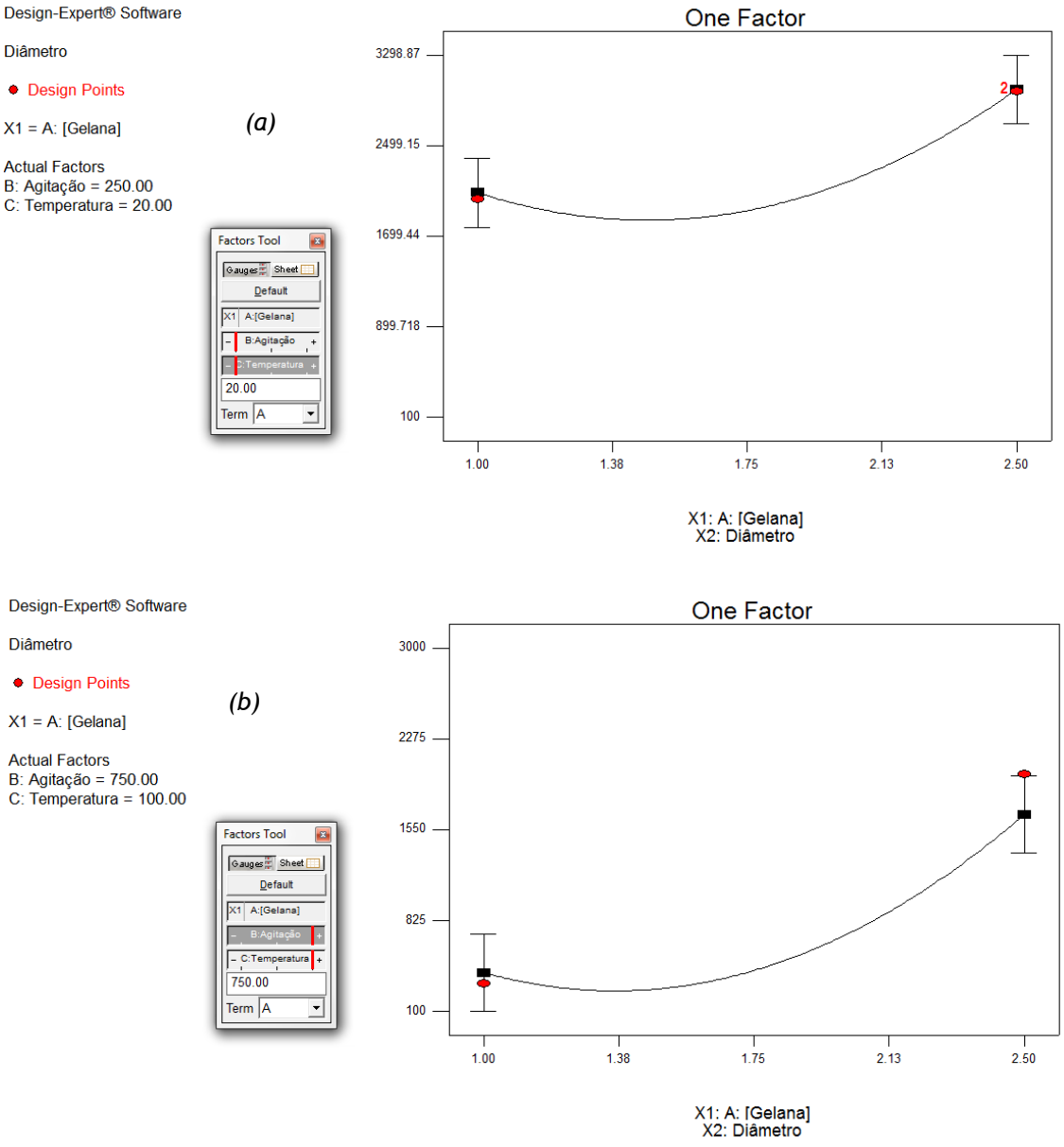

Figure 28. Interactions between stirring velocity and temperature, when assuming gellan concentration as a constant parameter on the beads diameter. (*a*) Effect when the stirring velocity is 250 rpm and temperature is 25 °C. (*b*) Effect when the stirring velocity is 750 rpm and temperature is 100 °C.

Based on the data of Figure 28, if stirring velocity and temperature are lower, larger beads are produced. An increase in both stirring velocity and temperature levels favors the production of gellan gum beads with smaller diameter. Figure 29 shows the effect of gellan gum concentration and temperature on the bead formulation.

B

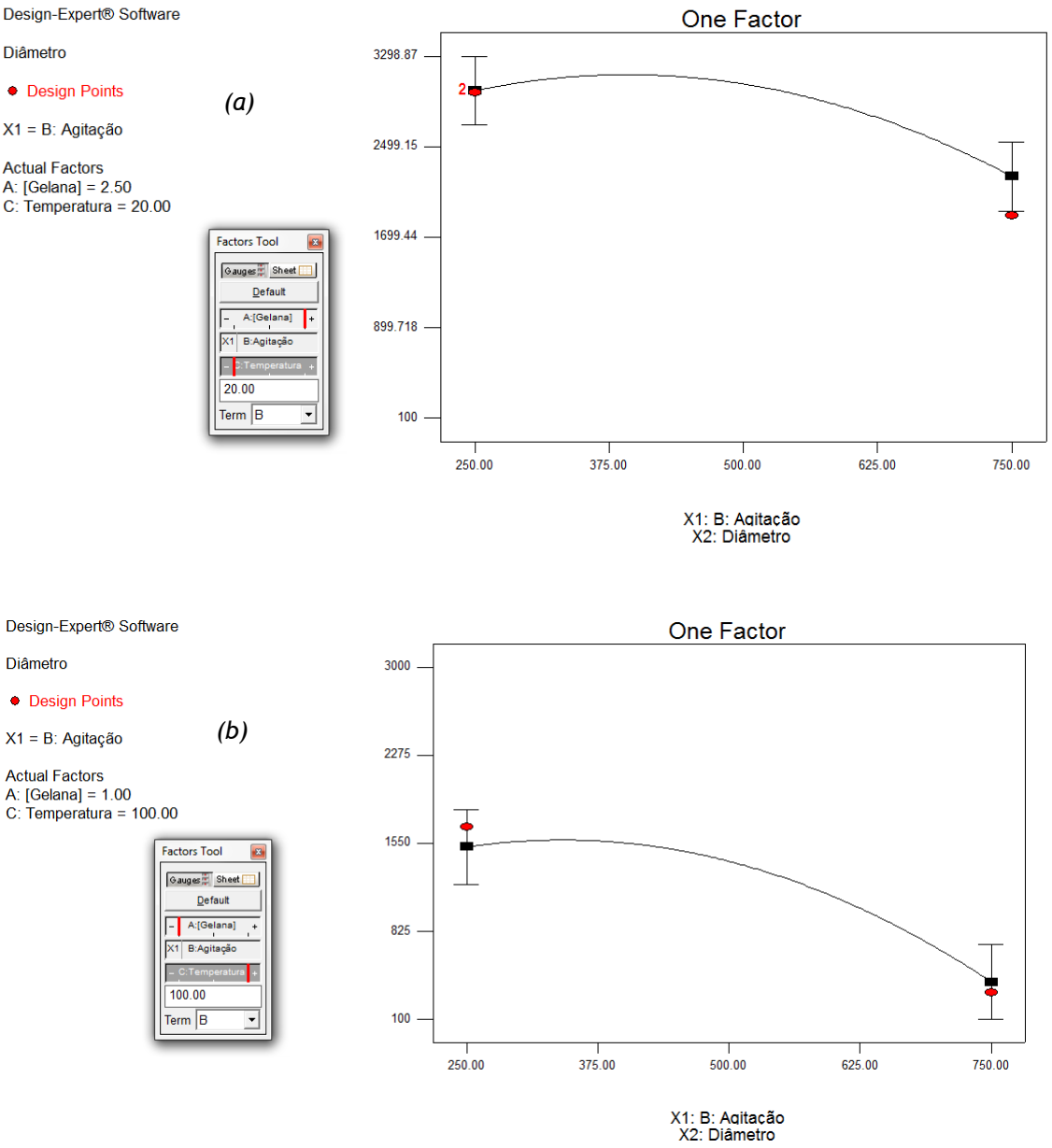

Figure 29. Interactions between gellan gum concentration and temperature, when assuming stirring velocity as a constant parameter on the beads diameter. (*a*) Effect when the gellan gum concentration is 2.5 % and temperature is 25 °C. (*b*) Effect when the gellan gum concentration is 1 % and temperature is 100 °C.

With the analysis of Figure 29, it is possible to view the effect of gellan gum concentration and temperature on formation of gellan gum beads. Gellan gum beads have a larger diameter when gellan gum concentration is higher and temperature is lower. If temperature is increased and the gellan concentration is lowered, the beads can have a smaller size. The interactions between gellan gum concentration and temperature are presented in Figure 30.

C

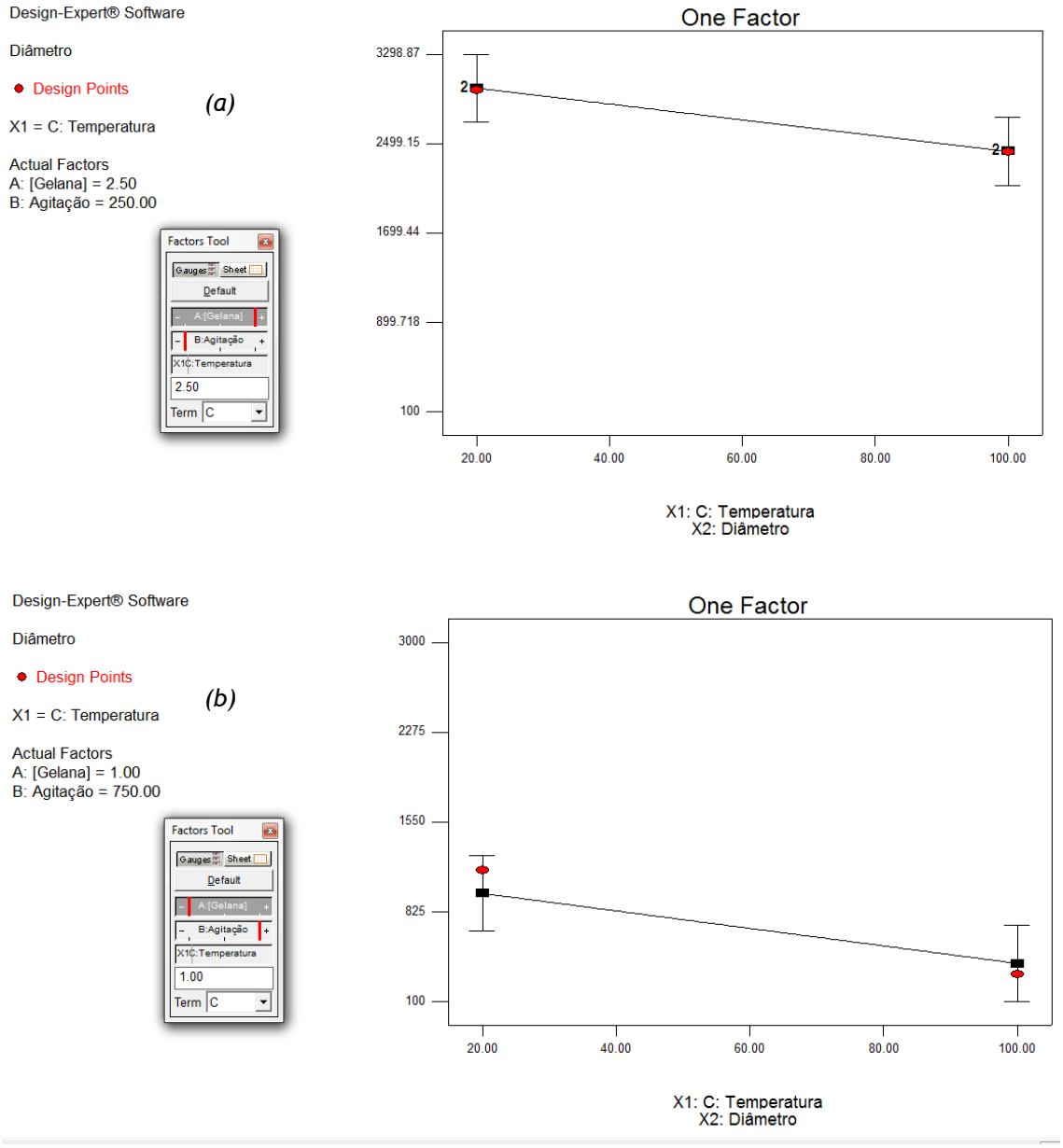

Figure 30. Interactions between gellan gum concentration and stirring velocity, when assuming temperature as a constant parameter on the beads diameter. (*a*) Effect when the gellan gum concentration is 2.5 % and stirring velocity is 250 rpm. (*b*) Effect when the gellan gum concentration is 1 % and stirring velocity is 750 rpm.

Figure 30 shows the effect of gellan gum concentration and stirring velocity on formation of gellan gum beads. Gellan gum beads have a much smaller diameter when gellan concentration is 1 % and when stirring velocity assumes higher values. If stirring velocity is lowered and gellan concentration is augmented, larger beads are produced. The effect of the temperature on the interaction between constant values of gellan gum concentration and stirring velocity can be seen in Figure 31.

AB

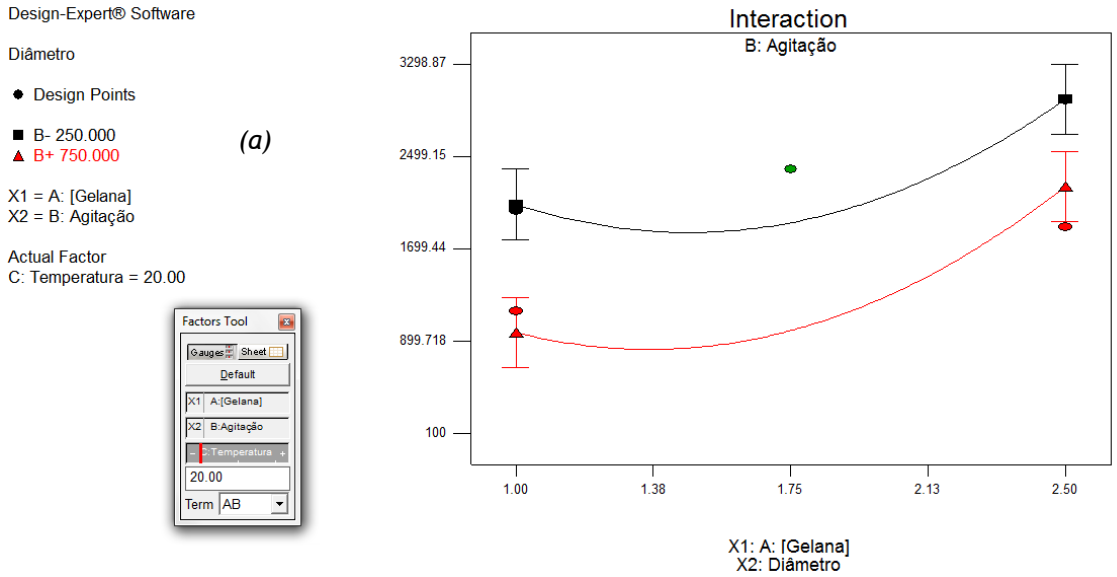

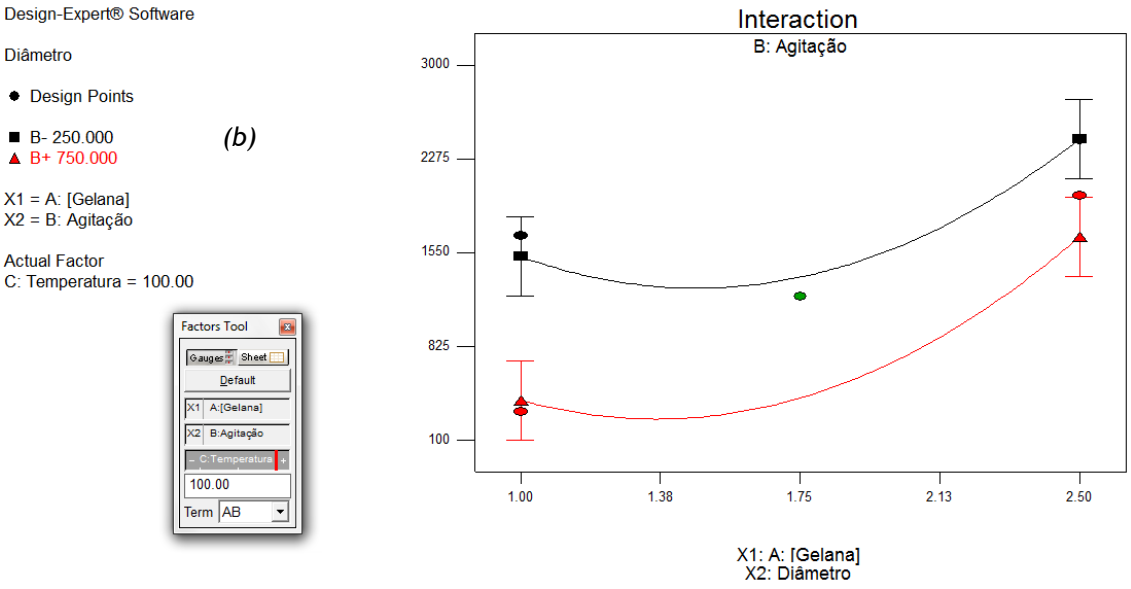

Figure 31. The effect of temperature, when assuming gellan gum concentration and stirring velocity as constant parameters, on the beads diameter. (*a*) Effect when the temperature is 20 ºC. (*b*) Effect when the temperature is 100 ºC.

Figure 31 allows us to understand the interactions between the three factors. When the gellan gum concentration and stirring velocity are constant, we could study how the temperature variation affects the beads formation. If we change the temperature from 20 ºC (Figure 31 *a*) to 100 ºC (Figure 31 *b*) it is possible to see that higher temperature values can produce smaller sizes of gellan beads.

These results allow comprehend which behaviors are more favorable to obtain the smallest gellan gum beads size possible. Moreover, it can also be seen, by analysis of the sum squares and p-values of each variable, how the parameters influence the model. From the results in Figure 32, the sum squares and F-values from every factor, it can be observed that temperature is the variable which has the least impact in this model, since it has the lower sum of squares and the lowest F-value, while the gellan gum concentration and stirring velocity have a more preponderant and intense role, due to its higher F-value and sum of squares values.

Response 1 Diâmetro

ANOVA for Response Surface Reduced Quadratic Model

Analysis of variance table [Partial sum of squares - Type III]

Source	Sum of Squares	df	Mean Square	F Value	p-value Prob > F	
Model	7.183E+006	6	1.197E+006	17.20	< 0.0001	significant
A-[Gelana]	*2.949E+006*	*1*	*2.949E+006*	*42.38*	*< 0.0001*	
B-Agitação	*2.174E+006*	*1*	*2.174E+006*	*31.25*	*0.0002*	
C-Temperatura	*7.965E+005*	*1*	*7.965E+005*	*11.45*	*0.0070*	
AB	*61973.12*	*1*	*61973.12*	*0.89*	*0.3676*	
A^2	*1.140E+006*	*1*	*1.140E+006*	*16.38*	*0.0023*	
B^2	*5.788E+005*	*1*	*5.788E+005*	*8.32*	*0.0163*	

Figure 32. Sum of squares and p-values of the different variables of the proposed model. Higher sum squares values means higher influence in the proposed model.

2.4 Response surface methodology

Numerical optimization technique based on minimum gellan bead diameter was carried out to determine the workable optimum conditions. Response surface graph incorporation can improve the understanding of the experimental data and helps finding the optimum levels of the factors implied. The graphics (Figure 33) were obtained using the Design Expert 7.0 software and are the representation of the resulting model regression equation [120].

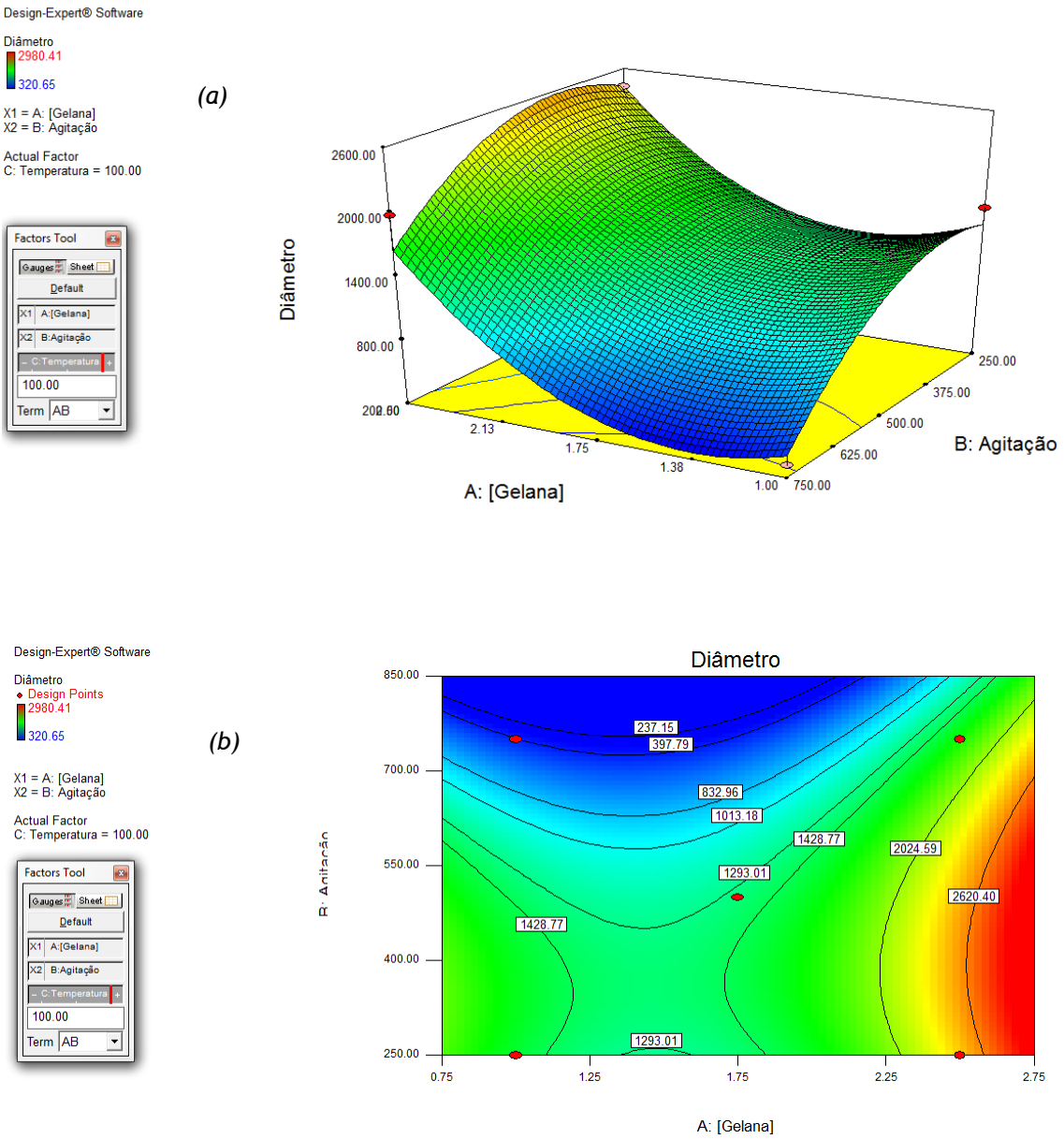

Figure 33. Response surface methodology. (a) Three-dimensional response surface plot of optimal conditions of gellan gum beads diameter. (b) Contour plot of interactions of variables gellan gum concentration, stirring velocity and temperature.

In order to provide an ideal case for this specific output with statistical significance, the goal was set to minimized response (minimum bead diameter). Analyzing the graphs of the response surface, the levels of gellan gum concentration, stirring velocity and temperature that reflect a blueish area are the conditions to achieve better response with temperature ate level +1 (100 ºC). The graphical representations are in agreement with the interactions presented. The optimal variables levels were achieved based in whole information provided by the CCD and RSM.

2.5 Scanning electron microscopy (SEM)

In order to obtain a more detailed analysis of the microscopic structure of the gellan gum beads, its reticulation and porosity, the scanning electron microscopy (SEM) was used. This technique allows accessing the surface topography and morphology of the microbeads. To perform this visualization, the beads needed to be in a lyophilized state. Since the all the beads have a very similar surface topography, the analysis was executed with the beads produced from the optimal point 2, given by the CCD model (Figure 34).

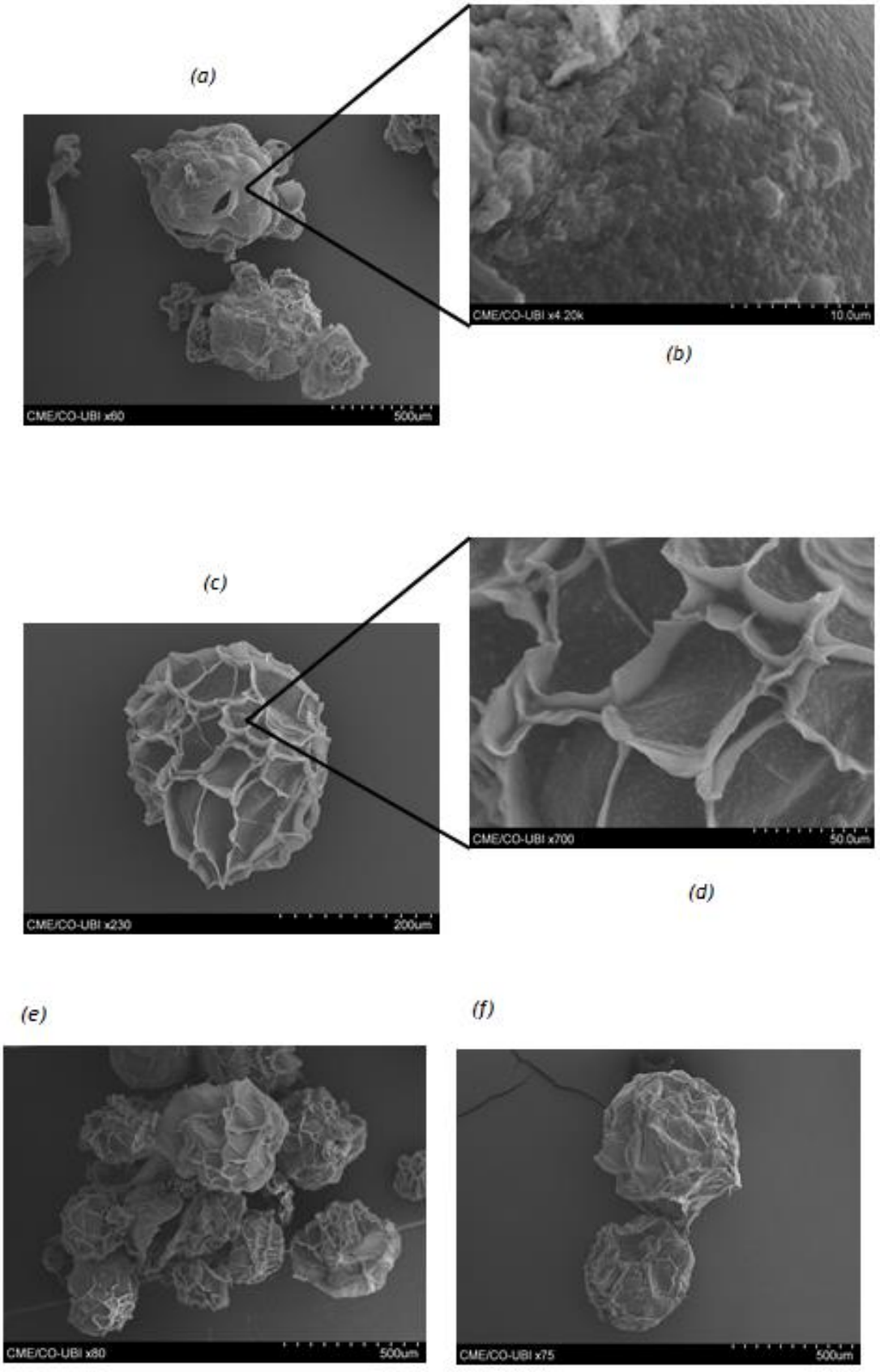

Figure 34. Representative pictures of lyophilized gellan gum beads by scanning electron microscopy (SEM). *(a)* Gellan gum bead with magnification of 60x. *(b)* Surface visualization from (a) with a magnification of 420x. *(c)* Gellan gum bead with magnification of 230x. *(d)* Surface visualization from (c) with a magnification of 700x. *(e) (f)* Gellan gum bead with magnification of 80x and 75, respectively.

The gellan gum beads show a very ordered and uniform spherical structure with some big cavity structures resembling to a “savoy cabbage” or a “honeycomb”. The outer rough surface is evident due to the presence of cracks. This alveolar structure may be due to its porosity degree. It appears that these cavities, and accordingly to the literature [79], are a great number of pores or channels which gives a rough surface to the beads. However, it is visible the absence of inner pores that drill the surface of the cavity from one side to another. These results suggest that the proteins will only bind to the surface of the bead, diminishing the total surface area that interacts with the target molecule to be purified.

3 Applicability of gellan gum beads in chromatography

Ion exchange chromatography (IEC) is one of the most powerful protein purification methods available and is frequently used in chromatographic processes. IEC separates biomolecules according to the differences in their surface charge to give high-resolution separation with high sample loading capacity [57].

After optimizing the conditions for the formulation of the gellan gum microbeads, it was intended to explore and study the possible interactions between the matrix as a stationary phase and loaded proteins on IEC. Thereby, after packaging 5 mL of an Econo-Pac column with the gellan gum beads of average size of 276.94 µm, chromatographic assays with three model proteins (BSA, α-chymotrypsin and lysozyme) were made. These assays aim to understand the sustainability and performance of the gellan matrix by exploiting its natural anionic nature and to establish the elution profiles of the proteins by taking into account their surface charge. The big advantage of using a stable gellan gum matrix resides on its anionic nature since the conventional matrices need to be functionalized with a specific ligand in order to explore the intended chromatographic interaction.

3.1 Chromatographic assays with isolated model proteins

In order to have an initial matrix characterization and to study the elution behavior of different proteins, basic assays with isolated model proteins were made. Each protein assay was constituted by two steps. First, the column was equilibrated with 10 mM MES buffer pH 6.2 and then 500 µL sample (BSA, α-chymotrypsin and lysozyme sample concentrations were 5 mg/mL, 10 mg/mL and 10 mg/mL, respectively) was loaded into the matrix under the same buffer. After elution of unbound material, the second step was imposed by changing the elution buffer to 750 mM NaCl in 100 mM $BaCl_2$ and 10 mM MES buffer pH 6.2. The addition of the barium ion in this buffer was necessary to avoid the loss of barium ions due to the

competition effect of sodium ions, maintaining the beads stability in the presence of high sodium chloride concentrations.

Figure 35 corresponds to the chromatographic profiles of the three isolated model proteins, BSA, α-chymotrypsin and lysozyme.

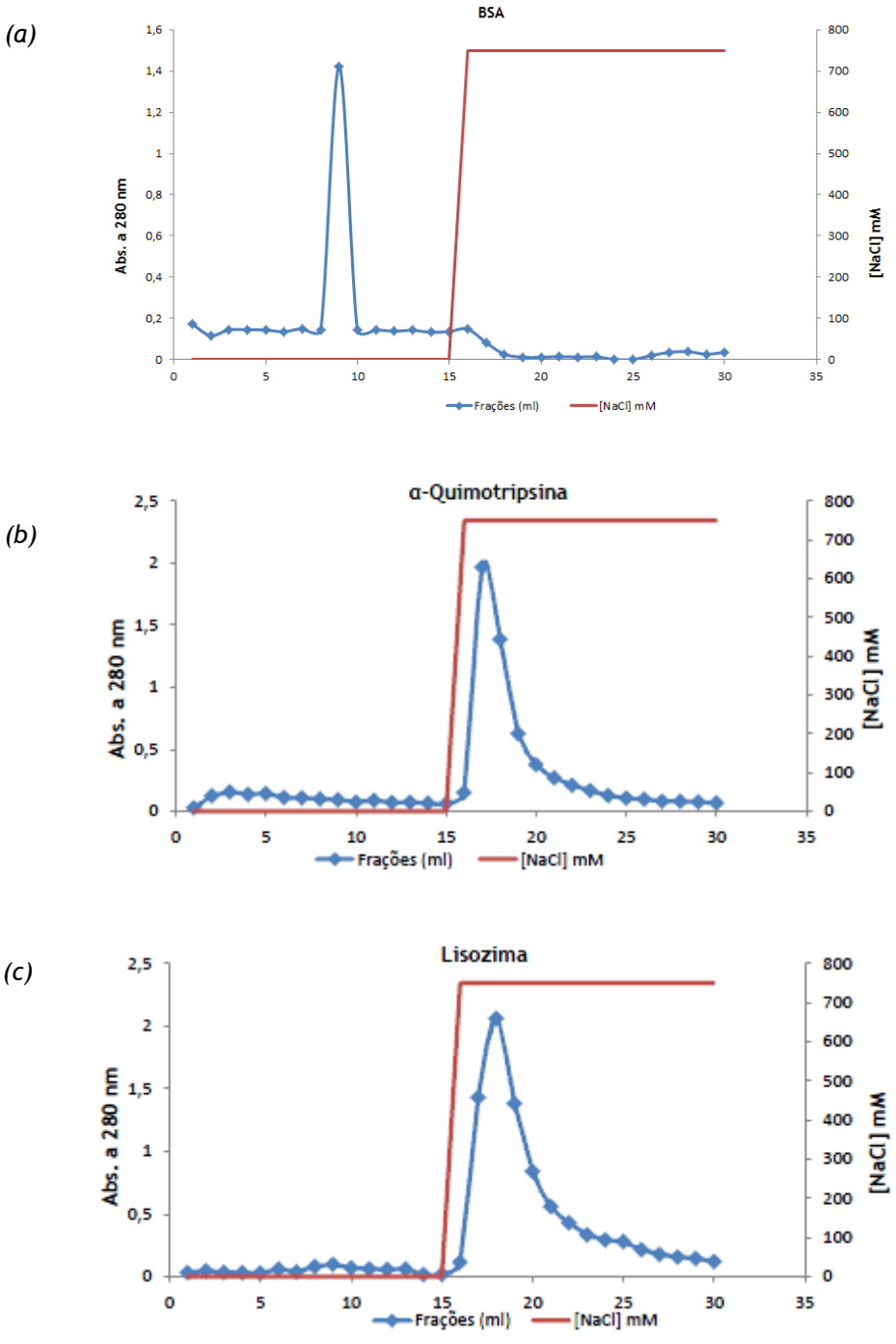

Figure 35. Chromatographic profile obtained for the isolated model proteins assay. (a) BSA. (b) α-chymotrypsin. (c) Lysozyme. The first step was performed with 10 mM MES buffer pH 6.2 and the second step was performed with 750 mM NaCl in 100 mM $BaCl_2$ and 10 mM MES buffer pH 6.2. The blue and red lines represent the absorbance at 280 nm of the fractions and salt concentration, respectively.

As expected, BSA was immediately eluted in the flowthrough and did not bind to the matrix. Given that the isoelectric point of this protein is 5.4 and the pH (pH 6.2) used in these assays had a higher value than its isoelectric point, BSA is negatively charged under these conditions and, consequently, did not interacted with the matrix, since gellan gum is also negatively charged. On the other hand, α-chymotrypsin and lysozyme proteins remained bound to the matrix after being injected. Since their isoelectric points are 8.6 and 11 respectively [49], retention was already expected because they are positively charged at this equilibirum pH. Nonetheless, the elution of these two proteins occurred when a second step with the addition of 750 mM NaCl and 100 mM $BaCl_2$ in MES buffer pH 6.2 was performed. The presence of NaCl in the buffer indicated that the interaction of α-chymotrypsin and lysozyme with the matrix was weakened by competition, resulting in its elution.

3.2 Chromatographic assays with combined model proteins

According to previous data, the separation of combined proteins should be possible due to the interaction and behavior of different charges. For the separation of BSA + α-chymotrypsin and BSA + lysozyme it was applied the previously described elution strategy for the isolated proteins, because under these equilibrium conditions BSA should be eluted and α-chymotrypsin and lysozyme should continue linked to the matrix.

Figure 36 shows the resulting chromatograms for the separation of combined BSA + α-chymotrypsin, BSA + lysozyme and α-chymotrypsin + lysozyme. For the assays of combined model proteins BSA + α-chymotrypsin and BSA + lysozyme, an equilibration step was performed with 10 mM MES buffer pH 6.2. Then, the respective sample was loaded with the same buffer, being achieved a first peak of unbound species. The elution step was performed with 750 mM NaCl in 100 mM $BaCl_2$ and 10 mM MES buffer pH 6.2 and a second peak was obtained. For the assay α-chymotrypsin + lysozyme, the column was equilibrated with 25 mM NaCl in 10 mM MES pH 6.2 and the sample was loaded with the same buffer. Furthermore, the second step was performed with 750 mM NaCl in 100 mM $BaCl_2$ and 10 mM MES buffer pH 6.2 and a second peak was obtained.

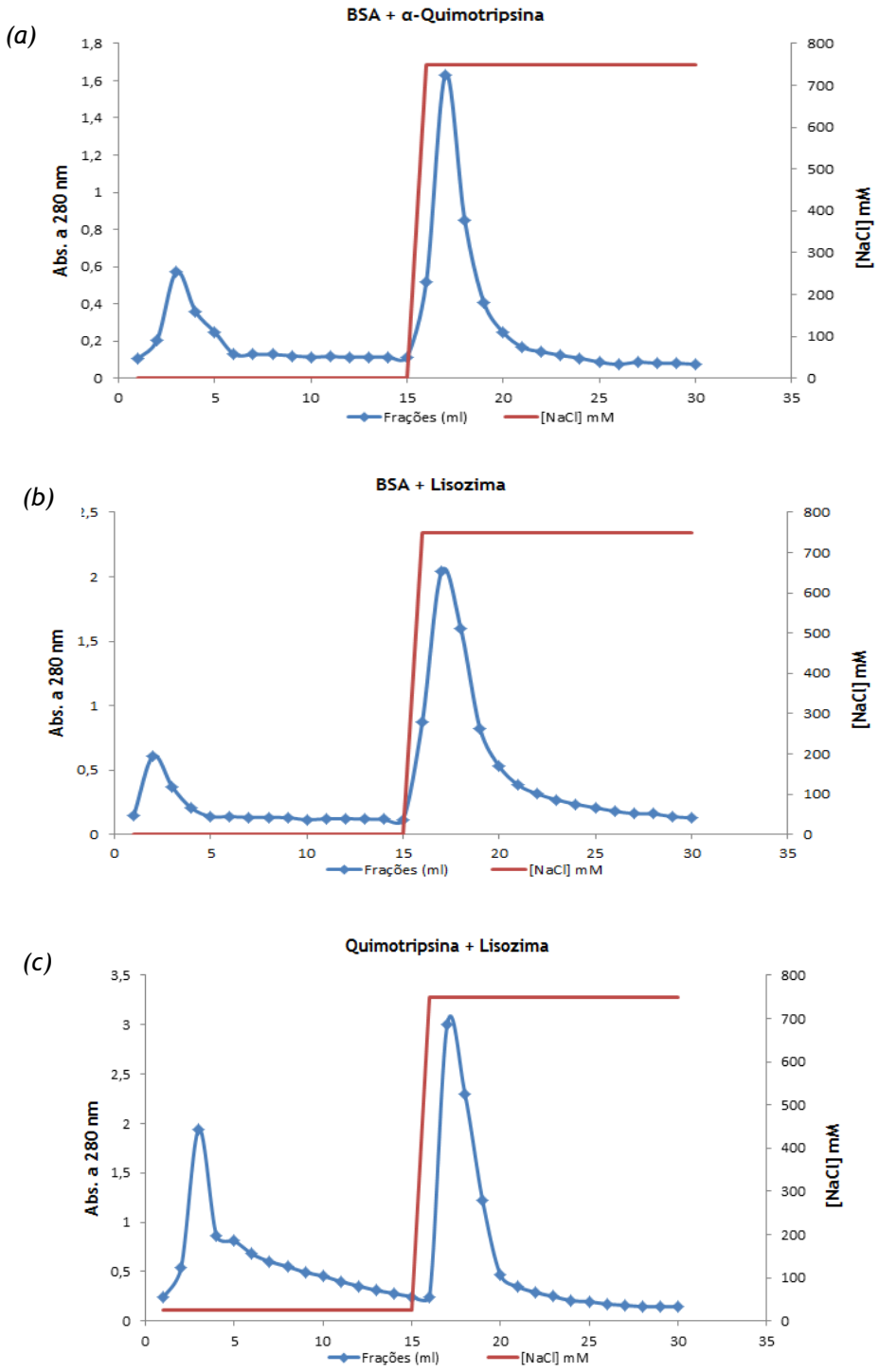

Figure 36. Chromatographic profile obtained for the combined model proteins assay. (a) BSA + α-chymotrypsin. (b) BSA + lysozyme. (c) α-chymotrypsin + lysozyme. The blue and red lines represent the absorbance at 280 nm of the fractions and salt concentration, respectively.

Figure 37 shows SDS-PAGE electrophoretic analysis of the peak fractions collected in the chromatographic assays of combined model proteins BSA + α-chymotrypsin, BSA + lysozyme and α-chymotrypsin + lysozyme. BSA, α-chymotrypsin and lysozyme molecular weights are 66 kDa [121], 25 kDa [122] and 14 kDa [123], respectively. By the visualization of Figure 37 (*a*),

we can say that lane IV is according to its BSA standard lane (lane I) whilst lane V corresponds to α-chymotrypsin since it is in accordance to lane II (α-chymotrypsin standard lane). In Figure 37 (*b*) lane IV corresponds to BSA because the bands are in the same migration zone of its standard lane (lane I) whilst lane V corresponds to lysozyme since it is in accordance to lane II (lysozyme standard lane). By visualization of Figure 37 (*c*), lane IV corresponds α-chymotrypsin because it is in agreement with the molecular weight marker and lane V is lysozyme because it matches lane II, the lysozyme´s standard lane.

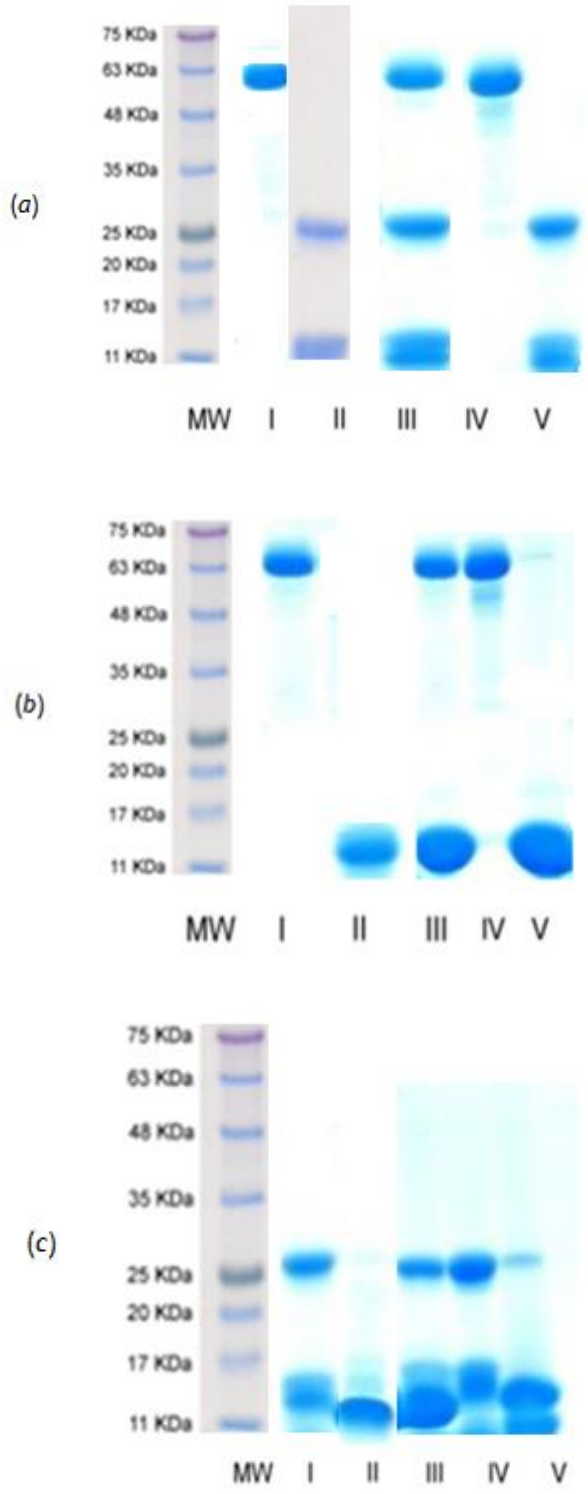

Figure 37. SDS-PAGE electrophoretic analysis of the peak fractions collected in the chromatographic assay of combined model proteins. (a) BSA + α-chymotrypsin. MW – Molecular weight standards; Lane I – BSA standard; Lane II – α-chymotrypsin standard; Lane III – sample inject onto the column; Lane IV - First peak from combined BSA + α-chymotrypsin; Lane V - Second peak from combined BSA + α-chymotrypsin (b) BSA + lysozyme. MW – Molecular weight standards; Lane I – BSA standard; Lane II – lysozyme standard; Lane III – sample inject onto the column; Lane IV - First peak from combined BSA + lysozyme; Lane V - Second peak from combined BSA + lysozyme. (c) α-chymotrypsin + lysozyme. MW – Molecular weight standards; Lane I – α-chymotrypsin standard; Lane II – lysozyme standard; Lane III - sample inject onto the column; Lane IV – First peak from combined α-chymotrypsin + lysozyme assay; Lane V – Second peak from combined α-chymotrypsin + lysozyme assay.

By analyzing the obtained peaks in Figure 36, and the electrophoretic assays in Figure 37, chromatographic profiles of the model proteins can be outlined and the results evidently indicate that a good separation occurred between them. In the BSA + α-chymotrypsin and BSA + lysozyme assays, since BSA has the same net charge than the matrix, this protein was, as expected, immediately eluted in the flowthrough, whilst α-chymotrypsin and lysozyme were eluted in the second peak. Unlike BSA, α-chymotrypsin and lysozyme were positively charged due to its isoelectric points be higher than the buffer pH value (6.2), which favored the interaction with the negatively charged matrix. The elution of α-chymotrypsin and lysozyme by increasing the NaCl concentration indicated that the ionic interaction was weakened by competition.

To determine the interaction force of α-chymotrypsin and lysozyme proteins to the matrix, a screening of several NaCl concentrations was performed in order to find a concentration in which one protein is eluted and the other not. The best separation between α-chymotrypsin and lysozyme was obtained when 25 mM NaCl was applied in the equilibrium buffer and α-chymotrypsin eluted while lysozyme was still linked to the gellan matrix. Lysozyme elution only happened when the buffer changed to 750 mM NaCl in 100 mM $BaCl_2$ and 10 mM MES buffer pH 6.2. As α-chymotrypsin elution occurred with lower NaCl concentration and lysozyme elution needed a greater amount of NaCl, we can say that the interactions of this protein with the gellan gum matrix are weaker than the interactions with lysozyme.

After studying the model proteins and its combination two by two, we proceeded to combining the three model proteins in simultaneous. This assay consisted in a three steps procedure. The column was equilibrated with 10 mM MES buffer pH 6.2 and the sample was loaded under the same buffer. After elution the unbound material, a second step was performed with 25 mM NaCl in 10 mM MES buffer pH 6.2 and a second peak was obtained. Finally, the third peak was eluted when the elution buffer was changed to 750 mM NaCl in 100 mM $BaCl_2$ and 10 mM MES buffer pH 6.2. Figure 38 shows the chromatographic profile resultant of the three combined model proteins and it is clear that different interactions occurred with the gellan gum matrix.

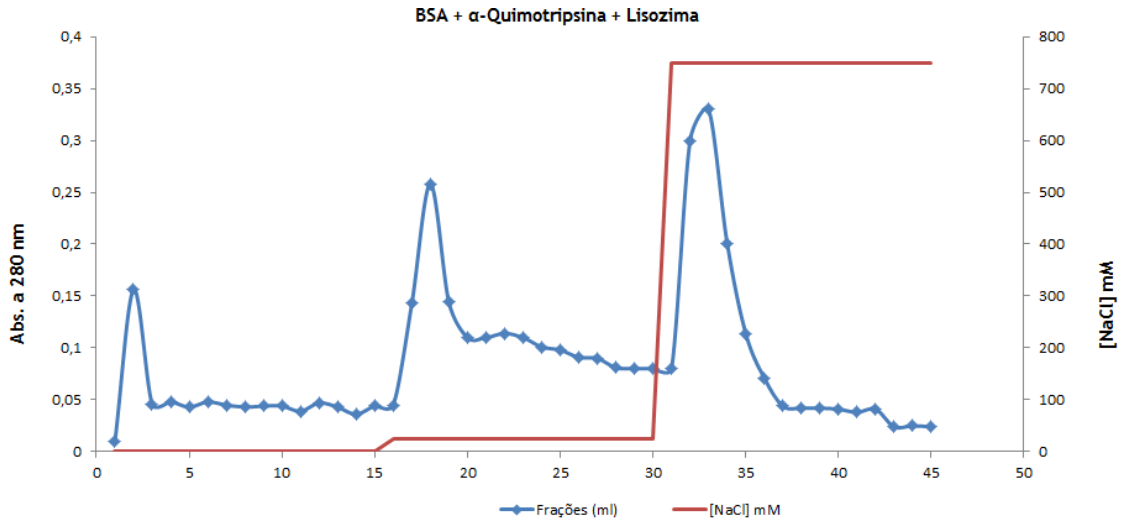

Figure 38. Chromatographic profile obtained for the combined model proteins assay. BSA + α-chymotrypsin + lysozyme. The first step was performed in 10 mM MES buffer pH 6.2, the second step was performed with 25 mM NaCl in 10 mM MES buffer pH 6.2 and the third step was performed with 750 mM NaCl in 100 mM $BaCl_2$ and 10 mM MES buffer pH 6.2. The blue and red lines represent the absorbance at 280 nm of the fractions and salt concentration, respectively.

Figure 39 shows the SDS-PAGE electrophoretic analysis with Comassie brilliant blue staining of the peak fractions collected in the chromatographic assay of combined model proteins BSA + α-chymotrypsin + lysozyme. Lane V is according to lane I (BSA standard), concluding that lane V corresponds to BSA that eluted in the first step. The bands appeared around 66 kDa [121], which is according to its molecular weight. Lane VI corresponds to α-chymotrypsin, because it was in accordance with line II, which matches to its standard. This protein has a molecular weight of around 25 kDa [122] and electrophoretic bands appeared around this value. Lane VII corresponds to lysosome, because its molecular weight is around 14 KDa [123] and the band is in agreement with the molecular weight marker. Also, when compared with the lysozyme standard, lane III, bands are in the same zone of migration. We can conclude that these results indicate that a clearly good separation occurred between BSA, α-chymotrypsin and lysozyme.

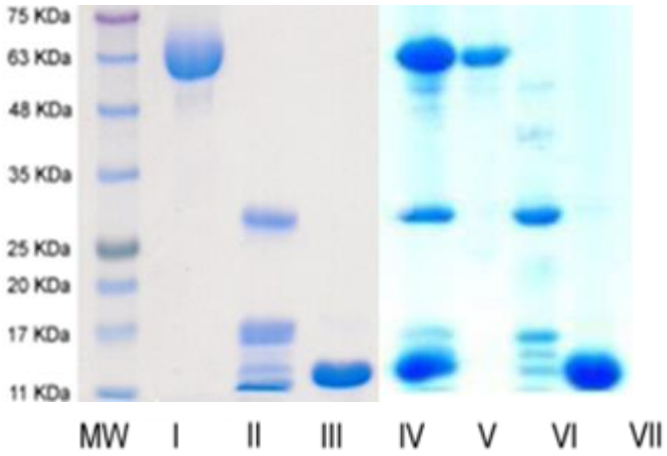

Figure 39. SDS-PAGE electrophoretic analysis of the peak fractions collected in the chromatographic assay of combined model proteins, BSA + α-chymotrypsin + lysozyme. MW – Molecular weight standards; Lane I – BSA standard; Lane II – α-chymotrypsin standard; Lane III – lysozyme standard; Lane IV – sample inject onto the column; Lane V – First peak from combined BSA + α-chymotrypsin + lysozyme assay; Lane VI – Second peak from combined BSA + α-chymotrypsin + lysozyme assay; Lane VII – Third peak from combined BSA + α-chymotrypsin + lysozyme assay.

By the visualization of Figures 38 and 39, we can say that BSA was eluted in the first step, which means that this protein was not bound to the matrix. In the second step, in order to cause the elution of α-chymotrypsin, only 25 mM NaCl was added to the 10 mM MES buffer pH 6.2 because this protein has a weak interaction with the matrix. In the third step, the NaCl concentration was again increased to 750 mM and the lysozyme, which promoted the stronger interaction to the gellan matrix, was eluted by salt competition.

After evaluating all the chromatograms and SDS-PAGE electrophoresis, it was concluded that gellan gum microbeads matrix reveals a behavior of cation exchange support that allows protein elution by salt manipulation.

3.3 Chromatographic assays with catechol-*O*-methyltransferase (COMT)

Since a good separation occurred between BSA, α-chymotrypsin and lysozyme, we intended to explore possible interactions between the matrix and a more complex protein, recombinant human soluble catechol-*O*-methyltransferase (hSCOMT), aiming its purification from a simple *P. pastoris* lysate by ion exchange chromatography.

For this assay, it was injected 1 mL of COMT sample (pre-purified by IMAC and concentrated by concentrators) into the column to study the profile that this enzyme had in the matrix and its chromatographic elution behavior based on its isoelectric point. This assay consisted in a three steps procedure. First, the column was equilibrated with 10 mM MES buffer pH 6.2 and

the sample was loaded under the same buffer. After elution of unbound material, a second step was performed with 100 mM NaCl in 50 mM $BaCl_2$ and 10 mM MES buffer pH 6.2. Finally, a third peak was obtained when the elution buffer was changed to 750 mM NaCl in 100 mM $BaCl_2$ and 10 mM MES buffer pH 6.2 (Figure 40).

Fractions of 1 mL were collected in each chromatographic step, then the absorbance of the collected fractions were monitored at 280 nm and, at last, the fractions corresponding to the chromatographic peaks were concentrated and desalted in centrifuges Macrosep® Advance.

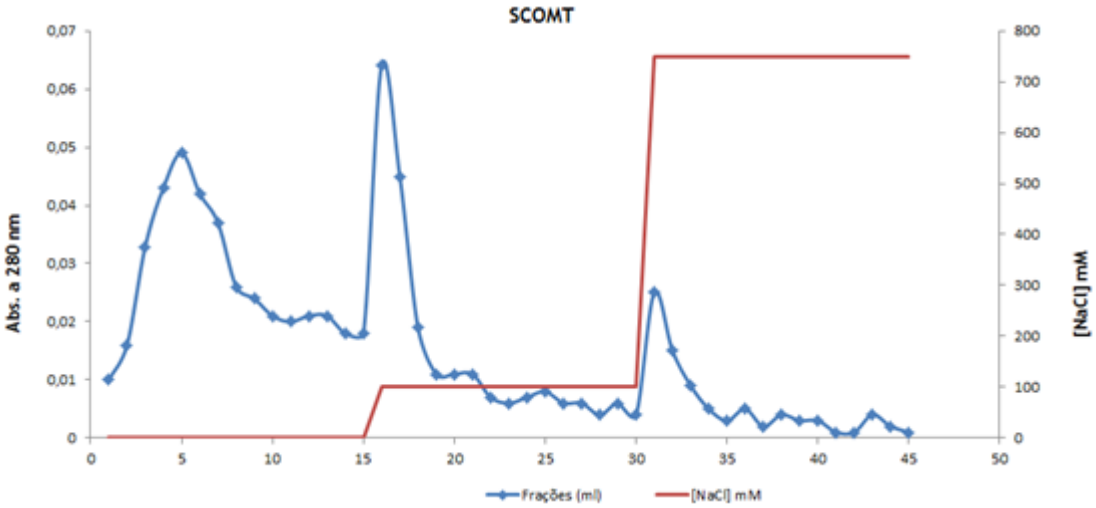

Figure 40. Chromatographic profile obtained for the pre-purified SCOMT protein assay. The first step was performed in 10 mM MES buffer pH 6.2, the second step was performed with 100 mM NaCl in 50 mM $BaCl_2$ and 10 mM MES buffer pH 6.2 and the third step was performed with 750 mM NaCl in 100 mM $BaCl_2$ and 10 mM MES buffer pH 6.2. The blue and red lines represent the absorbance at 280 nm of the fractions and salt concentration, respectively.

To confirm these results and validate these data, SDS-PAGE electrophoretic analysis with silver staining of the peak fractions collected in the chromatographic assay of SCOMT and dot-blot analysis were made, as we can see in Figure 41. Lane II is according to lane I (SCOMT sample injected in the gellan gum matrix), concluding that lane II corresponds to SCOMT that eluted in the first step. The band appeared around 25 kDa [124], which is according to its molecular weight. Lanes III and IV correspond to the second and third peak, respectively. Lane III and IV did not contain SCOMT, confirmed by SDS-PAGE electrophoresis and dot-blot. This may be due to the fact that peak 2 and peak 3 from the chromatogram are contaminants that, in a very small concentration, did not showed up in the gel. Moreover, as known, dot-blot is a highly specific method for SCOMT and the fact that lane III and lane IV did not appeared in the dot-blot analysis, supports the fact that those obtained peaks are, in fact, contaminants.

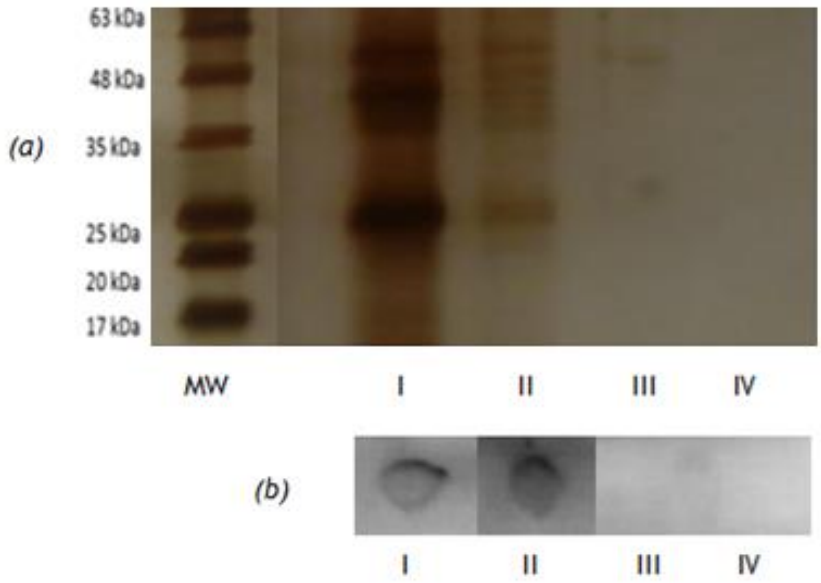

Figure 41. (a) SDS-PAGE electrophoretic analysis with silver staining of the peak fractions collected in the chromatographic assay of pre-purified SCOMT. (*b*) Dot-blotting analysis of the peak fractions collected in the chromatographic assay of pre-purified SCOMT. MW – Molecular weight standards; Lane I – Pre-purified SCOMT sample that was injected in the gellan gum matrix; Lane II – First peak from the assay; Lane III – Second peak from the assay; Lane IV Third peak from the assay.

Therefore, the results revealed that SCOMT did not bind to the matrix and was immediately eluted in the flowthrough of the first peak, together with other contaminant proteins as is visible in the electrophoresis. Given that the isoelectric point of this protein is 5.2 and the pH used in these assays (pH 6.2) had a higher value than its isoelectric point, SCOMT was negatively charged and, consequently, did not interacted with the matrix, due to the also negative character of gellan gum.

Thus, a new chromatographic assay was performed by changing the pH of the equilibrium step in order to favor the SCOMT retention. Since the SCOMT isoelectric point is 5.2 and we wanted the protein to assume a positive charge, the equilibration buffer solution was changed to a citrate buffer pH 4.0 (since an acid pH was intended).

This assay consisted in a four steps procedure. First, the column was equilibrated with 10 mM citrate buffer pH 4.0 and the sample was loaded under the same buffer. After elution the unbound material, a second step was performed with 10 mM MES buffer pH 6.4. Then, the third step was done with 100 mM NaCl in 50 mM $BaCl_2$ and 10 mM MES buffer pH 6.4. Finally, the fourth peak was eluted when the elution buffer was changed to 750 mM NaCl in 100 mM $BaCl_2$ and 10 mM MES buffer pH 6.4 (Figure 42).

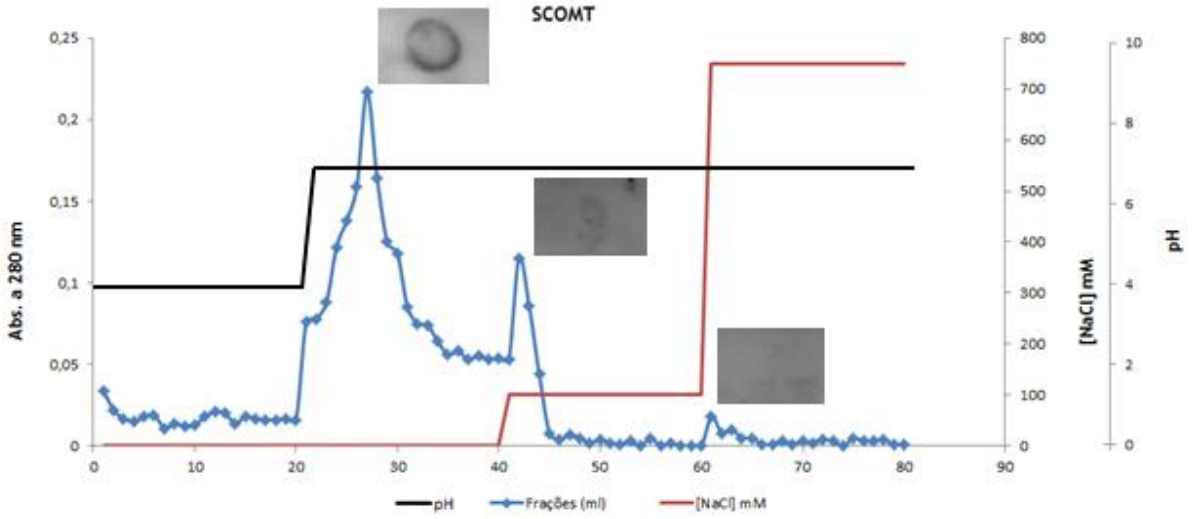

Figure 42. Chromatographic profile obtained for the pre-purified SCOMT protein and respective dot-blot analysis. The first step was performed in 10 mM citrate buffer pH 4.0 without salt addition; the second step was performed with 10 mM MES buffer pH 6.4 without salt addition; the third step was performed with 100 mM NaCl in 50 mM $BaCl_2$ and 10 mM MES buffer pH 6.4 and the fourth step was performed with 750 mM NaCl in 100 mM $BaCl_2$ and 10 mM MES buffer pH 6.4. The blue, red and black lines represent the absorbance at 280 nm of the fractions, salt concentration and pH values, respectively.

Figure 43 shows the SDS-PAGE electrophoretic analysis of the peak fractions collected in the second chromatographic assay of SCOMT. Lane I corresponds to the pre-purified SCOMT sample with all its contaminants that was injected in the gellan gum matrix. The band in lane II, which corresponds to the first peak of the chromatogram in Figure 42, appeared around 25 kDa [124], matching the molecular weight of SCOMT. Lanes III and IV correspond to the second and third peak, respectively.

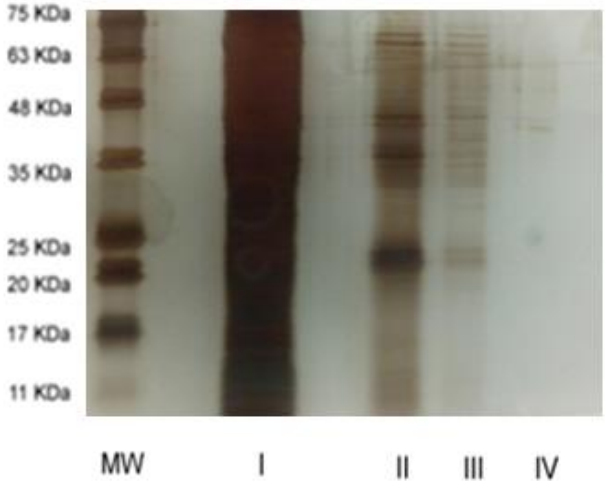

Figure 43. SDS-PAGE electrophoretic analysis with silver staining of the peak fractions collected in the chromatographic assay of pre-purified SCOMT. MW – Molecular weight standards; Lane I – Pre-purified SCOMT sample that was injected in the gellan gum matrix; Lane II – First peak from the assay; Lane III – Second peak from the assay; Lane IV Third peak from the assay.

Through the analysis of elution by dot-blot (Figure 42) and SDS-PAGE electrophoretic gel (Figure 43), it can be observed that SCOMT was retained at pH 4.0 and was eluted essentially at two different fractions at distinct NaCl concentrations. The major fraction is eluted on the first obtained peak at 10 mM MES buffer pH 6.4 with no addition of sodium chloride, resulting on an immunological active strong stain on dot-blot and a strong lane in SDS-PAGE. The second obtained peak, which resulted from the addition of 100 mM NaCl in 50 mM $BaCl_2$ and 10mM MES buffer pH 6.4, shows a weak stain on dot-blot and a weak lane on SDS-PAGE. The third peak shows no signs of SCOMT elution, result which is supported by the absence of any dot or lane on both analysis.

Given that isoelectric point of SCOMT is 5.2 and in this assay the pH used in the equilibration step was 4.0, the protein was positively charged and, consequently, it interacted and was bound with the negatively charged gellan gum matrix in equilibrium conditions. Therefore, to promote the successful SCOMT elution and taking into account the protein isoelectric point, a change in the pH of the buffer was performed. The addition of NaCl in the two last buffer solutions was in order to guarantee the removal of all contaminants and any vestigial protein still bounded to the matrix by weakening its interactions by salt competition.

These results suggest that gellan gum matrix has the capacity to retain the SCOMT sample injected onto the column. However, also other contaminants proteins elute along with the SCOMT at pH 6.4. In order to try the isolation of SCOMT from contaminants, a new chromatographic assay was made, by introducing a new pH step.

This third assay consisted in a four steps procedure. First, the column was equilibrated with 10 mM citrate buffer pH 4.0 and the sample was loaded under the same buffer. After elution the unbound material, a second step was performed with 10 mM citrate buffer pH 5.4. Then, the third step was done with 10 mM MES buffer pH 6.4. Finally, the fourth peak was eluted when the elution buffer was changed to 750 mM NaCl in 100 mM $BaCl_2$ and 10 mM MES buffer pH 6.4 (Figure 44).

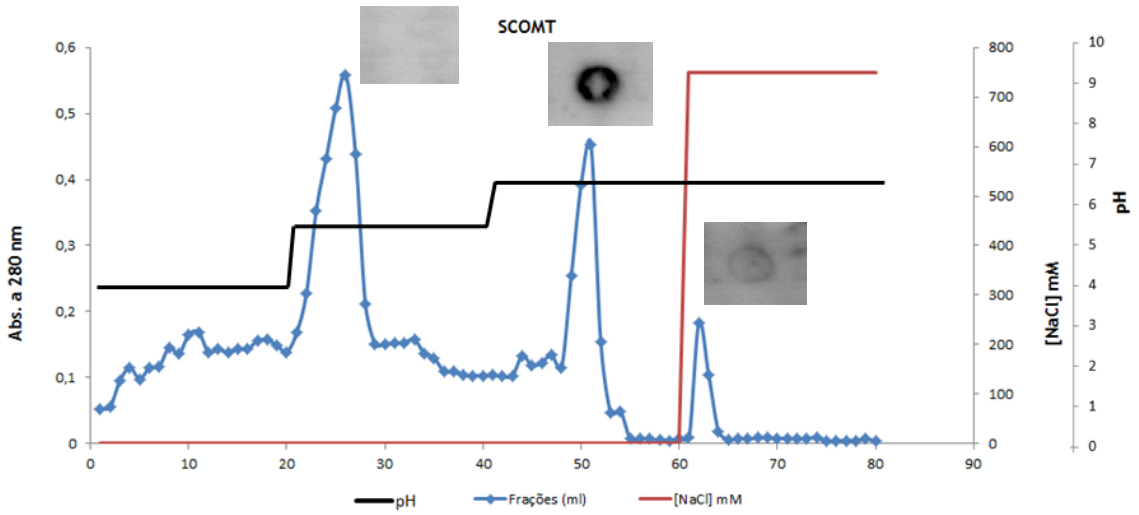

Figure 44. Chromatographic profile obtained for the pre-purified SCOMT protein and respective dot-blot analysis. The first step was performed in 10 mM citrate buffer pH 4.0 without salt addition; the second step was performed with 10 mM MES buffer pH 5.4 without salt additon; the third step was performed with 10 mM MES buffer pH 6.4 without salt addition and the fourth step was performed with 750 mM NaCl in 100 mM $BaCl_2$ and 10 mM MES buffer pH 6.4. The blue, red and black lines represent the absorbance at 280 nm of the fractions, salt concentration and pH values, respectively.

Figure 45 shows the SDS-PAGE electrophoretic analysis of the peak fractions collected in the last chromatographic assay of SCOMT. Lane I corresponds to the pre-purified SCOMT sample with all its contaminants that was injected in the gellan gum matrix. Lane II matches the first obtained peak whilst lane III corresponds to the second peak and has a band that appeared at 25 kDa, which is according to the molecular weight of SCOMT. Lane IV corresponds to the third peak of the chromatogram.

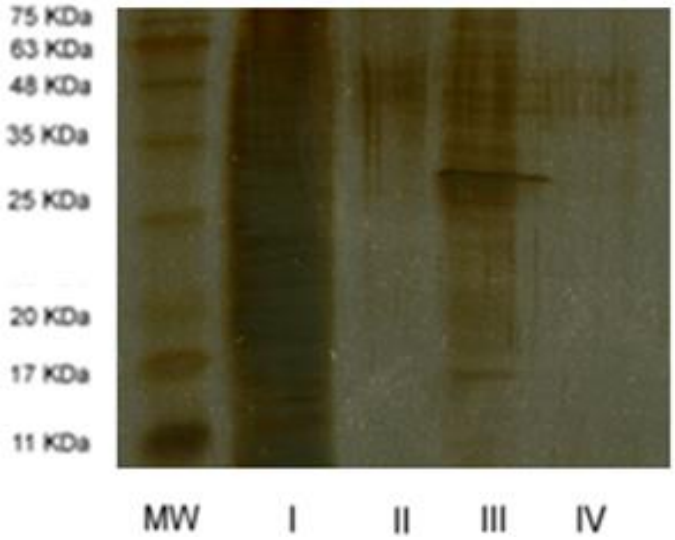

Figure 45. SDS-PAGE electrophoretic analysis with silver staining of the peak fractions collected in the chromatographic assay of pre-purified SCOMT. MW – Molecular weight standards; Lane I – Pre-purified SCOMT sample that was injected in the gellan gum matrix; Lane II – First peak from the assay; Lane III – Second peak from the assay; Lane IV Third peak from the assay.

By interpreting the information from the chromatogram, dot-blot analysis and SDS-PAGE electrophoretic assay, SCOMT was retained at pH 4.0 and major elution occurred on the second peak at 10 mM MES buffer pH 6.4, which corresponds to lane III of the SDS-PAGE analysis that evidence a strong band as well as an immunological active strong stain on the dot-blot assay. Lane II corresponds to the first peak obtained in the chromatogram, at buffer pH 5.4, containing only impurities, not showing any SCOMT evidence in the dot-blot analysis. The last peak, which resulted from the addition of 750 mM NaCl in 100 mM $BaCl_2$ and 10 mM MES buffer pH 6.4, shows no visible evidence in the electrophoretic assay (lane IV), however, a weak vestigial stain in the dot-blot analysis is visible.

These results indicate that SCOMT was retained in the matrix in equilibration conditions due to its positive charge and successful elution was performed when a change in pH value was applied. At buffer pH 5.4 part of contaminants were eluted and it was not visible any signal of SCOMT. This may be due to the proximity to the SCOMT´s isoelectric point (5.2), where it assumes neutral charge. Thus, the majorly successful protein elution was only verified when the difference was, at least, one pH value above its isoelectric point (10 mM MES buffer pH 6.4). In the last buffer, it was added sodium chloride to remove the remaining contaminants and any target protein still bound to the matrix. In this step, it was verified a small weak stain in the dot-blot analysis, which means that SCOMT interacted with the matrix and, although its primarily elution occurred with pH manipulation, the salt competition also had the capacity to remove the protein from the chromatographic support, despite of its vestigial concentration.

After analysis of all the data, we can conclude that the gellan gum microbeads matrix reveals a behavior of cation exchange support that allows the elution of proteins either by salt or pH manipulation. However, to more complex proteins, like SCOMT, further assays and studies are needed in order to obtain the biomolecule in a higher purity state with elimination of all contaminants proteins from the injected sample.

4 Dynamic binding capacity (DBC)

In order to characterize the application of the gellan gum beads as a new matrix in purification processes, dynamic binding capacity studies were made. DBC of a chromatographic media evaluates the amount of target protein that will bind to the matrix under adequate binding conditions until it reaches the saturation of the matrix.

Determination of dynamic binding capacity was carried out by recording breakthrough curves and calculating the amount of bound lysozyme per mL support at 10 % and 50 % of breakthrough curve. This assay was performed accordingly the experimental design conditions

and the column was equilibrated with 10 mM MES buffer pH 6.2. Then, the matrix was overloaded with 0.5 mg/mL of lysozyme in 10 mM MES buffer pH 6.2, at a flow rate of 1 mL/min. Afterwards, the elution of the bound lysozyme was achieved by increasing the ionic strength to 750 mM NaCl in 100 mM $BaCl_2$ and 10 mM MES buffer pH 6.2.

Dynamic binding capacity values were then obtained (Figure 46) by subtracting the value obtained under non-binding conditions, according follow equation:

$$\mathrm{DBC} = \frac{(\mathrm{VL} - \mathrm{V0}) \times \mathrm{Cp}}{\mathrm{Vc}} \quad (4)$$

where DBC is the dynamic binding capacity (mg/mL), VL corresponds to the volume loaded up to the breakthrough point (mL), V0 is the void volume of the column (mL), Cp corresponds to the concentration of protein (mg/mL) and Vc is the volume of the columns (mL) [49].

Figure 46 represents the breakthrough curve of the dynamic binding capacity assay of the gellan gum microbeads matrix. The values of DBC obtained at 10 % and 50 % are 2.43 mg/mL and 4.73 mg/mL, respectively. Taking into account that the binding of the protein only occurred at the external surface, fact that diminishes the total surface area that interacts with the target molecule, we can say that the capacity values obtained are satisfactory and strengthens the applicability of gellan gum beads matrix in chromatographic processes.

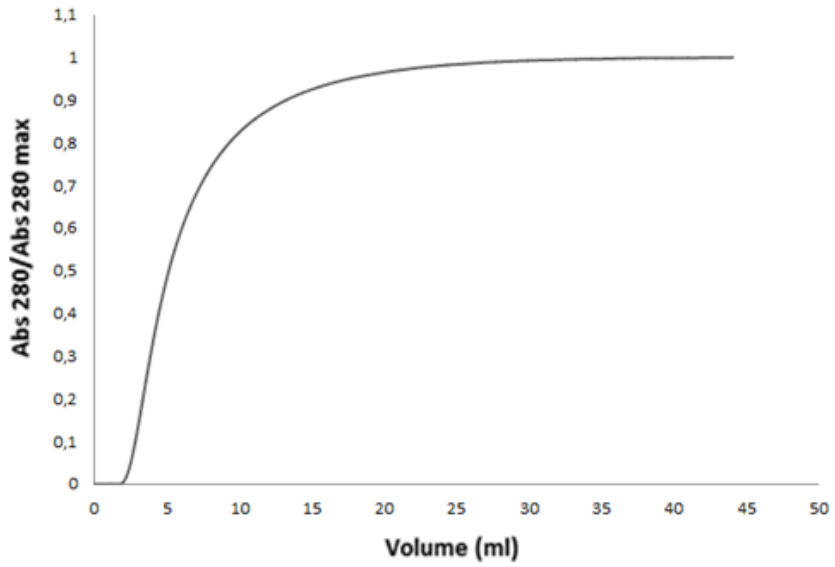

Figure 46. Dynamic binding capacity of gellan gum beads for 0.5 mg/mL solution lysozyme at 1 mL/min flow rate.

Table 16 shows DBC values of several chromatographic matrices with different structural properties and different ligands. For cation exchange chromatographic matrices (Fractogel SE HICAP (M), MacroPrep CM and SP Toyopearl 650m), values varied from 18 to 37 mg/mL, at 10 % and from 30 to 60 mg/mL at 50 % of breakthrough curves. For matrices used in affinity chromatography (Heparin Sepharose FF, Heparin and Heparin Toyopearl 650m Ceramic HYPERD M) range of values obtained at 10% and 50% of breakthrough curves were from 4 to 20 mg/mL and from 5 to 24 mg/mL, respectively [49].

Table 16. Dynamic binding capacity of cation-exchange resins and heparin for 0.5 mg/ml solution lysozyme (modified from [125].

Resin	*Flow rate (mL/min)*	*Lysozyme concentration (mg/mL)*	*Dynamic binding capacity (mg/mL)*	
			10 %	*50 %*
Fractogel SE HICAP (M)	1.3	1.0	37.0	60.0
MacroPrep CM	2.5	1.0	18.0	30.0
SP Toyopearl 650m	1.3	1.0	30.0	42.0
Heparin Sepharose FF	0.6	1.0	4.0	5.0
Heparin Toyopearl 650m	1.3	1.0	17.0	21.0
Heparin Ceramic HyperD M	4.0	1.0	20.0	24.0
Gellan gum beads	1.0	0.5	2.43	4.73

These values represent the functionality of the immobilized ligands at each support. DBC values of the present work, an innovative chromatographic matrix, are lower than the values of the commercial matrices used in cation exchange chromatography but, when comparing with the ones used in affinity chromatography, they are similar and satisfactory. Nonetheless, immobilization of specific ligands, as well as the formation of inner pores which increases the total surface area, can improve these values and be a good possibility to increase the support binding capacity of the gellan gum beads in the future.

Chapter V

Conclusion

The chromatographic technology is undoubtedly one of the most diverse and powerful purification methods for downstream process applications. The development of techniques and methods for protein separation and purification has been, over the years, essential for many of the advancements in biotechnology research.

Gellan gum is a natural exopolysaccharide with several versatile applications in different technological and industrial sectors due to its gelling ability. In a novel chromatographic approach, the proposed aim of this work was the optimization of gellan gum as a stable stationary phase by formulating an innovative gellan gum microbead support using an emulsion technique and design of experiments. Moreover, it was studied its applicability as a chromatographic matrix in the purification of model proteins, BSA, α-chymotrypsin and lysozyme, and a more complex biomolecule, human soluble catechol-*O*-methyltransferase (hSCOMT).

In order to formulate the gellan gum microbeads, the strategy adopted was an easy and low-cost water-in-oil emulsion technique. This method is advantageous for industrial purposes, since it can be easily scaled-up, it does not require expensive and complex instruments, and it is easy to control the process parameters. This manufacturing technique allowed, with the application of central composite design, the optimization of the chromatographic support by studying the effects and interactions between the different parameters used in the bead formation. In order obtain beads with minimum diameter (277.08 μm) the ideal conditions given by the experimental design application were 1.41 % gellan concentration, 749.47 rpm as stirring velocity and 99.20 ºC. To formulate this chromatographic support, it was necessary the presence of divalent ions in a reinforcer solution where the formed beads were hardened in order to give higher stability to the matrix. The chosen ion was barium because it is considered to be very effective in the gelation of gellan and, due to its large ionic size, it contributes to the formation of a rigid network with high tensile strength. Moreover, it allowed the formation of smaller and uniform microspheres with low swelling ratio. To obtain a detailed analysis of size and microscopic structure of the gellan gum beads, scanning electron microscopy was used, which allowed to evaluate the surface topography, morphology, reticulation and porosity of the spheres.

Gellan gum is as anionic polymer, so it can be used in cation exchange chromatography without the need of first being functionalized like other commercial chromatographic supports. Fact that constitutes an industrial valuable asset in purification of pharmacological biomolecules since the cost associated to the production of chromatographic matrices can be diminished. In this context, the applicability of gellan gum bead matrix was tested with BSA, α-chymotrypsin, lysozyme and hSCOMT. The interaction of the support with the loaded proteins was established in different levels. BSA did not interact with the matrix, while α-chymotrypsin and lysozyme were retained to the column, being eluted at different NaCl concentrations. As to SCOMT, it also was retained in the matrix, being majorly eluted and partially purified by pH manipulation. In fact, this gellan gum bead matrix revealed different interaction forces with positively charged proteins, which it is reflected in a characteristic chromatographic behavior.

In order to characterize this innovative support, it was determined the dynamic binding capacity. For this matrix, DBC values are according to the commercial resin values and are satisfactory, taking into account that the proteins only interacted with the surface of the microbeads.

This work represents a chromatographic approach of a new chromatographic support made by gellan gum microbeads by an innovative water-in-oil emulsion technique. Since it is an initial study, adapting the matrix to specific objectives is required in order to continue the characterization and applicability of the gellan gum beads in chromatographic processes, and, subsequently improve and get the best benefit from its use.

Chapter VI

Future perspectives

Since gellan gum microbeads application as a chromatographic matrix is a new approach, several chromatographic parameters have yet to be studied. In this context, binding strength, compressibility, swelling capacity and porosity assessment studies should be made. Moreover, gellan gum properties that allow increase the stability for separation purpose ought to be screened.

Also gellan gum matrix modifications with specific ligands should be explored in order to discover other chromatographic types, since it would give a versatility of interactions to this innovative chromatographic support with countless target molecules with different characteristics.

Gellan gum already interacts with more complex proteins, namely pre-purified SCOMT, however, it did not totally separated the target protein from all the other protein contaminants. A more efficient salt and pH manipulation is in order to obtain the enzyme in a higher state of purity. In addition, enzymatic activity studies also should be performed with the purified SCOMT to evaluate its functionality.

The gellan gum microbeads were handmade produced, without any mechanical system support. In order to optimize and standardize this manufacturing process, a method for micro or nanoparticles production should be adopted. The electrospinning technique seems to be adequate, plus, it has the advantage of controlling the flow rates and allows the formation of μm-sized drops using channels, which result in the production of beads with smaller diameter, at a nanoscale size.

In the future, if these studies are considered and conciliated with specific purification objectives, gellan gum microbeads can gain even more relevance and lead to a more important role in biotechnological industry.

Chapter VII

References

[1] F. Freitas, V. D. Alves, and M. A. M. Reis, "Advances in bacterial exopolysaccharides: From production to biotechnological applications," *Trends Biotechnol.*, vol. 29, no. 8, pp. 388–398, 2011.

[2] A. S. Kumar, K. Mody, and B. Jha, "Bacterial exopolysaccharides - A perception," *J. Basic Microbiol.*, vol. 47, no. 2, pp. 103–117, 2007.

[3] C. Roca, V. D. Alves, F. Freitas, and M. A. M. Reis, "Exopolysaccharides enriched in rare sugars: bacterial sources, production, and applications," *Front. Microbiol.*, vol. 6, no. April, pp. 1–7, 2015.

[4] F. Paul, A. Morin, and P. Monsan, "Microbial polysaccharides with actual potential industrial applications.," *Biotechnol. Adv.*, vol. 4, no. 2, pp. 245–259, 1986.

[5] K. S. Kang, G. T. Veeder, P. J. Mirrasoul, T. Kaneko, and I. W. Cottrell, "Agar-like polysaccharide produced by a pseudomonas species: production and basic properties.," *Appl. Environ. Microbiol.*, vol. 43, no. 5, pp. 1086–1091, 1982.

[6] M. Takeuchi, H. Sawada, H. Oyaizu, and A. Yokota, "Phylogenetic evidence for Sphingomonas and Rhizomonas as nonphotosynthetic members of the alpha-4 subclass of the Proteobacteria.," *Int. J. Syst. Bacteriol.*, vol. 44, no. 2, pp. 308–314, 1994.

[7] E. Yabuuchi and I. Yano, "Proposals of Sphingomonas paucimobilis gen . nov . and comb . nov ., Sphingomonas parapaucimobilis sp . nov ., Sphingomonas yanoikuyae sp . nov ., Sphingomonas adhaesiva sp . nov ., Sphingomonas capsulata comb . nov ., and Two Genospecies of the Genus Sph," vol. 34, no. 2, pp. 99–119, 1990.

[8] R. M. Banik, B. Kanari, and S. N. Upadhyay, "Exopolysaccharide of the gellan family: Prospects and potential," *World J. Microbiol. Biotechnol.*, vol. 16, no. 5, pp. 407–414, 2000.

[9] I. Sá-Correia, A. M. Fialho, P. Videira, L. M. Moreira, A. R. Marques, and H. Albano, "Gellan gum biosynthesis in Sphingomonas paucimobilis ATCC 31461: genes, enzymes and exopolysaccharide production engineering.," *J. Ind. Microbiol. Biotechnol.*, vol. 29, no. 4, pp. 170–176, 2002.

[10] C. J. Ferris, K. J. Gilmore, G. G. Wallace, and M. Panhuis, "Modified gellan gum hydrogels for tissue engineering applications," *Soft Matter*, vol. 9, no. 14, p. 3705, 2013.

[11] R. Chandrasekaran, R. P. Millane, and S. Arnott, "Gellan is a nonsulfated , anionic , extracellular polytetrasaccharide secreted by the bacterium Auromonas elodea . It is potentially useful in the food industry because of its gel-forming properties . The molecular basis of these properties had been inves," vol. 175, pp. 1–15, 1988.

[12] E. R. Morris, K. Nishinari, and M. Rinaudo, "Gelation of gellan - A review," *Food Hydrocolloids*, vol. 28, no. 2. Elsevier Ltd, pp. 373–411, 2012.

[13] H. Moritaka, H. Fukuba, K. Kumeno, N. Nakahama, and K. Nishinari, “Effect of monovalent and divalent cations on the rheological properties of gellan gels,” *Food Hydrocoll.*, vol. 4, no. 6, pp. 495–507, 1991.

[14] R. Chandrasekaran and V. G. Thailambal, “The influence of calcium ions, acetate and l-glycerate groups on the gellan double-helix,” *Carbohydr. Polym.*, vol. 12, no. 4, pp. 431–442, 1990.

[15] R. Chandrasekaran and A. Radha, “Molecular architectures and functional properties of gellan gum and related polysaccharides,” *Trends Food Sci. Technol.*, vol. 6, no. 5, pp. 143–148, 1995.

[16] G. R. SANDERSON, *Gellan gum*, Peter Harr. Elsevier Ltd, 1990.

[17] G. Sworn, G. R. Sanderson, and W. Gibson, “Gellan gum fluid gels,” *Food Hydrocoll.*, vol. 9, no. 4, pp. 265–271, 1995.

[18] V. D. Prajapati, G. K. Jani, B. S. Zala, and T. A. Khutliwala, “An insight into the emerging exopolysaccharide gellan gum as a novel polymer,” *Carbohydr. Polym.*, vol. 93, no. 2, pp. 670–678, 2013.

[19] K. M. Manjanna, T. M. Pramod Kumar, and B. Shivakumar, “Natural polysaccharide hydrogels as novel excipients for modified drug delivery systems: A review,” *Int. J. ChemTech Res.*, vol. 2, no. 1, pp. 509–525, 2010.

[20] P.E. Jansson, B. Lindberg, and P. A. Sandford, “Structural studies of gellan gum, an extracellular polysaccharide elaborated by Pseudomonas elodea,” *Carbohydr. Res.*, vol. 124, no. 1, pp. 135–139, 1983.

[21] M. A. O’Neill, R. R. Selvendran, and V. J. Morris, “Structure of the acidic extracellular gelling polysaccharide produced by Pseudomonas elodea,” *Carbohydr. Res.*, vol. 124, no. 1, pp. 123–133, 1983.

[22] K. S. Kang, “United States Patent [19],” 1982.

[23] A. M. Fialho, L. M. Moreira, A. T. Granja, A. O. Popescu, K. Hoffmann, and I. Sá-Correia, “Occurrence, production, and applications of gellan: Current state and perspectives,” *Appl. Microbiol. Biotechnol.*, vol. 79, no. 6, pp. 889–900, 2008.

[24] E. Dreveton, F. Monot, D. Ballerini, J. Lecourtier, and L. Choplin, “Effect of mixing and mass transfer conditions on gellan production by Auromonas elodea,” *J. Ferment. Bioeng.*, vol. 77, no. 6, pp. 642–649, 1994.

[25] B. Manna, A. Gambhir, and P. Ghosh, “Production and rheological characteristics of the microbial polysaccharide gellan,” *Lett. Appl. Microbiol.*, vol. 23, no. 3, pp. 141–145, 2008.

[26] K. M. Nampoothiri, R. R. Singhania, C. Sabarinath, and A. Pandey, “Fermentative production of gellan using Sphingomonas paucimobilis,” *Process Biochem.*, vol. 38, no. 11, pp. 1513–1519, 2003.

[27] P. A. Videira, L. L. Cortes, A. M. Fialho, and I. Sá-Correia, “Identification of the pgmG gene, encoding a bifunctional protein with phosphoglucomutase and phosphomannomutase activities, in the gellan gum- producing strain Sphingomonas paucimobilis ATCC 31461,” *Appl. Environ. Microbiol.*, vol. 66, no. 5, pp. 2252–2258, 2000.

[28] A. R. Marques, P. B. Ferreira, I. Sá-Correia, and A. M. Fialho, "Characterization of the ugpG gene encoding a UDP-glucose pyrophosphorylase from the gellan gum producer Sphingomonas paucimobilis ATCC 31461.," *Mol. Genet. Genomics*, vol. 268, no. 6, pp. 816–824, 2003.

[29] A. T. Granja, A. Popescu, A. R. Marques, I. Sá-Correia, and A. M. Fialho, "Biochemical characterization and phylogenetic analysis of UDP-glucose dehydrogenase from the gellan gum producer Sphingomonas elodea ATCC 31461," *Appl. Microbiol. Biotechnol.*, vol. 76, no. 6, pp. 1319–1327, 2007.

[30] E. Silva, A. R. Marques, A. M. Fialho, A. T. Granja, and I. Sá-Correia, "Proteins encoded by Sphingomonas elodea ATCC 31461 rmlA and ugpG genes, involved in gellan gum biosynthesis, exhibit both dTDP- and UDP-glucose pyrophosphorylase activities," *Appl. Environ. Microbiol.*, vol. 71, no. 8, pp. 4703–4712, 2005.

[31] N. E. Harding, Y. N. Patel, and R. J. Coleman, "Organization of genes required for gellan polysaccharide biosynthesis in Sphingomonas elodea ATCC 31461," *J. Ind. Microbiol. Biotechnol.*, vol. 31, no. 2, pp. 70–82, 2004.

[32] T. J. Pollock, L. Thorne, M. Yamazaki, M. J. Mikolajczak, and R. W. Armentrout, "Mechanism of bacitracin resistance in gram-negative bacteria that synthesize exopolysaccharides," *J. Bacteriol.*, vol. 176, no. 20, pp. 6229–6237, 1994.

[33] L. M. Moreira, K. Hoffmann, H. Albano, A. Becker, K. Niehaus, and I. Sá-Correia, "The gellan gum biosynthetic genes gelC and gelE encode two separate polypeptides homologous to the activator and the kinase domains of tyrosine autokinases," *J. Mol. Microbiol. Biotechnol.*, vol. 8, no. 1, pp. 43–57, 2004.

[34] R. F. Collins and J. P. Derrick, "Wza: a new structural paradigm for outer membrane secretory proteins?," *Trends Microbiol.*, vol. 15, no. 3, pp. 96–100, 2007.

[35] A. N. Reid and C. M. Szymanski, "Biosynthesis and Assembly of Capsular Polysaccharides," *Microb. Glycobiol.*, pp. 351–373, 2010.

[36] C. L. Dumitriu, M. Popa, S. Vasiliu, and V. Sunel, "Interpenetrated Network-Type Hydrogels Based on Gellan and Poly(Vinyl Alcohol) for Inclusion and Release of Cephotaxime," *J. Macromol. Sci. Part A*, vol. 41, no. 6, pp. 727–739, 2004.

[37] G. Péterszegi, I. Fodil-Bourahla, a. M. Robert, and L. Robert, "Pharmacological properties of fucose. Applications in age-related modifications of connective tissues," *Biomed. Pharmacother.*, vol. 57, no. 5–6, pp. 240–245, 2003.

[38] V. Ravelojaona, A. M. Robert, and L. Robert, "Expression of senescence-associated ??-galactosidase (SA-??-Gal) by human skin fibroblasts, effect of advanced glycation end-products and fucose or rhamnose-rich polysaccharides," *Arch. Gerontol. Geriatr.*, vol. 48, no. 2, pp. 151–154, 2009.

[39] L. Robert, J. Labat-Robert, and A. M. Robert, "Physiology of skin aging," *Clin. Plast. Surg.*, vol. 39, no. 1, pp. 1–8, 2012.

[40] Pszczola, "Gellan gum wins IFT´s Food Technology Industrial Achievement Award," *Food Technol. Biotechnol.*, 1993.

[41] F. Freitas, "Production and food applications of microbial biopolymers," *Eng. Asp. Food Biotechnol.*, 2013.

[42] I. W. Sutherland, “Microbial polysaccharides from Gram-negative bacteria,” *Int. Dairy J.*, vol. 11, no. 9, pp. 663–674, 2001.

[43] C. C. Lin and L. E. Casida, “GELRITE as a gelling agent in media for the growth of thermophilic microorganisms,” *Appl. Environ. Microbiol.*, vol. 47, no. 2, pp. 427–429, 1984.

[44] P. Moslemy, R. J. Neufeld, D. Millette, and S. R. Guiot, “Transport of gellan gum microbeads through sand: An experimental evaluation for encapsulated cell bioaugmentation,” *J. Environ. Manage.*, vol. 69, no. 3, pp. 249–259, 2003.

[45] P. Moslemy, S. R. Guiot, and R. J. Neufeld, “Production of size-controlled gellan gum microbeads encapsulating gasoline-degrading bacteria,” *Enzyme Microb. Technol.*, vol. 30, no. 1, pp. 10–18, 2002.

[46] K. Miyamoto, K. Sugihara, Y. Abe, T. Nobori, M. Tokita, and T. Komai, “Novel plasma-separation dilayer gellan-gellan-sulfate adsorber for direct removal of extra domain A containing fibronectin from the blood of rheumatoid arthritis patients,” *Int. J. Biol. Macromol.*, vol. 30, no. 3–4, pp. 197–204, 2002.

[47] S. Miyazaki, H. Aoyama, N. Kawasaki, W. Kubo, and D. Attwood, “In situ-gelling gellan formulations as vehicles for oral drug delivery,” *J. Control. Release*, vol. 60, no. 2–3, pp. 287–295, 1999.

[48] K. D. Cole, “Reversible gels for electrophoresis and isolation of DNA,” *Biotechniques*, vol. 26, no. 4, pp. 748–756, 1999.

[49] A. I. C. Gonçalves, L. A. Rocha, J. M. L. Dias, L. A. Passarinha, and Â. Sousa, “Optimization of a chromatographic stationary phase based on gellan gum using central composite design,” *J. Chromatogr. B Anal. Technol. Biomed. Life Sci.*, vol. 957, pp. 46–52, 2014.

[50] J. A. Queiroz, T. C. T., and Cabral J.M.S., “Hydrophobic interaction chromatography of proteins.,” *Methods Enzymol.*, vol. 270, pp. 27–47, 2001.

[51] Â. Sousa, F. Sousa, and J. A. Queiroz, “Advances in chromatographic supports for pharmaceutical-grade plasmid DNA purification,” *J. Sep. Sci.*, vol. 35, no. 22, pp. 3046–3058, 2012.

[52] J. Billen and G. Desmet, “Understanding and design of existing and future chromatographic support formats,” *J. Chromatogr. A*, vol. 1168, no. 1–2, pp. 73–99, 2007.

[53] C. Gölker, *Isolation and Purification*. 2007.

[54] G. E. Healthcare, “Recombinant Protein Purification Handbook,” pp. 1–167, 2010.

[55] A. Jungbauer, “Preparative chromatography of biomolecules,” *J. Chromatogr.*, vol. 639, no. 1, pp. 3–16, 1993.

[56] G. Guiochon, “Preparative liquid chromatography,” *J. Chromatogr. A*, vol. 965, no. 1–2, pp. 129–161, 2002.

[57] M. Hedhammar, A. Karlstrom, and S. Hober, “Chromatographic methods for protein purification,” *Stock. R. Inst. Technol.*, pp. 1–31, 2006.

[58] A. Jungbauer, “Chromatographic media for bioseparation,” *J. Chromatogr. A*, vol. 1065, no. 1, pp. 3–12, 2005.

[59] H. G. Barth, B. E. Boyes, and C. Jackson, “Size exclusion chromatography.,” *Anal. Chem.*, vol. 66, no. 12, p. 595R–620R, 1994.

[60] J. Li, W. Han, and Y. Yu, “Chromatography Method,” 2013.

[61] T. S. Planning, B. Protocol, T. A. Protocol, B. Protocol, B. Protocol, B. Protocol, S. Protocol, S. Protocol, and S. Protocol, “Ion-Exchange Chromatography,” 1999.

[62] Ö. B. Acikara, “Ion-Exchange Chromatography and Its Applications,” *Column Chromatogr.*, pp. 31–56, 2013.

[63] J. Porath, “Salt-promoted adsorption: recent developments.,” *J. Chromatogr.*, vol. 376, pp. 331–341, 1986.

[64] J.C. Janson and L. Rydén, “Protein Separation and Purification,” *Biotechnol. Set*, pp. 617–642, 2001.

[65] G. E. Healthcare, “Chromatography (Hydrophobic Interactions).”

[66] P. Jandera, “Stationary and mobile phases in hydrophilic interaction chromatography: A review,” *Anal. Chim. Acta*, vol. 692, no. 1–2, pp. 1–25, 2011.

[67] M. Hutta, R. Góra, R. Halko, and M. Chalányová, “Some theoretical and practical aspects in the separation of humic substances by combined liquid chromatography methods,” *J. Chromatogr. A*, vol. 1218, no. 49, pp. 8946–8957, 2011.

[68] D. S. Hage, “Affinity chromatography: a review of clinical applications.,” *Clin. Chem.*, vol. 45, no. 5, pp. 593–615, 1999.

[69] D. S. Hage, “High-performance affinity chromatography: A powerful tool for studying serum protein binding,” *J. Chromatogr. B Anal. Technol. Biomed. Life Sci.*, vol. 768, no. 1, pp. 3–30, 2002.

[70] F. Sousa, D. M. F. Prazeres, and J. A. Queiroz, “Affinity chromatography approaches to overcome the challenges of purifying plasmid DNA,” *Trends Biotechnol.*, vol. 26, no. 9, pp. 518–525, 2008.

[71] M. M. Diogo, J. A. Queiroz, and D. M. F. Prazeres, “Chromatography of plasmid DNA,” *J. Chromatogr. A*, vol. 1069, no. 1, pp. 3–22, 2005.

[72] S. R. Narayanan, “Review Preparative affinity chromatography of proteins,” *Pharmacia*, vol. 658, pp. 237–258, 1994.

[73] A. Jungbauer and R. Hahn, “Polymethacrylate monoliths for preparative and industrial separation of biomolecular assemblies,” *J. Chromatogr. A*, vol. 1184, no. 1–2, pp. 62–79, 2008.

[74] C. Horvath and W. Melander, “Liquid Chromatography With Hydrocarbonaceous Bonded Phases; Theory and Practice of Reversed Phase Chromatography.,” *J. Chromatogr. Sci.*, vol. 15, no. 9, pp. 393–404, 1977.

[75] R. E. F. Boto, U. Anyanwu, F. Sousa, P. Almeida, and J. A. Queiroz, “Thiacarbocyanine as ligand in dye-affinity chromatography for protein purification. II. Dynamic binding

capacity using lysozyme as a model," *Biomed. Chromatogr.*, vol. 23, no. 9, pp. 987–993, 2009.

[76] Y. K. Chang and I. P. Chang, "Method development for direct recovery of lysozyme from highly crude chicken egg white by stirred fluidized bed technique," *Biochem. Eng. J.*, vol. 30, no. 1, pp. 63–75, 2006.

[77] A. Jungbauer and R. Hahn, *Chapter 22 Ion-Exchange Chromatography*, 1st ed., vol. 463, no. C. Elsevier Inc., 2009.

[78] J. Jan-Christer, "Protein Purification," 2011.

[79] C. S. F. Picone and R. L. Cunha, "Influence of pH on formation and properties of gellan gels," *Carbohydr. Polym.*, vol. 84, no. 1, pp. 662–668, 2011.

[80] W. Kubo, S. Miyazaki, and D. Attwood, "Oral sustained delivery of paracetamol from in situ-gelling gellan and sodium alginate formulations," *Int. J. Pharm.*, vol. 258, no. 1–2, pp. 55–64, 2003.

[81] A. K. A. S. Brun-Graeppi, C. Richard, M. Bessodes, D. Scherman, and O. W. Merten, "Cell microcarriers and microcapsules of stimuli-responsive polymers," *J. Control. Release*, vol. 149, no. 3, pp. 209–224, 2011.

[82] D. J. McClements, "Critical review of techniques and methodologies for characterization of emulsion stability.," *Crit. Rev. Food Sci. Nutr.*, vol. 47, no. 7, pp. 611–649, 2007.

[83] T. Coviello, P. Matricardi, C. Marianecci, and F. Alhaique, "Polysaccharide hydrogels for modified release formulations," *J. Control. Release*, vol. 119, no. 1, pp. 5–24, 2007.

[84] S. A. Agnihotri and T. M. Aminabhavi, "Development of novel interpenetrating network gellan gum-poly(vinyl alcohol) hydrogel microspheres for the controlled release of carvedilol.," *Drug Dev. Ind. Pharm.*, vol. 31, no. 6, pp. 491–503, 2005.

[85] E. R. Morris, R. K. Richardson, and L. E. Whittaker, "Rheology and gelation of deacylated gellan polysaccharide with Na+ as the sole counterion," *Phys. Chem. Ind. Appl. Gellan Gum*, vol. 114, pp. 109–115, 1999.

[86] Ş. Racoviţă, S. Vasiliu, M. Popa, and C. Luca, "Polysaccharides based on micro- and nanoparticles obtained by ionic gelation and their applications as drug delivery systems," *Rev. Roum. Chim.*, vol. 54, no. 9, pp. 709–718, 2009.

[87] M. N. Ravi Kumar, "Nano and microparticles as controlled drug delivery devices.," *J. Pharm. Pharm. Sci.*, vol. 3, no. 2, pp. 234–258, 2000.

[88] L. V. A. Reddy, Y. J. Wee, J. S. Yun, and H. W. Ryu, "Optimization of alkaline protease production by batch culture of Bacillus sp. RKY3 through Plackett-Burman and response surface methodological approaches," *Bioresour. Technol.*, vol. 99, no. 7, pp. 2242–2249, 2008.

[89] C. M. Pan, Y. T. Fan, Y. Xing, H. W. Hou, and M. L. Zhang, "Statistical optimization of process parameters on biohydrogen production from glucose by Clostridium sp. Fanp2," *Bioresour. Technol.*, vol. 99, no. 8, pp. 3146–3154, 2008.

[90] R. M. Banik, A. Santhiagu, and S. N. Upadhyay, "Optimization of nutrients for gellan gum production by Sphingomonas paucimobilis ATCC-31461 in molasses based medium

using response surface methodology," *Bioresour. Technol.*, vol. 98, no. 4, pp. 792–797, 2007.

[91] D. B. Hibbert, "Experimental design in chromatography: A tutorial review," *J. Chromatogr. B Anal. Technol. Biomed. Life Sci.*, vol. 910, pp. 2–13, 2012.

[92] R. L. Mason, R. F. Gunst, and J. L. Hess, *Statistical Design and Analysis of Experiments*. 2003.

[93] S. Brainerd, "Design and Analysis of Engineering Experiments," 2001.

[94] S. R. Montoro, S. D. F. Medeiros, A. M. Santos, M. B. Silva, and M. L. Tebaldi, "Application of 2 K Experimental Design and Response Surface Methodology in the Optimization of the Molar Mass Reduction of Poly (3-Hydroxybutyrate- co -3-Hydroxyvalerate) (PHBHV)."

[95] N. Aslan, "Application of response surface methodology and central composite rotatable design for modeling and optimization of a multi-gravity separator for chromite concentration," *Powder Technol.*, vol. 185, no. 1, pp. 80–86, 2008.

[96] G. M. Espírito Santo, A. Q. Pedro, D. Oppolzer, M. J. Bonifácio, J. A. Queiroz, F. Silva, and L. A. Passarinha, "Development of fed-batch profiles for efficient biosynthesis of catechol-O-methyltransferase," *Biotechnol. Reports*, vol. 3, pp. 34–41, 2014.

[97] P. T. Männistö and S. Kaakkola, "Catechol-O-methyltransferase (COMT): biochemistry, molecular biology, pharmacology, and clinical efficacy of the new selective COMT inhibitors.," *Pharmacol. Rev.*, vol. 51, no. 4, pp. 593–628, 1999.

[98] N. Jatana, A. Sharma, and N. Latha, "Pharmacophore modeling and virtual screening studies to design potential COMT inhibitors as new leads," *J. Mol. Graph. Model.*, vol. 39, pp. 145–164, 2013.

[99] F. F. Correia, F. M. Santos, A. Q. Pedro, M. J. Bonifácio, J. A. Queiroz, and L. A. P. Passarinha, "Recovery of biological active catechol-O-methyltransferase isoforms from Q-sepharose," *J. Sep. Sci.*, vol. 37, no. 1–2, pp. 20–29, 2014.

[100] M. J. Bonifácio and J. A. Queiroz L. A. Passarinha, "Comparative study on the interaction of recombinant human soluble catechol-O-methyltransferase on some hydrophobic adsorbents," *Biomed. Chromatogr.*, vol. 21, no. 10, pp. 430–438, 2007.

[101] E. M. Tunbridge, P. J. Harrison, and D. R. Weinberger, "Catechol-o-Methyltransferase, Cognition, and Psychosis: Val158Met and Beyond," *Biol. Psychiatry*, vol. 60, no. 2, pp. 141–151, 2006.

[102] M. Jo and P. N. Palma, "Catechol- O -methyltransferase and Its Inhibitors in Parkinson ' s Disease," vol. 13, no. 3, pp. 352–379, 2007.

[103] J. A. Roth, "Membrane-bound catechol-O-methyltransferase: a reevaluation of its role in the O-methylation of the catecholamine neurotransmitters.," *Rev. Physiol. Biochem. Pharmacol.*, vol. 120, pp. 1–29, 1992.

[104] V. Licker, E. Kövari, D. F. Hochstrasser, and P. R. Burkhard, "Proteomics in human Parkinson's disease research," *J. Proteomics*, vol. 73, no. 1, pp. 10–29, 2009.

[105] L. A. Passarinha, M. J. Bonifácio, and J. A. Queiroz, "Application of a fed-batch bioprocess for the heterologous production of hSCOMT in Escherichia coli," *J. Microbiol. Biotechnol.*, vol. 19, no. 9, pp. 972–981, 2009.

[106] L. A. Passarinha, M. J. Bonifácio, P. Soares-da-Silva, and J. A. Queiroz, "A new approach on the purification of recombinant human soluble catechol-O-methyltransferase from an Escherichia coli extract using hydrophobic interaction chromatography," *J. Chromatogr. A*, vol. 1177, no. 2, pp. 287–296, 2008.

[107] A. Q. Pedro, M. J. Bonifácio, J. A. Queiroz, C. J. Maia, and L. A. Passarinha, "A novel prokaryotic expression system for biosynthesis of recombinant human membrane-bound catechol-O-methyltransferase," *J. Biotechnol.*, vol. 156, no. 2, pp. 141–146, 2011.

[108] F. M. Santos, A. Q. Pedro, R. F. Soares, R. Martins, M. J. Bonifácio, J. A. Queiroz, and L. A. Passarinha, "Performance of hydrophobic interaction ligands for human membrane-bound catechol-O-methyltransferase purification," *J. Sep. Sci.*, vol. 36, no. 11, pp. 1693–1702, 2013.

[109] S. R. Costa, M. J. Bonifácio, J. A. Queiroz, and L. A. Passarinha, "Analysis of hSCOMT adsorption in bioaffinity chromatography with immobilized amino acids: The influence of pH and ionic strength," *J. Chromatogr. B Anal. Technol. Biomed. Life Sci.*, vol. 879, no. 19, pp. 1704–1706, 2011.

[110] C. Tilgmann and I. Ulmanen, "Purification methods of mammalian catechol-O-methyltransferase," *J. Chromatogr. B Biomed. Appl.*, vol. 684, no. 1–2, pp. 147–161, 1996.

[111] A. Q. Pedro, D. Oppolzer, M. J. Bonifácio, C. J. Maia, J. A. Queiroz, and L. A. Passarinha, "Evaluation of MutS and Mut+ Pichia pastoris Strains for Membrane-Bound Catechol-O-Methyltransferase Biosynthesis," *Appl. Biochem. Biotechnol.*, pp. 3840–3855, 2015.

[112] L. Passarinha, F. Correia, A. Pedro, D. Oliveira, and J. Queiroz, "Biosynthesis, purification and biointeraction of human SCOMT with Parkinson's disease inhibitors," *N. Biotechnol.*, vol. 31, no. July, p. S193, 2014.

[113] M. Milas, X. Shi, and M. Rinaudo, "On the physicochemical properties of gellan gum.," *Biopolymers*, vol. 30, no. 3–4, pp. 451–464, 1990.

[114] S. K. Bajpai, S. K. Saxena, and S. Sharma, "Swelling behavior of barium ions-crosslinked bipolymeric sodium alginate-carboxymethyl guar gum blend beads," *React. Funct. Polym.*, vol. 66, no. 6, pp. 659–666, 2006.

[115] R. T. Thimma and S. Tammishetti, "Barium chloride crosslinked carboxymethyl guar gum beads for gastrointestinal drug delivery," *J. Appl. Polym. Sci.*, vol. 82, no. 12, pp. 3084–3090, 2001.

[116] R. Carlson, "Design of Experiments, Principles and Applications, L. Eriksson, E. Johansson, N. Kettaneh- Wold, C. Wikstrom and S. Wold, Umetrics AB, Ume Learnways AB, Stockholm, 2000, ISBN 91-973730-0-1, xii?+?329 pp.," *J. Chemom.*, vol. 15, no. 5, pp. 495–496, 2001.

[117] S. E. Agarry and O. O. Ogunleye, "Box-Behnken design application to study enhanced bioremediation of soil artificially contaminated with spent engine oil using biostimulation strategy," *Int. J. Energy Environ. Eng.*, vol. 3, no. 1, p. 31, 2012.

[118] Food and Drug Administration, "Guidance for Industry: Bioanalytical Method Validation," *U.S. Dep. Heal. Hum. Serv.*, no. May, pp. 4–10, 2001.

[119] S. L. C. Ferreira, R. E. Bruns, H. S. Ferreira, G. D. Matos, J. M. David, G. C. Brandão, E. G. P. da Silva, L. A. Portugal, P. S. dos Reis, A. S. Souza, and W. N. L. dos Santos, "Box-Behnken design: An alternative for the optimization of analytical methods," *Anal. Chim. Acta*, vol. 597, no. 2, pp. 179–186, 2007.

[120] S. A. Patil, S. N. Surwase, S. B. Jadhav, and J. P. Jadhav, "Optimization of medium using response surface methodology for l-DOPA production by Pseudomonas sp. SSA," *Biochem. Eng. J.*, vol. 74, pp. 36–45, 2013.

[121] A. K. Dunker and R. R. Rueckert, "Observations on molecular weight determination on polyacrylamide gels," *J.Biol.Chem.*, vol. 224, no. 18, pp. 5074–5080, 1969.

[122] F. C. Wedler, "a-Chymotrypsin : Enzyme Concentration and Kinetics," pp. 84–88.

[123] K. J. Palmer, M. Ballantyne, and J. a Galvin, "The molecular weight of lysozyme determined by the X-ray diffraction method.," *J. Am. Chem. Soc.*, vol. 70, no. 3, pp. 906–908, 1948.

[124] J. Chen, B. K. Lipska, N. Halim, Q. D. Ma, M. Matsumoto, S. Melhem, B. S. Kolachana, T. M. Hyde, M. M. Herman, J. Apud, M. F. Egan, J. E. Kleinman, and D. R. Weinberger, "Functional analysis of genetic variation in catechol-O-methyltransferase (COMT): effects on mRNA, protein, and enzyme activity in postmortem human brain.," *Am. J. Hum. Genet.*, vol. 75, no. 5, pp. 807–821, 2004.

[125] A. Staby, M. B. Sand, R. G. Hansen, J. H. Jacobsen, L. A. Andersen, M. Gerstenberg, U. K. Bruus, and I. H. Jensen, "Comparison of chromatographic ion-exchange resins: IV. Strong and weak cation-exchange resins and heparin resins," *J. Chromatogr. A*, vol. 1069, no. 1, pp. 65–77, 2005.